STUDIES ON THE ENERGETICS AND MECHANISM OF VISUAL PIGMENT RHODOPSINS.

SHEILA F. DIXON (B.Sc.)

A thesis submitted to the University of Glasgow for the degree of Doctor of Philosophy.

Department of Chemistry

April 1986

ProQuest LLC.
789 East Eisenhower Parkway
P.O. Box 1346
Ann Arbor, MI 48106 – 1346

ACKNOWLEDGEMENTS

There are several people I would like to thank who helped me in the course of this work. First and foremost, I would like to thank my supervisor Dr. Alan Cooper for all his patience, help and encouragement during the three years I spent doing this work. My thanks also to Mrs Margaret Nutley for whose technical help in the laboratory I am extremely grateful. I would also like to express my gratitude to Dr. Carolyn A. Converse for supplying the vertebrate antiserum, to Dr. Sahar A.H. Al-Mahdawi who helped me with the SDS gel electrophoresis, to Professor M. Tsuda for supplying the octopus microvilli and to the Science Research Council for the award of a research studentship. Last but not least, I would like to thank my husband Kim and my mother for all their help and tolerance as I wrote this thesis.

To my husband Kim, my mother and my late father.

Contents

Summary

Three aspects of vision are examined in this work. Firstly, the enthalpy of formation of each of the intermediates in the octopus rhodopsin photocycle were measured photocalorimetrically. The formation of the first intermediate (bathorhodopsin) proceeded endothermically, with storage of ~50% of the exciting photon energy. Formation of the later intermediates, lumirhodopsin, mesorhodopsin, acid metarhodopsin and alkaline metarhodopsin involved release of the stored energy. Experiments were performed on both octopus microvilli membranes and L1690 detergent extracted octopus rhodopsin and there was no significant difference in the results obtained.

Variation of the buffer system used in the experiments showed that the enthalpy of the rhodopsin to acid metarhodopsin reaction involved no contributions from protonation changes. In contrast to this, the rhodopsin to alkaline metarhodopsin reaction was found to proceed with the release of ~1 proton/rhodopsin molecule. The energy difference between acid and alkaline metarhodopsin was estimated calorimetrically to be ~ 50 KJ/mole, a value which was confirmed by Van't Hoff analysis on the temperature dependence of the reversible acid ⇌ alkaline metarhodopsin equilibrium.

The protonation changes in the acid ⇌ alkaline metarhodopsin equilibrium were studied in two ways:-

1. Directly, by formation of both acid and alkaline metarhodopsin in the absence of buffer. This gave a

value of 1.08 protons per molecule of rhodopsin, which reinforced the calorimetrically determined value. 2. By acid-base titration of the metarhodopsin equilibrium. This showed a non-ideal titration curve with a value of 0.8 protons per molecule of rhodopsin.

The energy profile obtained for octopus rhodopsin was compared with that which had been measured for bovine rhodopsin and a general mechanism for the primary photoreaction step is proposed. Differences which occur between vertebrates and invertebrates at the later intermediates are considered in relation to their environment and pigment regeneration requirements.

In the second part of the work, the quantum yield for the forward and backward octopus rhodopsin photoreaction was measured. Potassium ferrioxalate and cattle rhodopsin were used as actinometers. Both systems gave the same result within experimental error. The rhodopsin to acid metarhodopsin reaction was found to have a value of 0.689 ± 0.016 . The regeneration reaction acid metarhodopsin to rhodopsin had a quantum yield of 0.430 ± 0.017. Two different methods of analysis were used to interpret the results. One was based on theory developed by H.Dartnall, the other on a method devised by A.Kropf. Both methods had to be modified to allow for photoreversal of the acid metarhodopsin to rhodopsin. The results for both methods of analysis were essentially identical.

In the third part of the work, the question of hydrolysis of the chromophore-protein bond during the metarhodopsin I to metarhodopsin II transition in cattle

rhodopsin was investigated using O^{18} labelled water. The uptake of label was monitored by mass spectroscopy and infrared spectroscopy. Both methods seem to suggest that Schiff base hydrolysis does indeed occur during the metarhodopsin I to metarhodopsin II transition in bovine rhodopsin.

Chapter 1

Introduction

CHAPTER 1

Introduction

Vision is generally considered to be the most important of the five senses known to mankind, and as such it has been the centre of a great deal of research and controversy over the years.

In order to see, two basic requirements have to be met: 1. There must be light. 2. There must be something to detect the light and process the information i.e. the eye. There are three basic types of eye:- the very basic "pin-hole" eye Fig.(1.1a), the compound eye Fig.(1.1b) and the refracting eye Fig.(1.2).

The first type of eye is found in creatures such as the mollusc "nautilus". Narrow beams of light from an object in the visual field enter the eye and form an inverted image on the back of the eye. This very basic type of eye is not particularly efficient. The second type of eye is found in insects, crustacea and some molluscs. In this type of eye, light travels through bundles of fibres termed ommatidia before it reaches the back of the eye. Only light travelling in the direction of these ommatidia reaches the back of the eye and gives rise to an erect image. The third type of eye is found in vertebrates and some invertebrates such as octopus and squid. It is the one of interest in this work. Light enters the eye through the cornea where it is focussed by the lens on to the back of the eye Fig.(1.2). The ciliary muscles control the focussing function of the lens and the iris controls the amount of light entering the eye. The optic nerve conducts the optical signal to the brain. Before light can interact with matter, it has to be absorbed, and

(a)

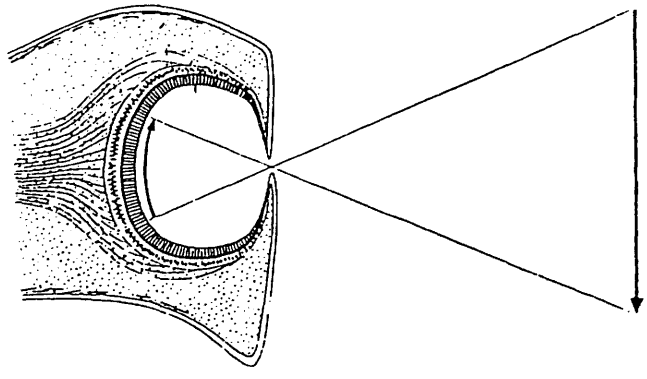

(b)

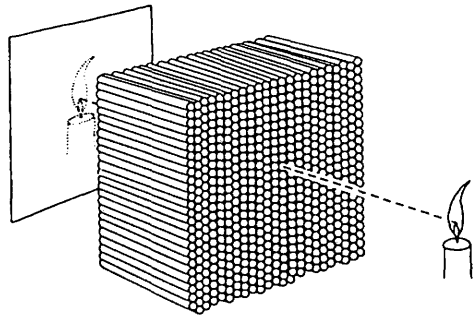

Fig.(1.1). (a) The "pin-hole" eye. An inverted image is formed on the retina.

(b) The compound eye. An erect image is formed on the retina.

(Taken from Davson 1977).

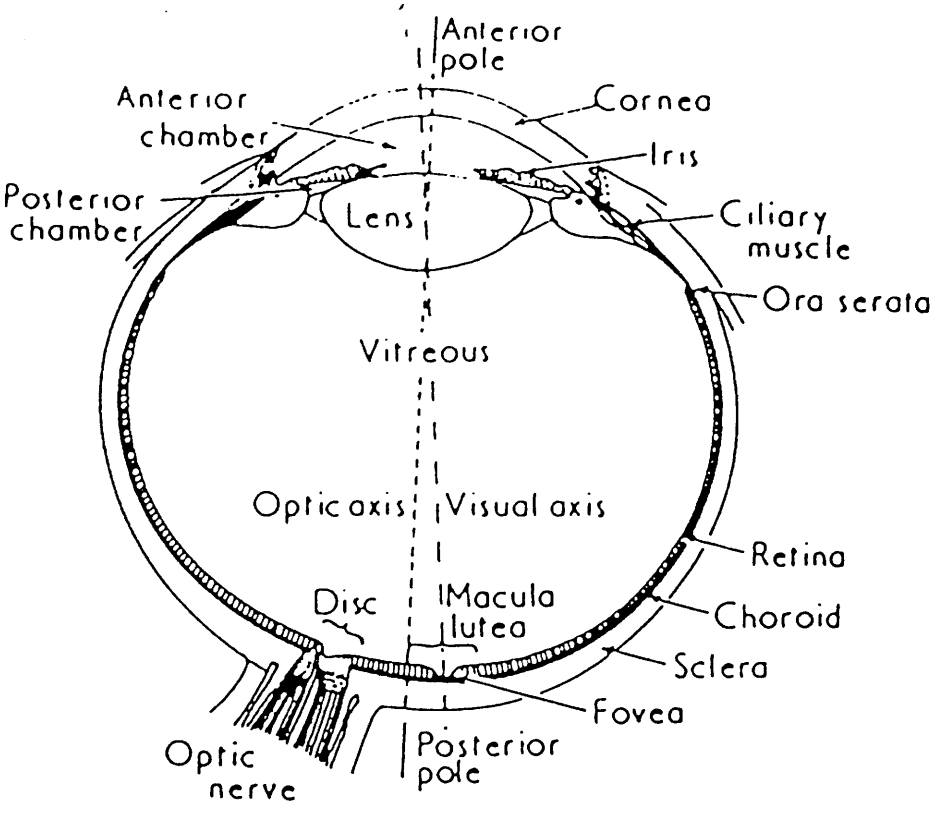

Fig.(1.2). The refracting eye: Horizontal section of the human eye.

(Taken from Davson 1977).

so the back of the eye is lined with a thin membranous substance called the retina which contains the visual pigment rhodopsin responsible for absorption of light.

Rhodopsin is an intrinsic membrane protein consisting of a protein part, opsin, plus a chromophore, 11-cis retinal linked via a protonated Schiff base Fig.(1.3). The role of rhodopsin is to absorb the incident light and trigger the neural impulse responsible for vision. Thus rhodopsin is very important. Its existance was appreciated as early as the 1860's but although pioneer investigators like Schultz (1866) observed the red, satiny appearance of rods, none of these investigators associated this red colour with light or photochemical events in visual cells. Boll (1876) was the first to connect an observed colour change with vision. Kuhne (1879) also did a lot of work on what he called "sehpurpur" and was the first to extract rhodopsin with bile salts. He made the first crude absorption spectrum of rhodopsin and studied the bleaching effectiveness of light of different wavelengths as well as commencing studies on regeneration reactions.

Although a prodigious amount of work was carried out by these workers, it was not until the 1930's that a more detailed structure and function analysis of rhodopsin was undertaken.

Nature of the chromophore: During the first world war, it had been noticed that vitamin A deficiency led to night blindness. Fridericia and Holm (1925) and Tansley(1931) showed a direct relationship between the two by observing

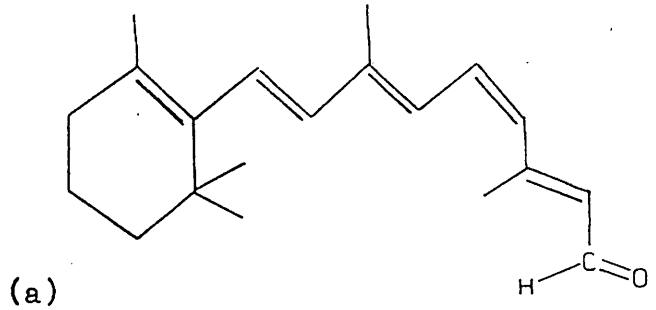

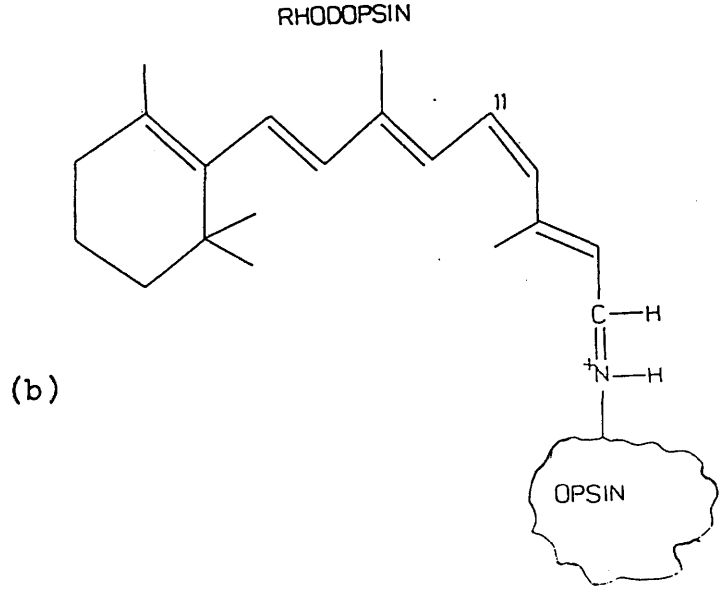

Fig.(1.3). (a) 11-cis retinal.

(b) Rhodopsin :- 11-cis retinal linked to opsin via a protonated Schiff base.

that visual pigment formed more slowly in retinas of rats raised on a vitamin A deficient diet. Wald (1933, 1935a) then identified vitamin A in eye tissues and postulated its participation in a visual cycle (1935b) with another extractable substance which he called retinene (now called retinal).

Retinene and vitamin A were believed to be closely related, but it was not until 1944 that Morton suggested that retinene was the aldehyde corresponding to vitamin A which is an alcohol. This was confirmed in 1950 by Wald and Brown who added synthetic retinal to extracted opsin which then recombined to give rhodopsin identical to that extracted from dark adapted retinas.

The fact that a specific isomer of retinal was involved was not appreciated until 1951 when Hubbard and Wald showed that rhodopsin could be regenerated by reaction of retinol with opsin in crude rod outer segments. The original sample of retinol was from fish liver oil which was known to contain a number of isomers of retinol. When this sample was purified the yield of rhodopsin dropped, from which they postulated that a specific isomer of retinol was required. Various isomers were synthesised and tried and it was found that 11-cis retinal would react spontaneously with opsin to give a stable pigment (Brown and Wald 1956).

Structure of rhodopsin: Determination of the nature of the protein component was much more difficult. It is insoluble in water and can only be brought in to solution as a micellar suspension in a detergent. Added to this is the fact that it is thermally unstable, difficult to purify

and appears to vary in physical properties with method of purification.

Various estimates have been made for the molecular weight of rhodopsin. The first measurements were made by Hecht and Pickels (1938) who obtained a value of 270,000 Dalton by the ultracentrifuge method. This high value was due to the weight of digitonin micelles whose presence was not appreciated by the investigators. Hubbard (1954) was the first to make an accurate measurement of the molecular weight of rhodopsin. She also used the ultracentrifuge technique on frog rhodopsin and obtained a value of 40,000 Dalton. Since then, other groups have measured the molecular weight by a variety of techniques including gel electrophoresis, gel filtration, and amino acid analysis. The results have ranged from 35,000 to 43,000 Dalton for vertebrates and from 35,000 to 43,000 Dalton for invertebrates,

This however gives no real indication of the structure. No crystallographic structure at adequate resolution is available for rhodopsin. Although small crystals of rhodopsin can be produced under certain conditions, (Dratz et al 1985, Corless et al 1982) none have yet been suitable for detailed X-ray or electron microscopic structural studies. This can be contrasted with the case of bacteriorhodopsin, whose 2-dimensional crystallinity in purple membranes has facilitated elegant structural studies (Henderson and Unwin 1975, Henderson 1975, Engelman et al 1980). Structural predictions for visual rhodopsins so far are based, by analogy, on this work.

More recently, the aim has been to determine the amino

acid sequence of rhodopsin from which a three dimensional structure might be predicted. The complete amino acid sequence for bovine rhodopsin was discovered almost simultaneously by Ovchinnikov et al (1982) and Hargrave et al (1983). Although the results are not completely identical, the overall picture is the same. There are regions in rhodopsin which are predominantly polar and hydrophilic in composition and others which are predominantly non-polar and hydrophobic. Since these regions alternate along the system, a model was predicted where the rhodopsin polypeptide chain traversed the lipid bilayer, exposed a hydrophilic loop region and then reentered and traversed the lipid bilayer Fig.(1.4). The hydrophobic sections are predicted to be seven α-helices although work done by Findlay et al (1982) on ovine rhodopsin suggests that there is a distortion in the α-helix containing the binding site of the chromophore retinal and also in the helix immediately adjacent. Subsequent amino acid analysis of ovine, porcine and equinine opsin (Findlay et al 1984) gave very similar results to bovine opsin with a low overall rate of mutation. Surprisingly however, the amino acid sequence of the fruit fly differs from opsin of vertebrates by about 70% (O'Tousa et al 1985) yet the sequence is such that it too is made up of seven α-helices with loops. The explanation for the differences in the amino acid sequence of invertebrate and vertebrate opsins may lie in the venerable age of opsin. In such an "old" protein, neutral mutations that change the sequence of amino acids but not necessarily the shape and function of the protein may gradually accumulate.

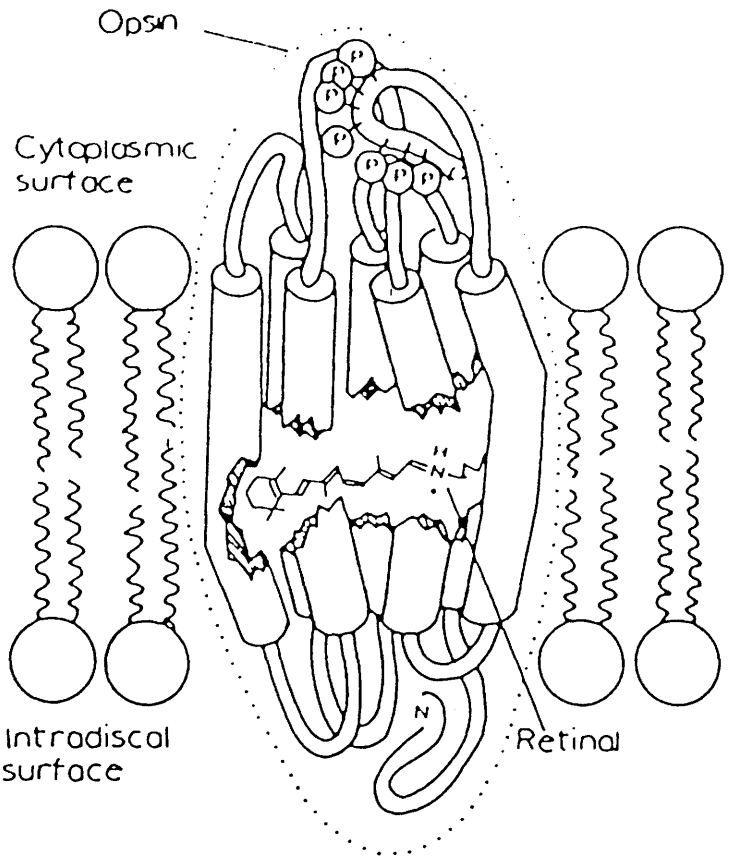

Fig.(1.4). Schematic representation of rhodopsin in the disc membrane.

(Taken from Vines 1985).

On the other hand, proteins with distinctly different origins may end up with a similar shape merely because this confers a similar photochemistry. For example, the pigment bacteriorhodopsin has a very different sequence of amino acids (Ovchinnikov 1978) yet in shape it is rather like a truncated animal opsin bereft of its loops. The barrel-shaped molecule is embedded in the membrane, its seven α-helices traversing the membrane. This too behaves as a light energy transducer converting light energy in to the form of a proton gradient that generates metabolic energy for the bacteria. (Reviews: Henderson 1977, Lanyi 1978, Stoeckenius 1979). Thus perhaps this shape is the most efficient for the photochemistry required.

Location of rhodopsin in vertebrate and invertebrate rod outer segments: The visual photoreceptor cells in the animal kingdom are of two basic types, the ciliary cells of vertebrates and allied phyla and the rhabdomeric cells of the invertebrate phyla. Both contain an inner and outer segment Fig.(1.5). The inner cell contains the cell nucleus, mitochondria and synthetic machinery, while the outer segment contains the visual pigment embedded in tightly packed membranes.

The rod outer segments in vertebrates are composed of a stack of disc-like membranes enclosed by a plasma membrane. The interior and exterior of the discs are aqueous and the rhodopsin is situated in the walls of the disc membrane Fig.(1.6a).

The photoreceptor cells of invertebrates also have an inner and outer segment, but no connecting cilium. There is

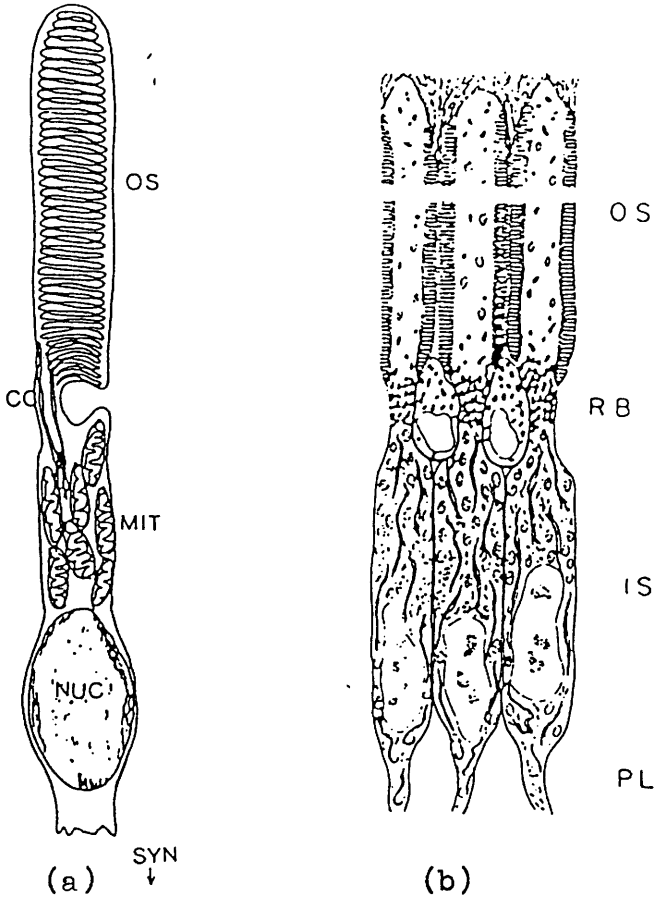

Fig.(1.5). Schematic view of (a) vertebrate and(b) invertebrate rod cell.

(Taken from Abrahamson and Fager 1973).

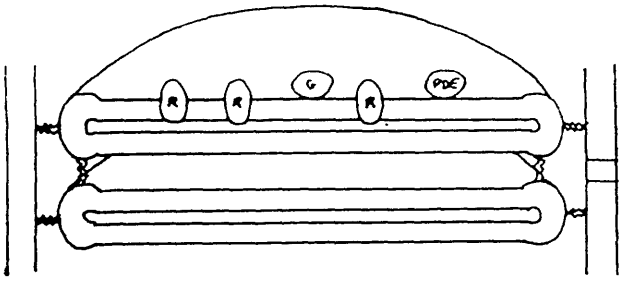

(a)

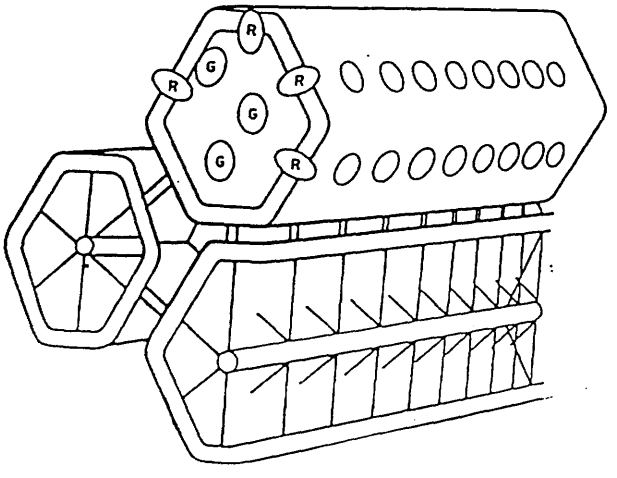

(b)

Fig.(1.6). (a) Vertebrate discs enclosed by the plasma membrane.

(b) Invertebrate microvilli in the invertebrate photoreceptor cell.

(Taken from Vines 1985).

only a single internal aqueous compartment along the axis of the outer segment which is surrounded by a tightly packed cluster of finger-like projections of the plasma membrane (microvilli) orientated perpendicular to the axis. In this case, the rhodopsin is situated in the walls of the microvilli. Several of these cells are packed in to clusters called rhabdomes Fig.(1.6b).

Since rhodopsin is an integral part of a membrane, it is of interest to know what the physical properties of the membrane are. Chemically, evidence can be obtained as to the rigidity or fluidity of the membrane by analysis of its lipid composition. The lipid composition has been determined by several groups of workers for different species and is summarised by Abrahamson and Fager (1973). They concluded that vertebrates have a membrane which is fluid-like in composition since they have little or no cholesterol and a high percentage of long chain polyunsaturated fatty acids. This can be contrasted to invertebrate membranes which show a high cholesterol content and are thought to be more rigid.

In support of the lipid analysis is the fact that in vertebrates, rhodopsin molecules undergo continual lateral and rotational diffusion in the disc membrane. Cone(1972) found that the momentary dichroism induced by bleaching rhodopsin with linearly polarised light is totally randomised within 60μs due to rapid rotation. Also when a rod is selectively bleached, there is an initial decrease in absorbance at the site of illumination, but within 40s the absorbance increases again accompanied by a decrease in absorbance in the surrounding unbleached area due to lateral diffusion

of rhodopsin molecules in the disc membrane. (Poo and Cone 1974, Liebman and Entine 1974).

By contrast, the relatively fixed nature of the invertebrate rhodopsin and its regular array in the microvilli means that invertebrates can detect polarised light. Waterman (1979) proposed that this feature was used by invertebrates for orientation and navigation. Another possibility is that they use this ability to detect prey. Many fish camouflage themselves with mirror-like scales that reflect light and match background illumination. Light reflected from mirrors becomes polarised and so invertebrates like octopus and squid who can detect polarised light can see through the camouflage and catch their prey. (Vines 1985).

Protein-chromophore interactions: The physical and chemical properties of the intact visual pigments are different to their isolated components opsin and the chromophore group. The interaction of these parts of the molecule is a very unusual one and the exact nature of the bond between them has been the subject of much attention and speculation.

It is now believed that the chromophore forms a protonated Schiff base with the protein (Morton and Pitt 1955, Hubbard 1969) via a lysine residue, but early experiments gave conflicting results. In both vertebrate and invertebrate rhodopsins , before light exposure the chromophore linkage is inaccessible to reduction by sodium borohydride at room temperature, whereas after light exposure, reduction proceeds rapidly. (Bownds and Wald 1965). Also hydroxylamine which has no effect on either vertebrate

or invertebrate rhodopsin before light exposure, rapidly extracts the chromophore and forms retinal oxime after light exposure. This appears to indicate that the chromophore in native rhodopsin is sequestered in a hydrophobic pocket of the molecule and cannot be reached by small water-soluble molecules. This made it difficult to study the protein-chromophore link in the unbleached state. The work done by Bownds and Wald in 1965 gave lysine as the binding site on reduction of light exposed rhodopsin with sodium borohydride.

In contrast to this however, Poincelot et al (1969,1970) found that extraction of dried bovine rod outer segments or digitonin micelles of rhodopsin gave retinal bound to a lipid, phosphatidylethanolamine. Other groups found a mixture of lipid and protein bound chromophore (Zorn 1971, Girsch and Rabinovitch 1972)depending on the conditions of reduction.

There was serious doubt about these results for two reasons:(1) Under the conditions employed, Schiff bases of retinal readily undergo hydrolysis and (2) the chromophore protein link was only accessible after illumination.

The controversy has apparently been resolved since it was found that the lipid ethanolamine:rhodopsin ratio was less than unity (Borggreven et al 1971). and also reduction of the unilluminated binding site was accomplished using the more hydrophobic sodium cyanoborohydride (Fager et al 1972) yielding lysine as the binding site.

Accumulated evidence favours the primary bond in native rhodopsin with the protein, but the presence of the

phospholipid has a stabilising effect upon the molecule. The proximity of the phospholipid group also perhaps allows transimmination to occur under certain extracting conditions giving the chromophore bound to phospholipid.

Although it is now generally believed that the chromophore-protein linkage is a protonated Schiff base, there have been a variety of other theories put forward. A major problem is the fact that the absorption maximum of rhodopsin is markedly red shifted compared to that of free retinal e.g. bovine rhodopsin λmax.=500nm, retinal in ethanol, λmax.=380nm. There are several ways in which the absorption of a conjugated molecule can be displaced to longer wavelengths:-

(1) Increase in the length of the conjugated system by the addition of further alternating single and double bonds.

(2) Introduction of a heteroatom e.g. N, O, S in to the system.

(3) Addition to, or removal from the system of an electron with subsequent formation of an ion or free radical. Change in the polarity or polarisability of the surrounding medium can also cause a red shift.

The first of the models put forward was for an aldimine linkage (Morton and Pitt 1955) Fig.(1.7a). In acid solution, the protonated form of these aldimines can go as high as 460nm. This falls short of the required 500nm. A second model proposed was for retinal with a secondary amine to give an enamine salt Fig.(1.7b) (Toth et al 1968). This could give a suitable absorbance maximum, but enamine salts

(a)

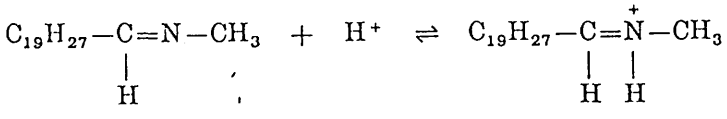

Neutral form of N-retinylidene methylamine

λ_{max} = 365 nm

Protonated form

λ_{max} = 438 nm

(b)

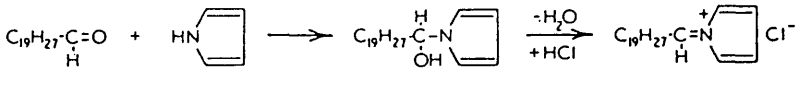

Retinal λ_{max} = 380nm

Pyrrole

Carbinol λ_{max} = 380nm

Enamine salt λ_{max} = 655 nm

The formation of the enamine salt between all-*trans*-retinal and pyrrole. (Toth and Rosenberg, 1968).

(c)

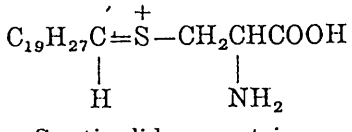

S-retinylidene cysteine

λ_{max} = 485 nm

Fig.(1.7). Models of the different postulated chromophore-protein linkages.

(a) Aldimine linkage.

(b) Enamine salt.

(c) Thioacetal bond.

are readily hydrolysed in solution and their spectral properties and thermal stability are strongly dependant upon pH. A third model proposed a thioacetal bond (Mizuno et al 1966) Fig.(1.7c), although this too did not have suitable chemical properties.

An aldimine bond is the favoured model and the discrepancies in absorbance obtained between rhodopsin and model Schiff bases was explained by invoking a secondary interaction between the chromophore and the protein. Two models were proposed:- (1) The Morton-Pitt and Kropf-Hubbard theory which considered the primary binding as a protonated Schiff base.(Morton and Pitt 1955, Kropf and Hubbard 1958). Bathochromic shifts are provided by optimally positioned negatively charged groups adjacent to the polyene chain Fig.(1.8a). The theory is that optical excitation induces a transition dipole moment along the polyene chain in which an electron moves towards the positively charged nitrogen atom, the energy of the transition being substantially lowered in a controlled fashion by properly placed negative groups. (2) The Dartnall "lock and key" theory (Dartnall 1957). This theory assumes that the primary bond linking the 11-cis retinal to the protein is an unprotonated Schiff base (Bridges 1962). Secondary binding of the polyene chain to the lipoprotein backbone is achieved by an optimally placed pair of charges which can produce massive permanent dipoles in the highly polarisable chain.

The Morton-Pitt and Kropf-Hubbard theory was later refined by Nakanishi et al (1979) who proposed the external point charge model shown in Fig.(1.9). From studies on hydro-

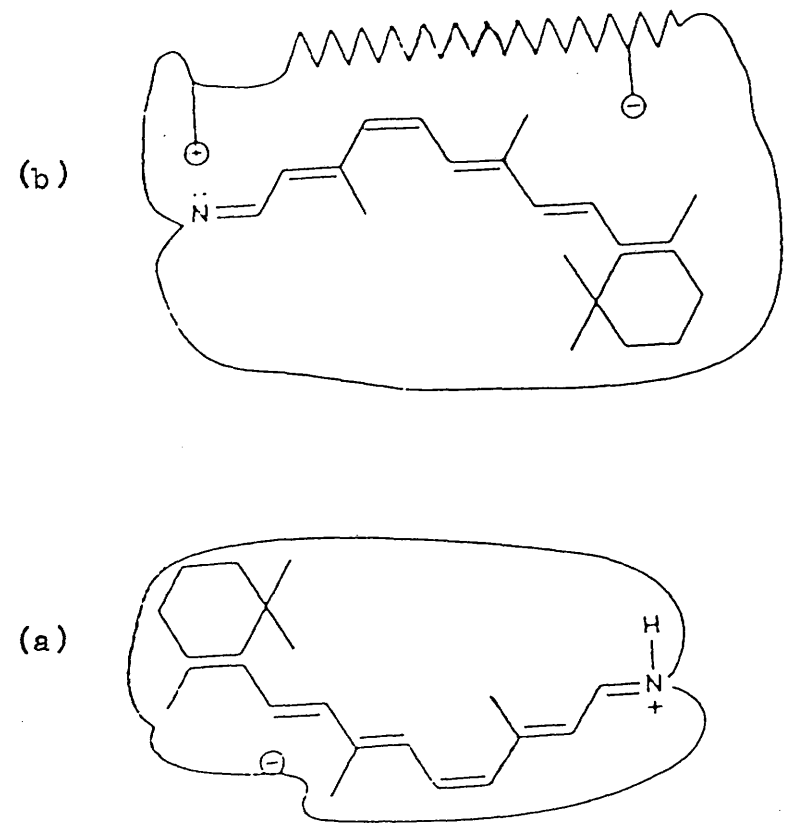

Fig.(1.8). The rhodopsin prosthetic chromophore according to:

(a) The Morton-Pitt-Kropf-Hubbard theory.

(b) The Dartnall lock and key theory.

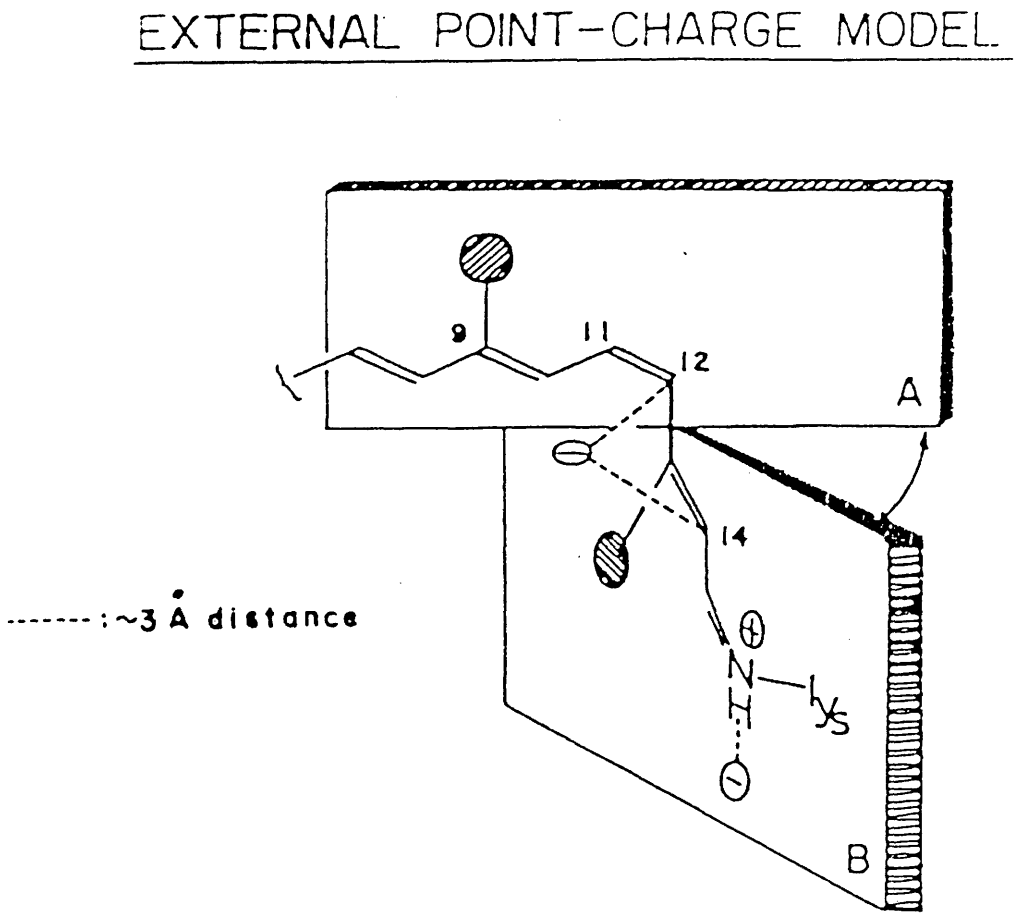

Fig.(1.9). The external point-charge model.

(Taken from Nakanishi et al 1979).

retinals prepared as Schiff bases and incorporated in to analog pigments, they concluded that there must be significant electrostatic interactions in the vicinity of the chromophoric unit of 11,12-dihydroretinal i.e. from C-13 to the nitrogen. A clear requirement of the model was that it should explain the red shift not only in artificial pigments but of rhodopsin itself. This could be obtained by placing a counterion near the nitrogen and a second negative charge between C-12 and C-14. They also proposed that the observed range of absorbance maxima in rhodopsins from different species could be obtained by variation in the position of the external charges around the chromophore.

Other evidence supporting the point charge model comes from the resonance Raman work of Eyring et al (1979) who found that interaction with a negatively charged residue (near $C_{11}=C_{12}$) could lead to the low value ($922cm^{-1}$) of the $C_{11}=C_{12}$ hydrogen out of plane bending mode in rhodopsin by reduction of the bond order.

The model can also explain the apparent inconsistency between resonance Raman experiments (Mathies 1976) supporting a protonated Schiff base and C^{13} NMR results which support an unprotonated Schiff base. Shriver et al (1977) found that the chemical shift for carbon-14 in 11-cis retinal and its Schiff base with propylamine to be 130ppm while the shift in the corresponding protonated Schiff base was at 120.1ppm. In the rhodopsin prepared from a 14-C^{13} labelled retinal, the chemical shift for carbon-14 was at 130.8ppm. The authors concluded that in rhodopsin, the Schiff base must be unprotonated.

However, the C^{13} NMR data can also agree with the existence of a protonated Schiff base linkage in rhodopsin by taking in to account the external point charge model. Calculated II-electron densities at carbon-14 are: for 11-cis retinal 77, its Schiff base 78, the protonated Schiff base 79, and rhodopsin 80 (Balogh-Nair and Nakanishi 1982). According to this calculation, the point charge close to carbon-14 could reduce the charge density at this point (by coulombic repulsion) and thus deshield carbon-14, leading to the observed value of 130.8ppm.

Photochemical response: A better knowledge of the structure of rhodopsin did not however explain how it worked. On absorption of a photon of light, rhodopsin undergoes a series of changes which can be characterised spectroscopically Fig.(1.10). In vertebrates, the sequence of changes ends with opsin plus liberated all-trans retinal. In invertebrates, the photoreaction halts at the metarhodopsin stage with the chromophore still attached. The reaction may be stopped at any of the intermediates by appropriate choice of pH and temperature and can be photoreversed to the original rhodopsin by irradiation at the appropriate wavelength.

Historically, the first of the intermediates studied were the indicator yellows. Lythgoe (1937) observed a yellow colour produced on bleaching frog rhodopsin. He also discovered that cooling the solution to 3°C produced evidence of another intermediate which he and Quilliam (1938) called transient orange, later named pararhodopsin by Wald in 1968. It is now known also as metarhodopsin III.

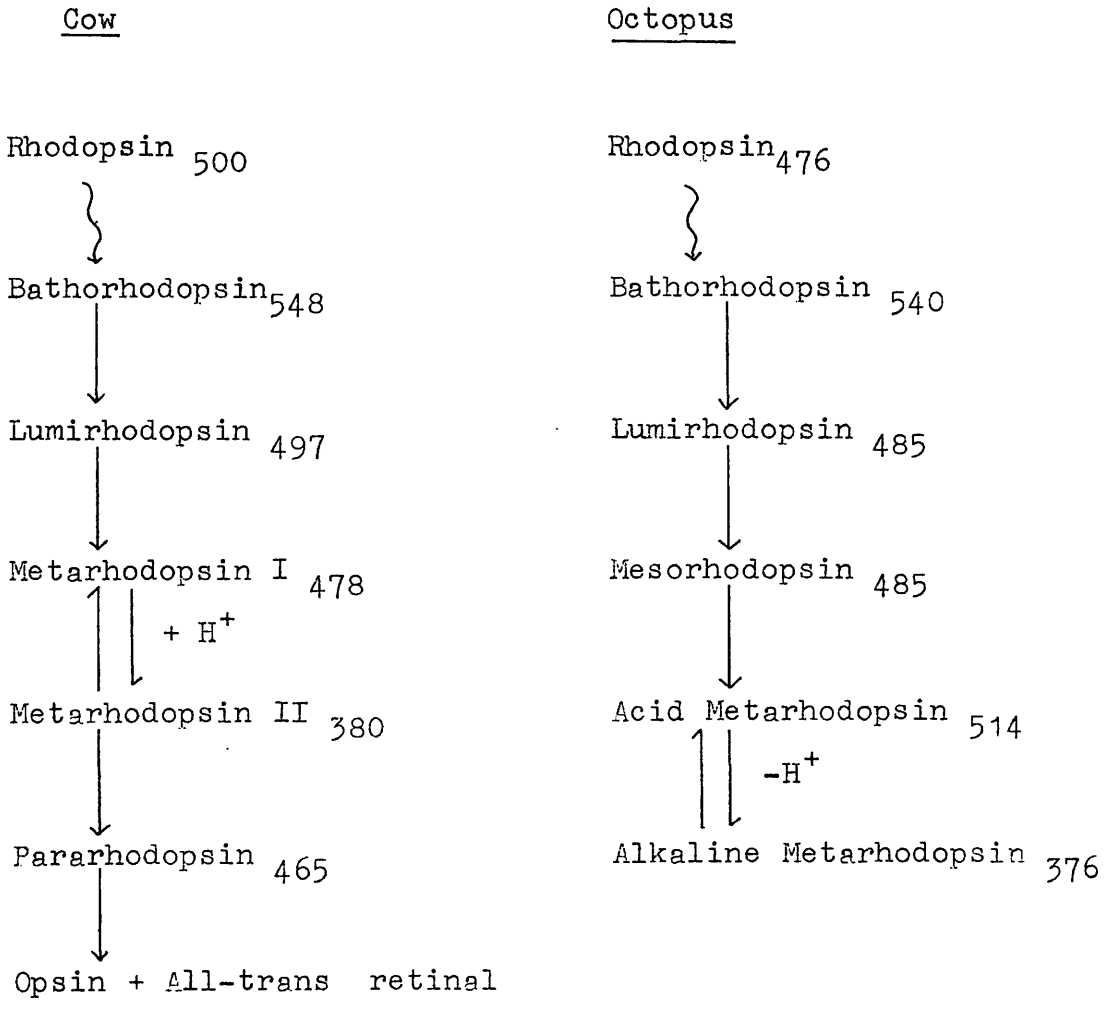

Fig.(1.10). Intermediates in the light activated absorbance changes in cow and octopus rhodopsin. The subscripts indicate the absorbance maxima (in nm) of the appropriate species.

Lumirhodopsin was first observed in 1941 by Broda and Goodeve who diluted a digitonin extracted solution of rhodopsin with three times its volume in glycerol and cooled it down to -73°C before irradiation. They mistakenly assumed however that it was the same as transient orange. It was not until 1950 that Wald, Durell and St.George reinvestigated it and discovered that it was in fact another intermediate. They also discovered metarhodopsin I by warming lumirhodopsin to -15°C.

Metarhodopsin II was first detected by Matthews, Hubbard and Wald in 1963. They showed that metarhodopsin existed in two tautomeric forms. The position of the equilibrium between the two being affected by temperature, pH, neutral salts and glycerol. Increasing any of these factors favours metarhodopsin II.

Bathorhodopsin can be trapped by cooling the solution to -190°C before irradiation. It was first observed by Yoshizawa and Wald (1963) who named it pre-lumirhodopsin. As its modern name implies, it is the only intermediate with λmax. longer than its parent rhodopsin.

For several years it was believed that bathorhodopsin formation was the primary photoreaction step, the later intermediates being thermal reactions. Later studies in 1969 (Yoshizawa and Horiuchi) found an apparent precursor to bathorhodopsin by irradiating rhodopsin at 4K. This intermediate was called hypsorhodopsin, but Yoshizawa noted that hypsorhodopsin does not necessarily precede bathorhodopsin. It may be a branching reaction (Abrahamson and Fager 1973,

or it may not be a genuine intermediate at all (Cooper 1983). Yoshizawa has also detected another possible intermediate photorhodopsin which has not been thoroughly investigated. (Yoshizawa 1984).

The invertebrate photoreaction is similar in a number of respects. It also has a bathorhodopsin and lumirhodopsin. Instead of lumirhodopsin decaying directly to metarhodopsin however, another intermediate subsequently called mesorhodopsin was detected by Tokunaga et al (1975). Also as has already been mentioned, the metarhodopsins differ from the vertebrate case. The acid $\rightleftharpoons$ alkaline metarhodopsin equilibrium would seem to correspond to simple protonation and deprotonation of a Schiff base (Hubbard and St.George 1957-58). Matthews et al (1963) found a small entropy change on going from acid to alkaline metarhodopsin which they found to be typical of deprotonation of an aldimine nitrogen atom. This is in direct contrast to the vertebrate metarhodopsin I to metarhodopsin II transition which proceeds with the uptake of a proton and a large increase in entropy.

An interesting question is which of these intermediates trigger the neural impulse ? The visual signal has to occur at or before the metarhodopsin stage since subsequent intermediates are too late to participate in visual transduction. (The neural impulse occurs within milliseconds).

The first step i.e. rhodopsin to bathorhodpsin has been explained by several theories but is now generally believed to be isomerisation about the $C_{11}=C_{12}$ bond to give a twisted

trans species (Hubbard and Kropf 1958). This will be discussed more fully in chapter three. Lumirhodopsin, metarhodopsin I and metarhodopsin II were postulated to be due to protein conformational changes, although Cooper and Converse (1976) proposed a model in which the metarhodopsin I to metarhodopsin II transition corresponded to hydrolysis of the chromophore linkage from the protein. Later intermediates i.e. para-rhodopsin and the indicator yellows received less attention since they were not involved in generation of the neural signal.

Although it is not known which of the intermediates is important, several attempts have been made to explain how rhodopsin works as a visual transducer.

Biochemical response:- How does rhodopsin activate vision? In the dark, a steady current flows through the rod cells. Sodium ions enter the the outer segments through channels in the plasma membrane in response to an ionic gradient. Inside the cell the ions diffuse to the far end where they are pumped out in a process fuelled by ATP hydrolysis. Fig(1.11).

In vertebrates when light interacts with rhodopsin, the dark current is shut down, the rods hyperpolarise and stop releasing neurotransmitter. It is not very likely that rhodopsin itself can block the channels directly for several reasons:-

1. There does not appear to be any obvious correlation between rate of change of dark current and the kinetics of the rhodopsin photocycle.
2. Rhodopsin is situated in the disc membranes which are not physically connected to the plasma membrane.

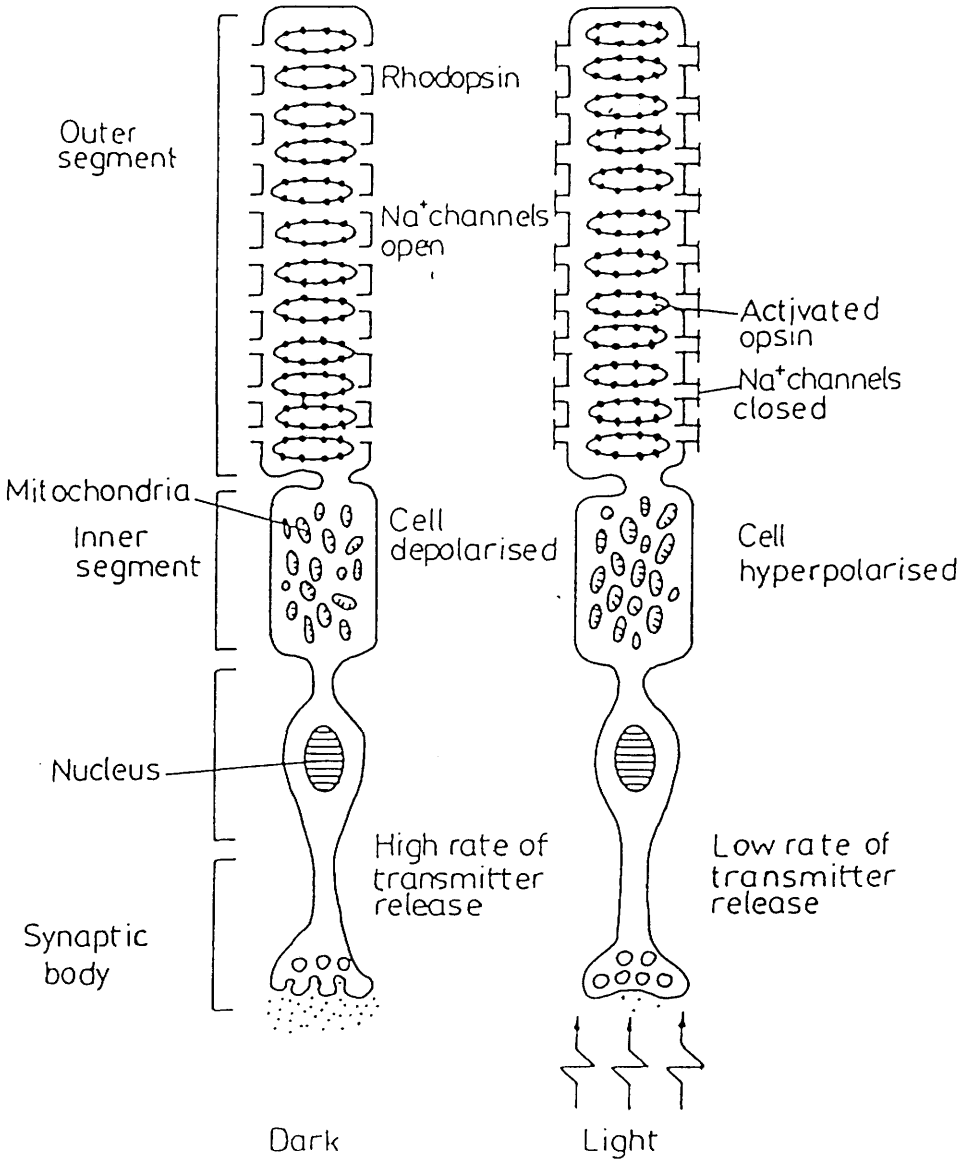

Fig.(1.11). Schematic representation of the effect of light on the rod outer segments.

(Taken from Vines 1985).

3. there is not a direct relationship between the number of rhodopsin molecules bleached and the number of channels closed. ie. Many channels are closed for every rhodopsin molecule bleached and the signal has been somehow amplified.

Any model for the transduction process in rod outer segments has to explain how the excitation of a single rhodopsin molecule in the disc membrane causes the closure of large numbers of sodium channels in the plasma membrane at some distance away. The simplest explanation of these two important features of amplification and transmission is that photoexcitation of rhodopsin leads to the release of a transmitter substance that migrates to the plasma membrane and there binds at sites of the sodium channels and causes them to close.

Hagins (1972) suggested that calcium ions are the transmitter and that rhodopsin acts as a light regulated ionic channel in the disc membrane, photoexcitation causing the release of Ca^{2+} ions in to the cytoplasm Fig.(1.12). The Ca^{2+} ions block the sodium channels causing the cell to hyperpolarise.

There has been conflicting evidence for rhodopsin acting as a channel. Downer and Englander (1977) examined the structure of rhodopsin using the tritium exchange method. The method measures the exchange of protein amide hydrogens with water and can distinguish between protons which are internally bonded from those which are hydrogen bonded to water. They discovered that 70% of rhodopsins peptides were exposed to water. This was much higher than

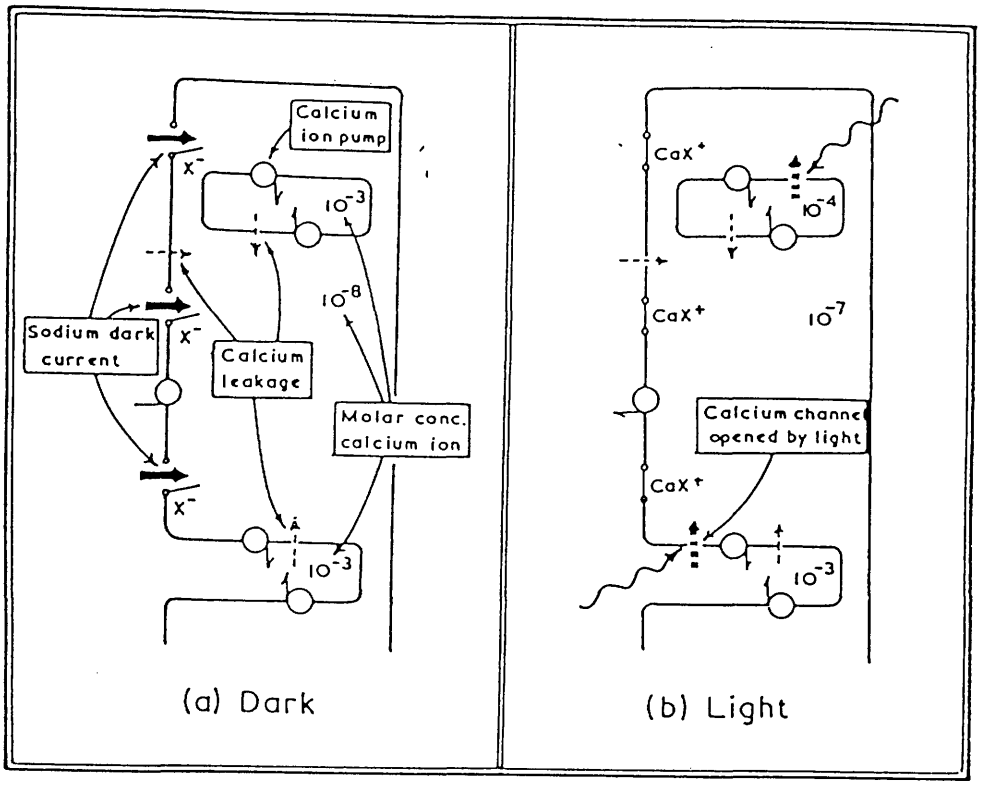

Fig.(1.12). Schematic diagram showing the proposed transmitter function of calcium ions in the vertebrate ROS. (a) In the dark-adapted rod, sodium ions flow steadily through the outer membrane in to the cytoplasm. Ionic pumps remove Ca^{2+} from the cytoplasm,passing it in to the discs or out of the cell. (b) Light causes a Ca^{2+} channel in the disc membrane to open and let ions flow in to the cytoplasm. These close sodium channels in the outer membrane, stopping the flow of sodium ions and hence reducing the dark current.

(Taken from Davson 1977).

the 20% to 40% generally found for other proteins. They suggested on the basis of this evidence that rhodopsin formed a channel 10-12 Å wide penetrating the disc membrane.

Montal et al (1977) measured the conductance of rhodopsin in planar bilipid membranes and postulated that the bilayer permeability changed on exposure to light in a pattern consistent with the formation of a channel.

Evidence against a polar channel in rhodopsin was presented by Osborne and Nabedryk-Viala (1977) who performed a deuterium-hydrogen exchange study on rhodopsin. They found that their studies suggested that rhodopsin had a considerable number of its amide protons buried in a "heart" shielded from the solvent water. They further postulated that the difference between the tritium and deuterium results were due to incomplete exchange-in of label in the tritium case and that their results were more specific for amide protons and contained no contribution from side chains. There is no conclusive evidence for or against rhodopsin acting as a channel.

The detection of a number of light-activated enzymes in the rod outer segments over the past decade has lead to the development of an alternative hypothesis based on a multistage cascade of enzyme reactions that entails a greater number of consecutive reactions. (Reviews: Zurer 1983, Knowles 1984, Kuhn 1984, Vines 1985).

In this theory, the sodium channels are held open in the dark by cyclic guanosine 3,5-monophosphate (cyclic GMP) , a nucleotide present in high concentrations in dark adapted

rod outer segments. Absorption of light by the chromophore converts rhodopsin to its "active" form which then binds to a so called G protein Fig.(1.13). This in turn activates a phosphodiesterase (PDE), an enzyme which rapidly destroys cGMP and the sodium channels close causing the cell to hyperpolarise.

The G-protein can exist in two forms, one that binds guanosine diphosphate (GDP) and one that binds guanosine triphosphate (GTP). The GDP-binding form of G-protein associates with light activated rhodopsin. However if GTP is present, a molecule of GTP exchanges for the GDP and the rhodopsin and G-protein move apart. At that point , the G-protein now with bound GTP forms a complex with PDE. By removing an inhibitor from PDE, the G-protein turns on that enzyme thus activating hydrolysis of cyclic GMP.

Amplification of the enzyme cascade occurs at two stages Fig.(1.14). Firstly, the rhodopsin molecule can activate many G-proteins and secondly, each G-protein turns on PDE's each of which can hydrolyse 2000 cyclic GMP's per second.

The cascade is turned off in two stages. Firstly, GTP bound to G-protein is hydrolysed to GDP, so the G-protein reverts to its inactive state. Secondly, another membrane protein, opsin kinase, adds phosphate groups to opsin from adenosine triphosphate. The multiply phosphorylated opsin no longer activates G-protein and once all active G-protein has reverted to the inactive state, cyclic GMP hydrolysis comes to a halt.

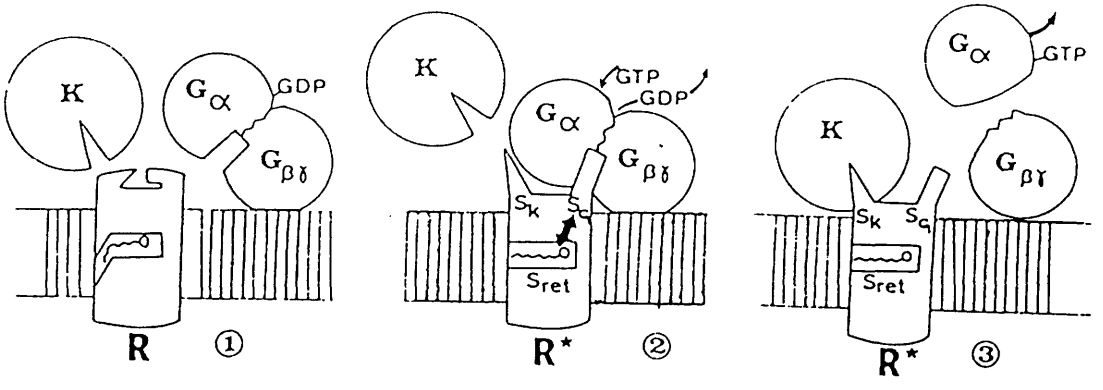

Fig.(1.13). Interaction between photoexcited rhodopsin (R^*), rhodopsin kinase (K) and GTP-binding protein ($G_\alpha G_{\beta\gamma}$).

State 1:- Dark adapted rhodopsin (R): No particular affinity for kinase or G.

State 2:- Photoexcited rhodopsin (R^*), probably meta II: the two cytoplasmic binding sites for kinase and G are exposed. G associates with its binding site S_G; steric constraints resist access of the kinase to S_K, S_{ret}, the retinal binding domain interacts with S_G stabilising MII at the cost of MI and M III as long as G is bound to S_G. If GTP is present: rapid exchange of GTP for bound GDP on G_α.

State 3:- After nucleotide exchange: G_α- GTP dissociates from R^* and from $G_{\beta\gamma}$ in to the cytoplasm. R^* is now free to bind further G molecules and catalyse their nucleotide exchange.

(Taken from Kuhn 1984).

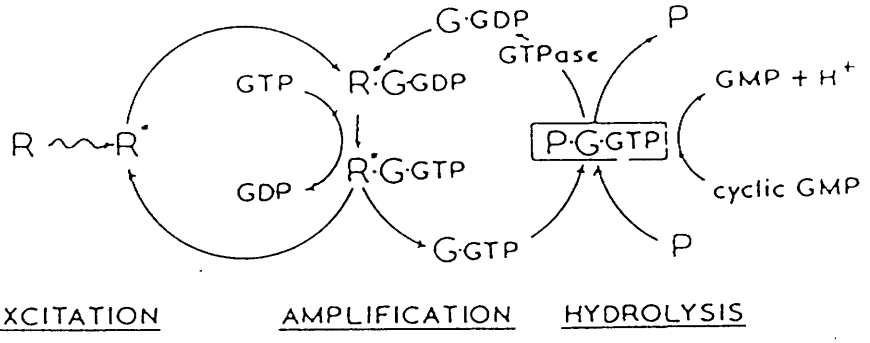

Fig.(1.14). Enzyme cascade: Amplification occurs in two stages. Firstly, each activated rhodopsin (R^*) can turn on many G-proteins and secondly, each G-protein turns on many PDE's each of which can hydrolyse 2000 cyclic GMP's per second.

What then is the role of calcium ions? Electrophysiology has shown that cGMP and Ca^{2+} modulate the Na^{+} conductance. (Brown et al 1977, Miller and Nichol 1979). This prompted Fatt (1982) to suggest that cGMP controls calcium uptake by a calcium binding protein Fig.(1.15). In his model, a group of rhodopsin molecules form a pore through the disc in response to light. This pore transmits $\sim$ 5000 Ca^{2+} ions per second and these ions diffuse to the plasma membrane and there close the sodium channels. The excited rhodopsin also activates the G-protein which in turn activates PDE and the cytoplasmic cGMP level falls. This stimulates the calcium binding protein which scavenges the Ca^{2+} from the cytoplasm thus accelerating the recovery of the receptor. Full dark adaptation would result from calcium pumps removing Ca^{2+} from the cytoplasm while the rising cGMP concentration would result in the release of bound Ca^{2+} from the cGMP.

Another theory proposed by Mueller and Pugh (1983) suggested that it was the protons produced on cGMP hydrolysis Fig.(1.16) which were important and not the level of cGMP itself. They showed that the sensitivity of the effect depended on the calcium level from which they postulated an ion exchange mechanism between the protons and bound calcium ions. The active form of rhodopsin in these theories has been postulated to be metarhodopsin II although it is not yet clear that this is so.(Bennet et al 1982, Emeis et al 1982).

The enzyme cascade also fits well with invertebrate vision. A G-protein has been detected in the photoreceptors

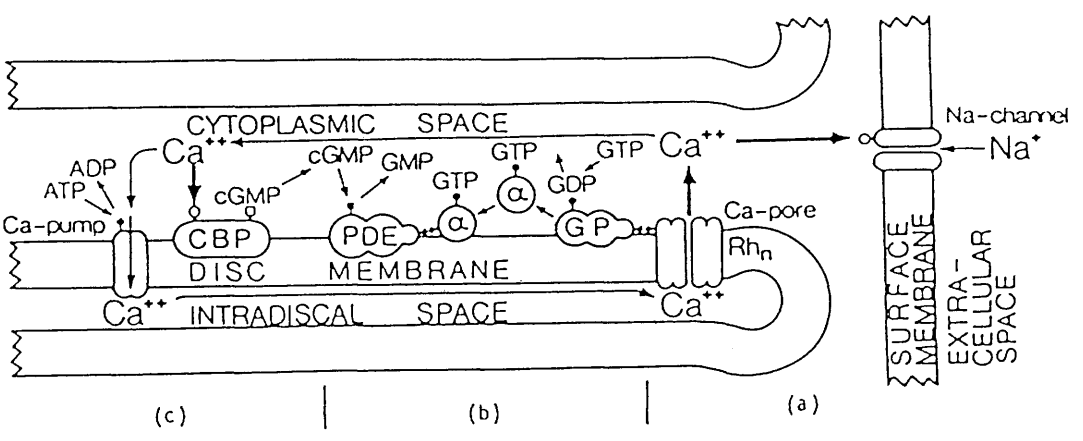

Fig.(1.15). A model for the transduction mechanism. The action of Ca^{2+} as transmitter is shown on the right hand side of the diagram (a): Activation of PDE is shown in (b); Cyclic GMP-controlled Ca^{2+} binding and the Ca^{2+} pump are in (c). Other active sites on the protein are indicated as follows: (○) site of reversible Ca^{2+} binding; (□) site of reversible cyclic GMP binding; (●) site of GTP binding and hydrolsis; (■) site of cyclic GMP hydrolysis; (◆) site of ATP hydrolysis.

(Taken from Fatt 1982).

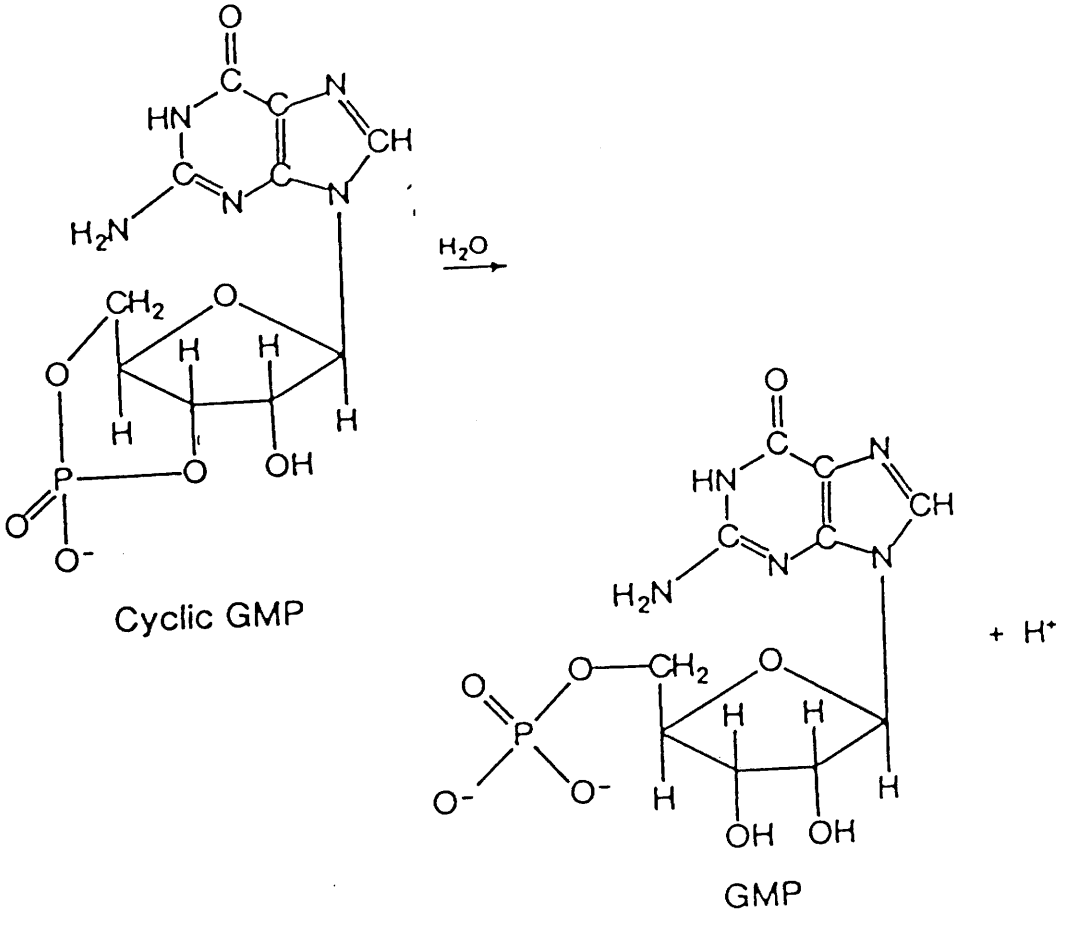

Fig.(1.16). Hydrolysis of cyclic GMP.

of squid (Saibil and Michel-Villaz 1984) and it has been found that light causes a change in the level of cGMP within the photoreceptor (Saibil 1984). In the case of invertebrates however, a rise rather than a fall of cGMP is observed. This inversion of pattern common to vertebrates makes excellent sense if both rely on the same molecular machinery, because the photoreceptors of squid depolarise when light strikes, whereas vertebrate rods hyperpolarise. The change in the electrical potential of their cells is similar in form but opposite in sign.

The mechanism of vision has still not been unambiguously identified and continues to provide a stimulating and rewarding challenge to scientists from diverse disciplines.

Investigations undertaken in this work:

The work presented in this thesis relates to physico-chemical aspects of the molecular processes involved in the rhodopsin photoreaction. The major part concerns experimental determination of the energy changes associated with the various intermediate stages of the photochemistry of octopus rhodopsin in comparison to previous studies of the bovine system. Light-induced protonation changes in octopus rhodopsin are also revealed by these and related experiments. Subsequent sections deal with measurements of the hitherto undetermined quantum yields for the reversible octopus photoreaction and examine the possibility of Schiff base hydrolysis at the metarhodopsin stage of bovine rhodopsin using isotope labelling techniques.

Chapter 2

The Energetics Of Octopus Rhodopsin

Introduction

When rhodopsin absorbs a photon of light, it undergoes a series of changes which at some point triggers the neural impulse responsible for vision. The intermediates in the sequence of changes can be characterised spectroscopically and are different for vertebrates and invertebrates Fig.(1.10). Although both visual pigments are similar in a number of respects ie. 11-cis retinal as chromophore, similar absorbance maximum, similar trend in intermediates, there are two fundamental differences.

The first is that in vertebrate visual pigments, the Schiff base bond is hydrolysed at some stage after photon absorption to give opsin plus all-trans retinal, whereas in the case of invertebrate visual pigments, the photo-reaction halts at the metarhodopsin stage. At this point the chromophore is still attached to the protein and the pigment is photoregenerable.

The second fundamental difference is also at the metarhodopsin stage. The spectrocopic pH response in the octopus metarhodopsin equilibrium is opposite to that in the vertebrate case.

Although the energetics of the photoreaction are important (Wald 1973), it is only relatively recently that the energy profile of bovine rhodopsin has been obtained (Cooper and Converse 1976, Cooper 1979a, Cooper 1979b). The energetics by themselves cannot define a mechanism for the reaction, but they provide definite

boundaries within which a mechanism may be developed.

It is of interest to measure and compare the energetics of octopus and bovine rhodopsin because they come from such evolutionary distinct species.

2.1 Materials and methods.

Dark adapted microvilli membranes isolated in Sapporo by Professor M. Tsuda from freshly obtained eyes of the edible octopus Paroctopus defleini by the method of Tsuda (1979), were frozen and shipped to Glasgow over solid carbon dioxide where they were stored at -70°C until use.

Sodium dodecyl sulphate gel electrophoresis of the microvilli showed several bands due to proteins in the range 27,000 to 88,000 A.M.U. (Appendix 1). This showed that the sample was not particularly pure in the conventional chemical sense, but is typical of intact microvilli. This is not important for the type of experiment performed here where only those molecules in the mixture which respond to light will give rise to a measurable effect. It is assumed that only the rhodopsin component of the preparation is photosensitive.

The concentration of rhodopsin and the extent of photoreaction in the calorimeter were determined spectophotometrically from optical absorbance changes (Pye-Unicam SP-1800). Molar extinction coefficients at the appropriate wavelength were taken from Tsuda et al (1982) and are as follows:- $\epsilon_R = 29700\ M^{-1}cm^{-1}$, $\epsilon_{\text{acid meta}} = 43500\ M^{-1}cm^{-1}$, $\epsilon_{\text{alkaline meta}} = 47800\ M^{-1}cm^{-1}$. The relative absorbances of the three species is shown in Fig.(2.1).

For measurement of spectral changes in membrane suspensions, the sample cuvette was placed in the secondary (scattering) cell position adjacent to the face of the photomultiplier and the reference cell was orientated with

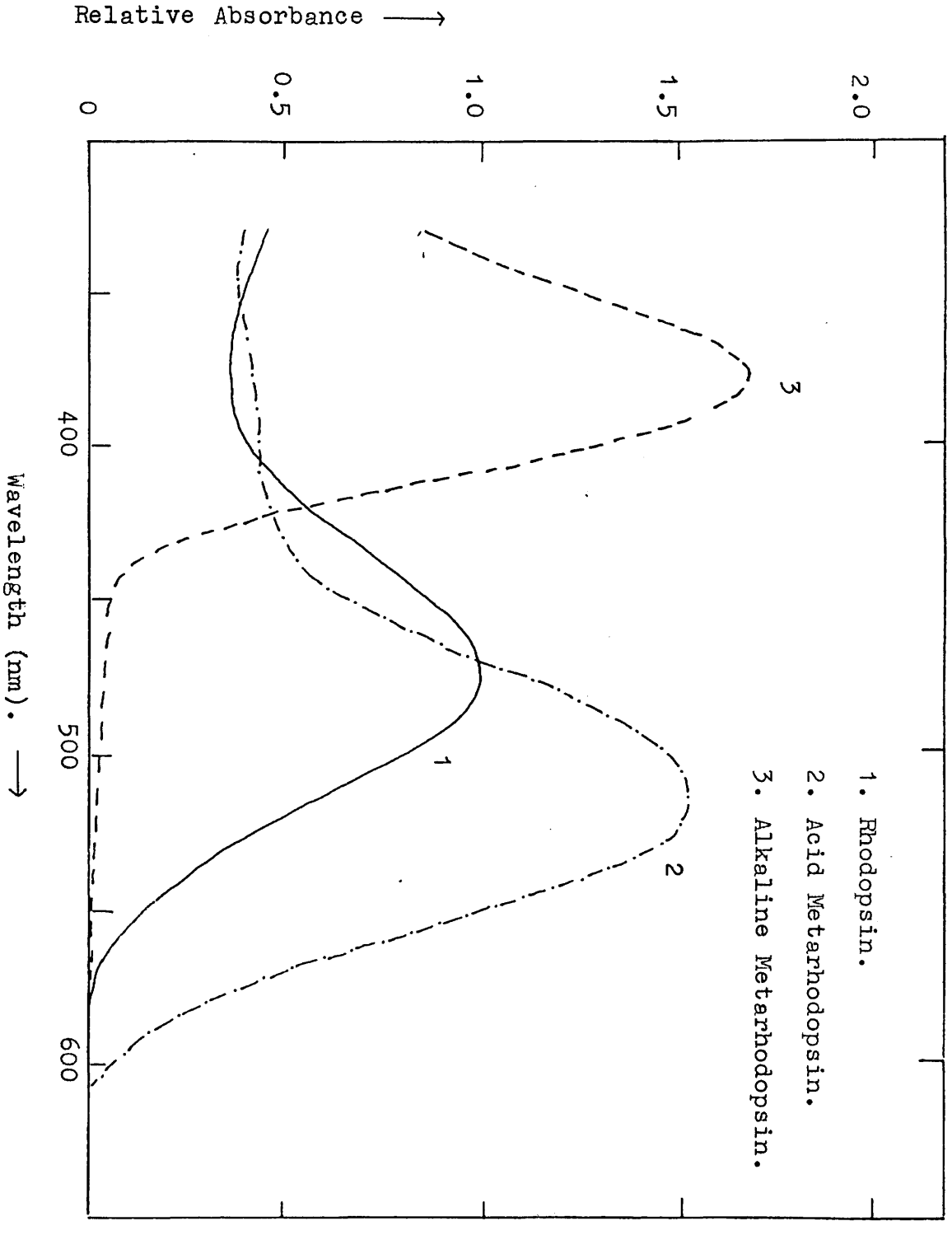

Fig.(2.1). Relative absorbances of rhodopsin, acid metarhodopsin and alkaline metarhodopsin.

(Taken from Tsuda et al 1982).

the ground glass face in the light path to compensate for scattering. Measurements of L1690 detergent-extracted rhodopsin were also performed in the secondary position with a corresponding detergent reference.

Samples for calorimetry were prepared as follows:- The membranes were sedimented at 18,000 rpm, 5°C on an MSE 18 centrifuge. The supernatant was removed and the pellet was resuspended in the appropriate buffer. The procedure was repeated and this time the pellet was resuspended in the appropriate buffer or detergent mixture. This procedure removed or at least greatly diluted any other buffers or salts present.

All manipulations were carried out in the dark or under dim red light unless otherwise specified, and samples for low temperature studies also contained glycerol in proportion 2:1 by volume. Detergent-extracted rhodopsin solutions were clarified by further centrifugation after extraction.

Sonicated membrane samples were prepared by cooling the rhodopsin in ice and sonicating it with an Ultrasonic probe sonicator for ~30s.

The sucrose lauryl ester L1690 was a kind gift of the Ryoto Company Ltd. (Tokyo). This is one of the few detergents capable of solubilising octopus photoreceptor membranes whilst maintaining the integrity of the rhodopsin. Trials carried out using Emulphogene, Triton X100, Tween 80, Ammonyx LO and sodium dodecyl sulphate detergents showed rapid rhodopsin denaturation and these detergents were

obviously unsuitable for use with octopus rhodopsin.

Trizma HCl and Trizma base were from the Sigma Chemical company, imidazole and ethylene diamine dihydrochloride were from BDH, sodium orthophosphate, sodium dihydrogen phosphate and sodium tetraborate were from May and Baker, butylamine was from Koch-Light and was redistilled before use and sodium chloride was from Formachem.

The buffer concentrations were normally 0.1M with 0.3M sodium chloride to maintain ionic strength. Glass distilled water was used throughout.

2.2 Photocalorimetry

The photocalorimeter was that designed and described by Cooper (1982). It is shown schematically in Fig.(2.2). Light from a Xe/Hg arc lamp travels through a monochromator and down fibre optic light guides in to the sample cell. The design is such that all light entering the sample is absorbed by either the sample or the walls of the container. The heat evolved by the reaction vessel is conducted through a thermopile to a comparitively large surrounding heat sink. The voltage generated by the thermopile is proportional to the temperature difference across it which in turn is proportional to the heat generated by the sample. Thus after appropriate calibration, integration of the output voltage over the period of the reaction gives the total heat of reaction.

ie. Rate of heat transfer across the thermopile is :-

$$\frac{dQ}{dt} = K_1 \Delta T$$

Thermopile voltage, $V = K_2 \Delta T$

$$\frac{dQ}{dt} = K_3 \cdot V$$

$$\text{and total } Q = \int_0^\infty \frac{dQ}{dt}\, dt = K_3 \int_0^\infty V\, dt$$

where K_1, K_2, K_3 are instrumental constants.

Dual reaction vessels with the thermopiles connected in opposition are used so as to minimise the effects of

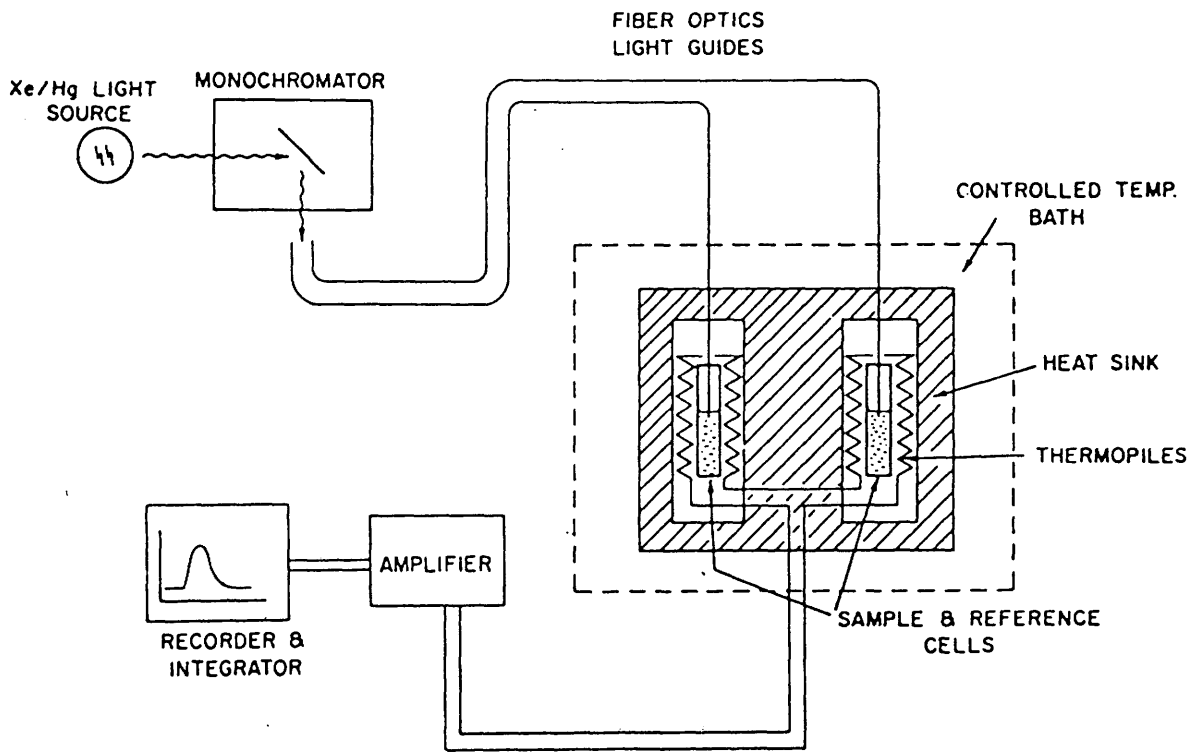

Fig.(2.2). Schematic layout of photocalorimeter system.

thermal fluctuations within the system.

The output voltage of the calorimeter thermopiles is connected to a Keithley Model 149 microvoltmeter (usually used at 10 μV or 30 μV full scale) and thence to a chart recorder connected to an electronic integrator with print out. The instrument is calibrated electronically and checked using the potassium ferrioxalate actinometry system (Hatchard and Parker 1956). (See section 2.4).

The total energy flux in the reaction vessels of this instrument can be measured with a precision of 1-2% and overall heat effects as low as 0.2 mJ can be detected. With the lamp used, illumination in the reaction vessel corresponds to energy fluxes in the range 0.01-0.30 mW depending on the wavelength. This means that for samples with a reasonably high quantum efficiency, irradiation times of a minute or so are generally sufficient to give a significant amount of photochemical reaction and that enthalpies of these reactions may be determined with a precision of $\pm$ 5KJmol^{-1}.

In the photocalorimeter, reactions are initiated by irradiating the sample with light of the appropriate wavelength. In the case of an inert sample all the light energy is converted to heat and the calorimeter measures merely the total light energy flux in to the cell. If however the light energy induces a photochemical reaction in the sample, one observes an additional heat of reaction over and above the energy of the incident light itself. Thus by comparison of the photochemically active sample with some suitable inert reference and by determining the

extent of the light induced reaction, it is possible to measure directly the absolute enthalpy of the reaction.

In a typical experiment, a known volume of rhodopsin solution is loaded in to the calorimeter and after a period of equilibration, is irradiated repeatedly with identical 2 minute bursts of light applied at regular intervals. The wavelength of irradiation depends on the experiment being performed. The output obtained is of the form shown in Fig.(2.3). The total energy in each pulse may be obtained by integrating the peaks, and since any reaction takes place within the first one or two peaks, subtraction of the earlier peak areas from the average of later peak areas allows estimation of the energy changes due to photochemical changes.

The peak areas were estimated by entering the integrator output in to an Apple computer and applying a peak integration program written specially for the purpose. In the program, a best fit line is drawn through the pre- and post-peak data to correct for instrumental drift, and this is used as the base for each peak.

Low temperature measurements were made by suspending the calorimeter over liquid nitrogen in a stainless steel dewar vessel fitted with a cryogenic level controller to maintain the liquid nitrogen level over a period of days to weeks. The layout of the liquid nitrogen calorimeter arrangement is shown in Fig.(2.4).

Experiments performed at 5°C were performed with the calorimeter immersed in a thermostatted bath. Control of temperature was achieved as in Fig.(2.5). The calorimeter was immersed in a water filled tank which was itself seated

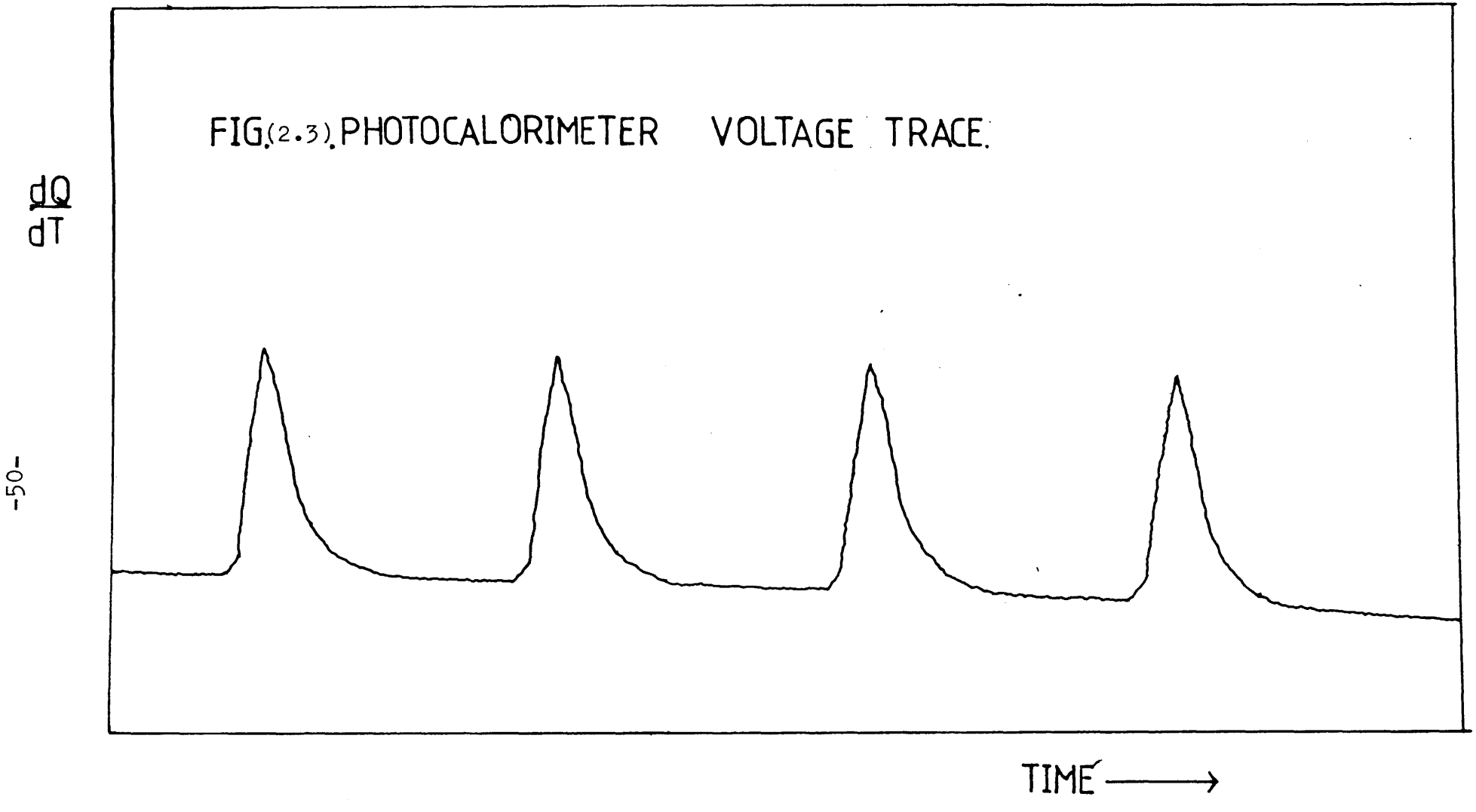
FIG.(2.3). PHOTOCALORIMETER VOLTAGE TRACE.
dQ/dT
TIME

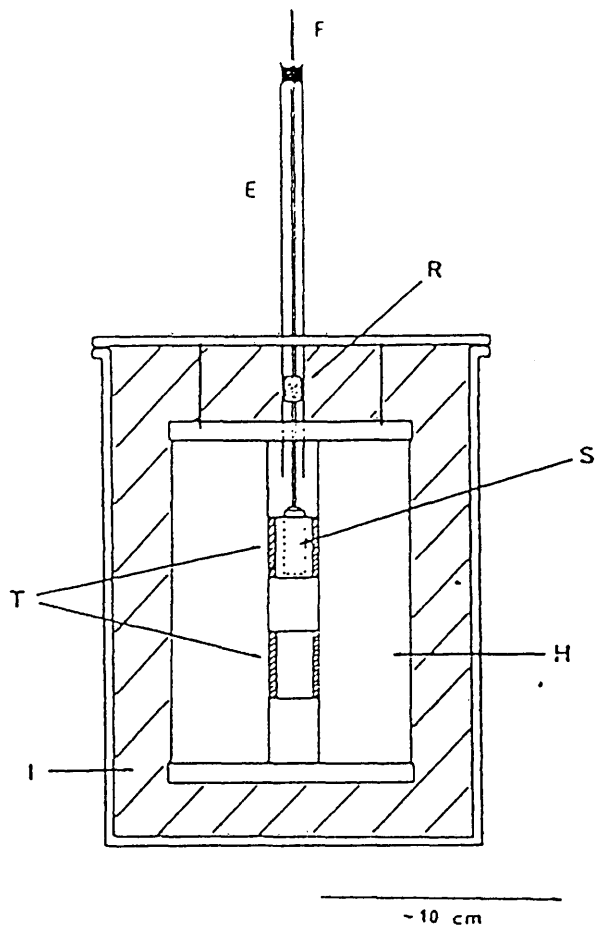

Fig.(2.4). Low temperature photocalorimeter. The sample is enclosed in a cylindrical gold-plated, stainless steel cell (S) fitted with flexible fibre-optics light guides (F) for illumination. A coaxial thermal radiation shield (R) minimises thermal leakage down the sample entry tube (E). The thermo-electric sensors (T) are solid-state Peltier cooling devices, the output of which is proportional to the rate of heat flow between the sample block and heat sink (H). Insulation (I) is with expanded polystyrene foam. The entire unit was suspended in a liquid nitrogen Dewar vessel.

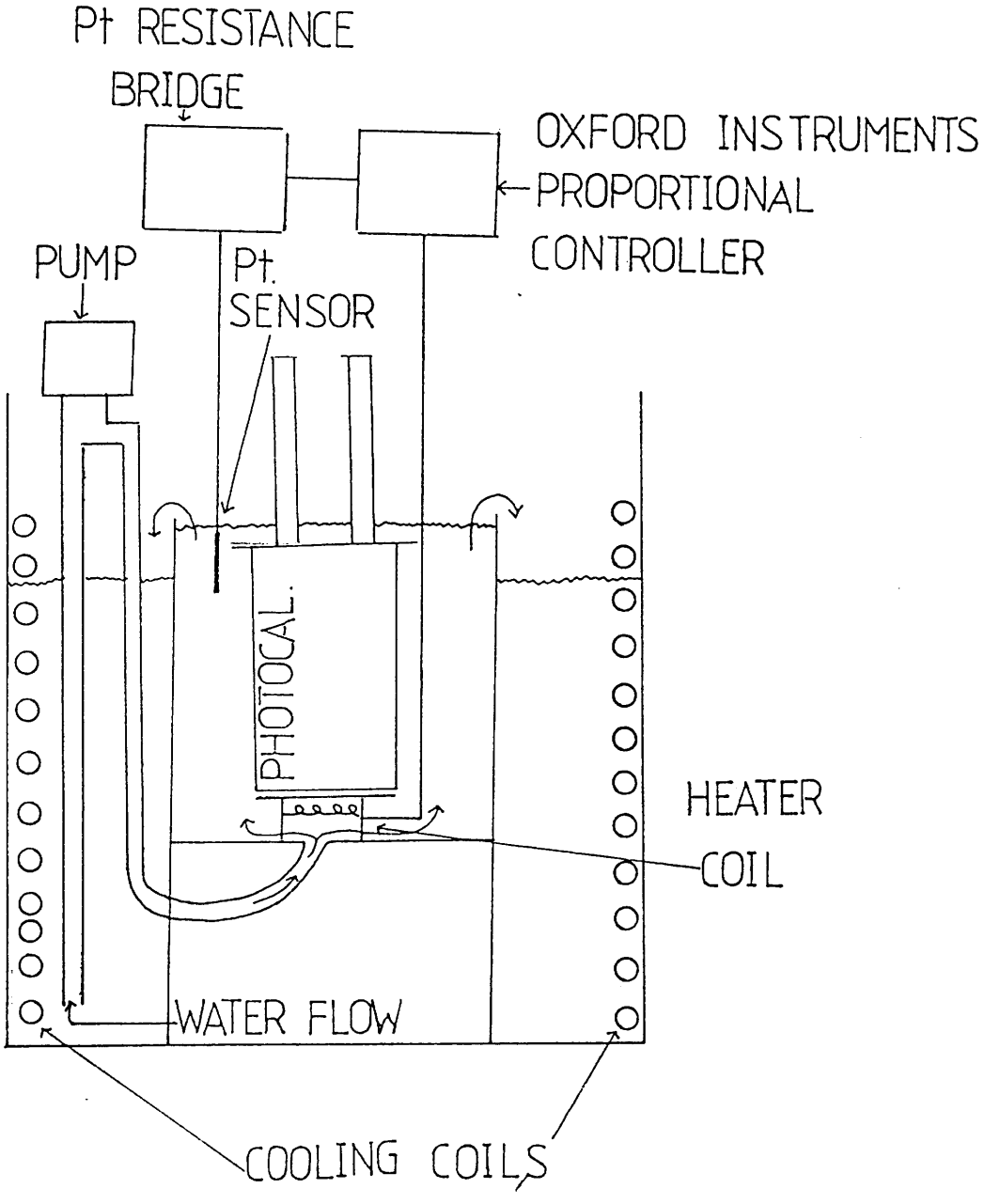

Fig.(2.5).Photocalorimeter arrangement for experiments performed at 5 °C.

in a bigger tank. The pump took water from the bottom of the larger tank and pumped it through a hole in the smaller tank, up past the calorimeter and over the top back to the larger tank. Crude temperature control was achieved from the copper cooling coils circulating H_2O at 5°C from a Landa refrigerator unit. Fine control was achieved using a platinum resistance thermometer. Small temperature changes detected by the sensor are passed through the bridge and used by the Oxford Instruments proportional conroller to switch a small heater coil on or off. The heater coil is mounted directly below the calorimeter to have the most direct effect. In this manner temperature control of $\pm$ 10^{-4}°C, or better could be achieved at the calorimetric unit, with negligible long term drift.

2.3 Electrical calibration of photocalorimeter.

Before commencing any experiments using the photocalorimeter, it is necessary to obtain a relationship between the voltage output on the chart recorder and the heat flow across the thermopiles (ie. K_3 in section 2.2). This is achieved by passing different currents through heaters mounted in the calorimeter for a fixed period of time. Since the resistance of the calibration heaters is known and since $E = I^2R$, it is possible to plot a calibration graph of energy (for different values of I) against integrated voltage response. The integrated voltage response is calculated by an integrator attached to a chart recorder and thus the voltage response is expressed in arbitrary integrator units (I.U.).

The calibration graph gives a line of gradient J/I.U., the calibration factor. Fig.(2.6) shows a typical calibration line, plotted in this case for $T=20^{\circ}C$.

The thermopile response varies with temperature, so it is necessary to repeat the calibration for each temperature used. A graph of calibration variation with temperature is shown in Fig.(2.7).

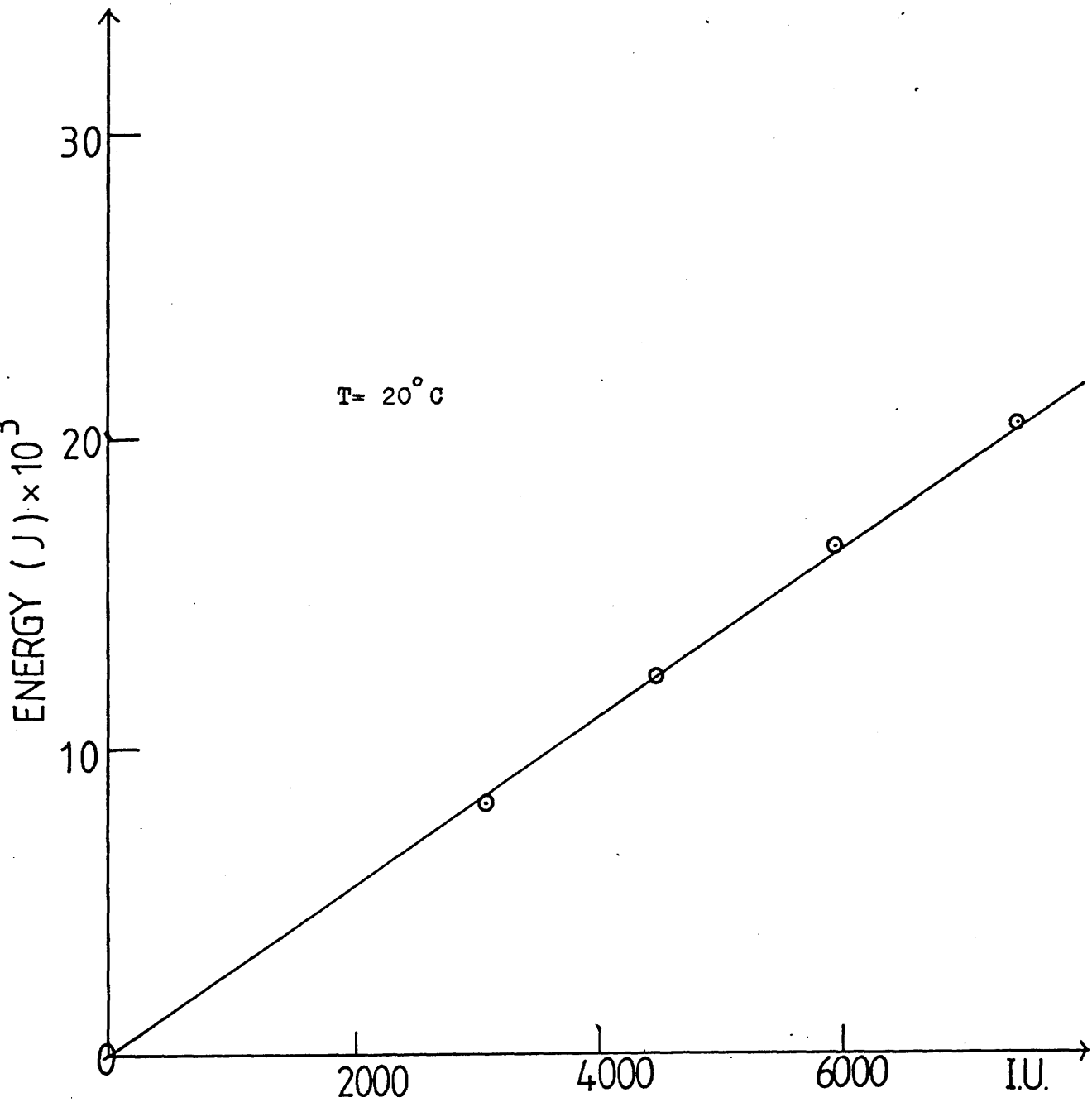

Fig.(2.6).Typical calibration graph for photocalorimeter.

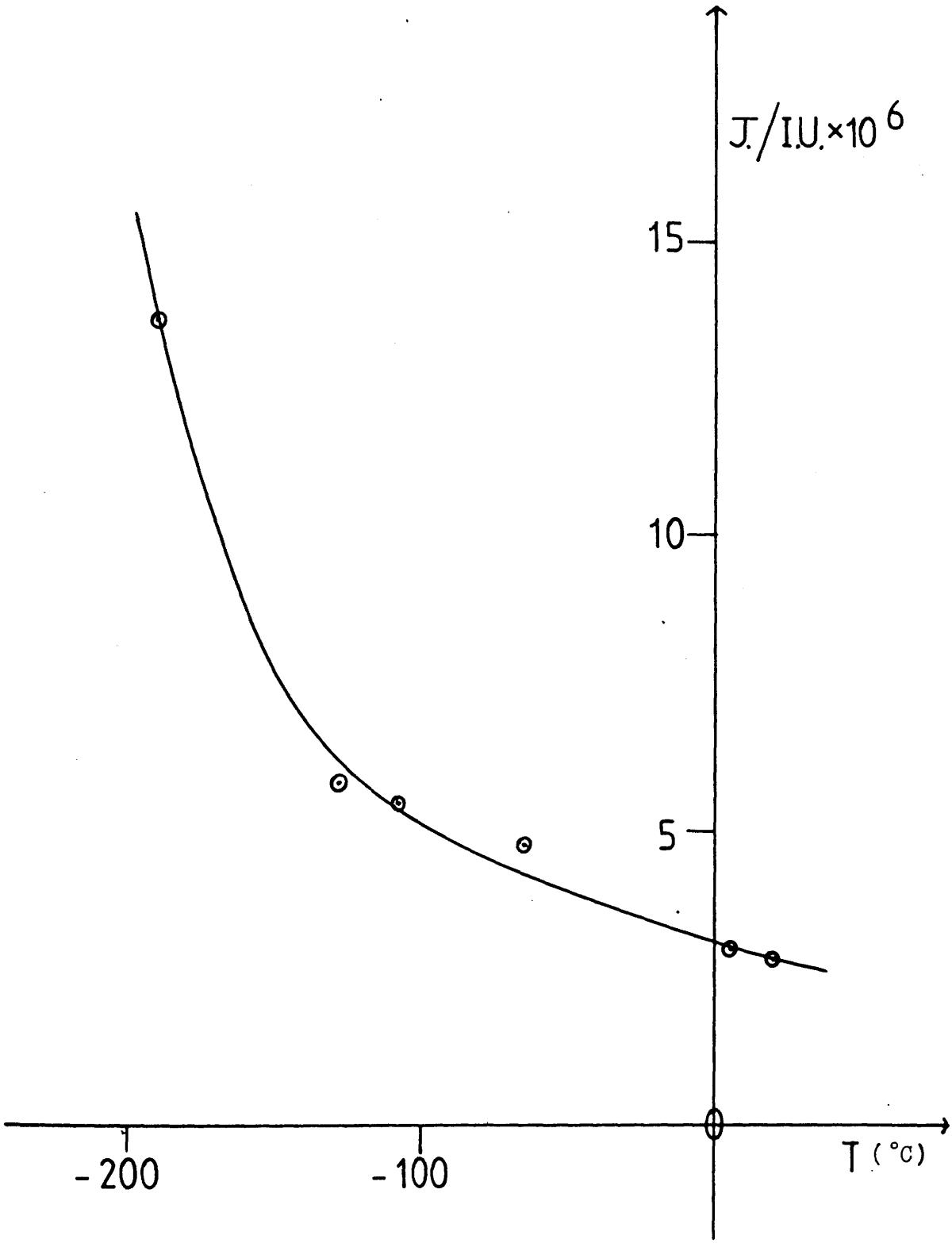

Fig(2.7). Variation of calorimeter voltage output with temperature.

2.4 Accuracy of photocalorimeter using the standard potassium ferrioxalate reaction.

The accuracy of the photocalorimeter system was tested using potassium ferrioxalate as a chemical actinometer (Hatchard and Parker 1956). This system was chosen since it is a relatively simple photoreaction which has a high quantum yield in the visible region. It also has a known enthalpy of reaction (Cooper and Converse 1976). The overall reaction may be written :-

$$2Fe^{3+} + C_2O_4^{2-} \longrightarrow 2Fe^{2+} + 2CO_2$$

The extent of reaction was followed by measuring the amount of ferrous ions produced. This was detected by complexing the Fe^{2+} produced with o-phenanthroline to produce a red coloured solution with an absorbance maximum at 510nm. A calibration graph was prepared prior to the experiment using standard iron sulphate solutions. A series of solutions were made up with a different concentration of Fe^{2+}:-

Flask	1	2	3	4	5	6	
Fe^{2+}(1mM)	0	0.3	0.6	0.9	1.2	1.5	ml
o-phen.	1.0	1.0	1.0	1.0	1.0	1.0	ml
buffer	1.5	1.5	1.5	1.5	1.5	1.5	ml
H_2O	7.5	7.2	6.9	6.6	6.3	6.0	ml

A calibration graph of A_{510} versus $[Fe^{2+}]$ was plotted Fig.(2.8). In a typical experiment, 1.5ml of 0.15M potassium ferrioxalate in 0.1N H_2SO_4 is loaded in to the calorimeter

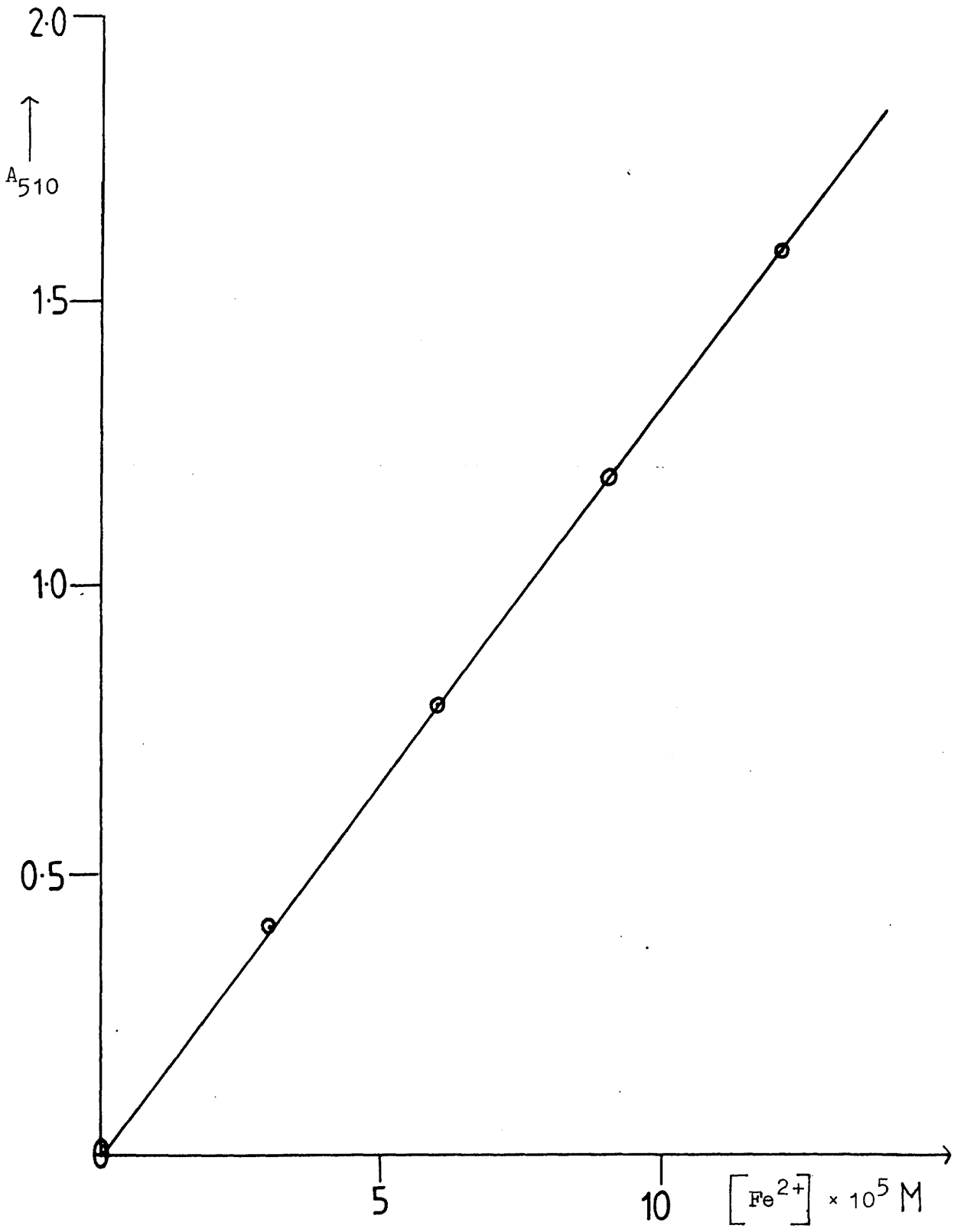

Fig.(2.8). Calibration graph of A_{510} versus $[Fe^{2+}]$.

and irradiated at 440nm. As can be seen in Fig.(2.9), the heat effect on irradiation of ferrioxalate is at all times greater than that due to the light energy alone, and corresponds to an additional light induced exothermic reaction.

The extent of the reaction is determined by taking 1ml of the solution, adding 1ml of 10% o-phenanthroline, 1.5ml of H_2SO_4/sodium acetate buffer and making up to 10ml with H_2O. After allowing it to develop for 30 minutes, A_{510} is measured. A reference solution is prepared in the same way using unexposed potassium ferrioxalate. For a typical experiment:-

$$A_{510} = 0.126$$

$$\therefore \left[Fe^{2+}\right] = 9.47 \times 10^{-6} M$$

$\therefore$ number of moles of Fe^{2+} produced in 1.5ml $= 1.42 \times 10^{-7}$

Energy due to reaction $= -6.93 \times 10^{-3}$ J

$\therefore$ Enthalpy of reaction $= -48.80$ KJ/mole

This agrees well with the enthalpy estimated from the heats of reaction of reactants and products :- -47.28 KJ/mole (Cooper and Converse 1976).

The potassium ferrioxalate system can in addition be used to check the photic efficiency of the photocalorimeter since the quantum yield of the reaction is accurately known.(1.01 at 440nm).

$$\text{Quantum Yield} = \frac{\text{number of chromophores affected}}{\text{number of quanta absorbed}}$$

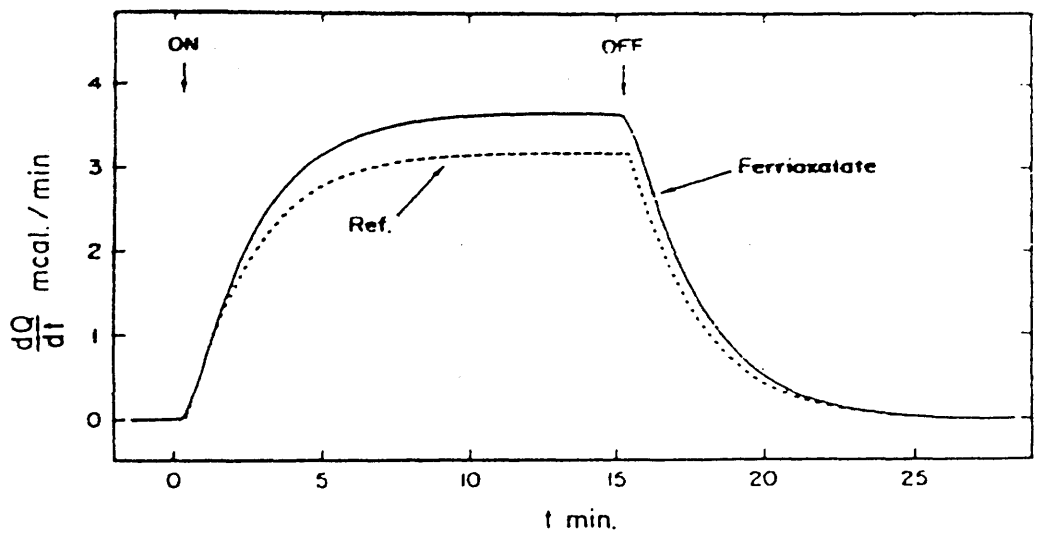

Fig.(2.9).Photocalorimeter voltage traces, converted to heat output rate, of 15-min irradiations of a potassium ferrioxalate solution and of an inert reference , at 436 nm, 25°C. Two separate experiments are shown superimposed.The difference in area of the two curves, obtained by integration, gives the total photochemical heat of reaction which is exothermic in this case.

Thus expected number of moles of photons incident = 1.41×10^{-7}.
Actual number of moles of photons incident = 2.00×10^{-7}.
Thus only 70% of the light energy entering the photocalorimeter is available for photochemistry. The remaining 30% appears to be dissipated as heat in the cell walls and in the end of the optical fibres.

2.5 Rhodopsin calorimetry.

As was mentioned in the introduction, when octopus rhodopsin absorbs a photon of light, it undergoes a series of changes halting at the metarhodopsin stage. It is possible to trap each of these intermediates in the calorimeter by suitable choice of temperature and pH.

The first intermediate, bathorhodopsin is trapped at -197°C, using the low temperature arrangement for the photocalorimeter described in section (2.2). At this temperature, it is necessary to use a detergent extract of rhodopsin and mix it 1:2 with glycerol so that the sample forms a reasonably transparent glass. Preliminary experiments showed that if membranes alone were used, light scattering at the surface of the sample would not allow sufficient light in for a measurable amount of reaction to occur. Light scattering occurs due to original membrane turbidity plus the appearance of freeze fractures at low temperatures.

The lumirhodopsin and mesorhodopsin intermediates, trapped at -118°C and -65°C repectively are measured using the same arrangement as that for bathorhodopsin by allowing the calorimeter to warm up from liquid nitrogen temperature. This works well for the lumirhodopsin intermediate since the temperature changes very slowly around -120°C. For the mesorhodopsin however, the temperature change is much more rapid. This results in two problems: 1. The baseline drift is so rapid that only one or two irradiations can be performed before it is necessary to adjust the pen to zero and obtain a fresh baseline. This repeated adjustment

increases the duration of the experiment. Secondly, the calibration factor of the calorimeter varies over the period of the experiment and an average of the pre- and post experiment calibration peaks has to be used. For these reasons, the value of the rhodopsin to mesorhodopsin enthalpy is very tentative.

The acid and alkaline metarhodopsin intermediates were measured both at 5°C and 20°C. Detergent-extracted samples and sonicated membrane preparations were used to see if any differences were obtained.

The acid metarhodopsin was obtained by preparing the rhodopsin sample in pH 7 buffer. The alkaline metarhodopsin was obtained by preparing the rhodopsin sample in a high pH buffer, range pH 9.5-10.5.

For the regeneration reaction, acid metarhodopsin to rhodopsin, a detergent-extracted sample of rhodopsin in pH 7 buffer was irradiated at 460nm in the dark with stirring to give as much acid metarhodopsin as possible. This was then loaded in to the calorimeter and irradiated at 540nm.

The bathorhodopsin to rhodopsin experiment was performed in the same arrangement as the forward reaction. A sample of rhodopsin was irradiated for sufficient time to give bathorhodopsin. This was then regenerated in situ using λ=550nm. The amount of bathorhodopsin present at the start of the regeneration experiment was estimated from previous forward reactions.

In all experiments, the irradiation wavelength was

chosen to reduce the possibility of any backward reaction eg. since rhodopsin ($\lambda_{max.}$ 480nm) and acid metarhodopsin ($\lambda_{max.}$ 520nm) have absorbance spectra which overlap, irradiation of rhodopsin gives an equilibrium of rhodopsin and acid metarhodopsin. Irradiation of the sample at 460nm however, reduces the extent of acid meta regeneration and shifts the equilibrium towards acid metarhodopsin.

2.6 Results.

The consistent observation throughout these calorimetric measurements was that irradiation of octopus rhodopsin always resulted in an uptake of energy, regardless of the intermediate being produced. In other words, all photoreactions of this rhodopsin are endothermic. This is illustrated in Fig.(2.10) for the rhodopsin to bathorhodopsin and rhodopsin to metarhodopsin reactions, where it can be clearly seen that earlier irradiations result in a lower integrated calorimetric response compared to the later irradiations of the now photoequilibrated mixtures. Details of the experimentally determined enthalpies under various conditions are given in Table 2.1 and summarised in Table 2.2.

Confirmation that this energy uptake is directly related to the rhodopsin photoprocess comes from photoreversal experiments in which regeneration of the original pigment rhodopsin from either bathorhodopsin or metarhodopsin intermediates is exothermic, releasing the photochemically stored energy.

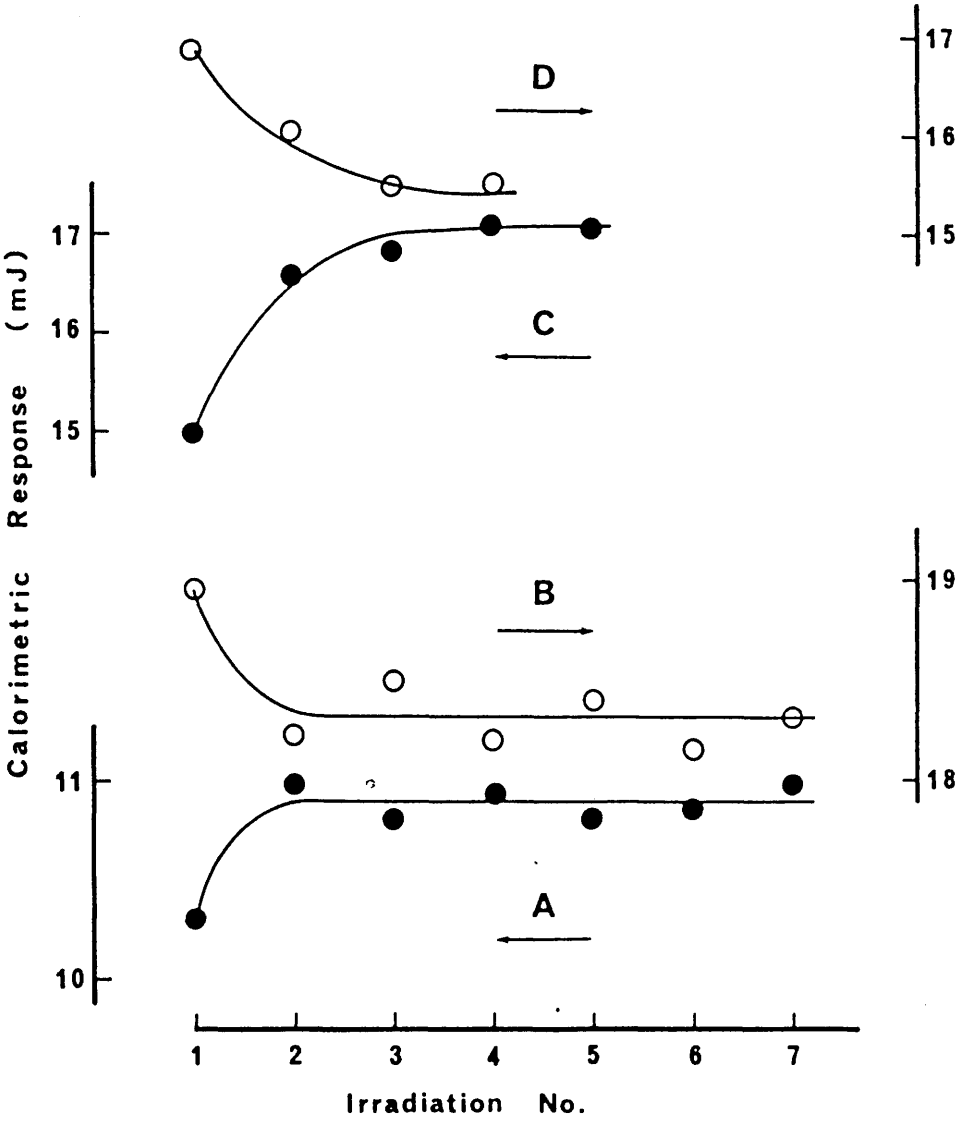

Fig.(2.10).Calorimetric response versus irradiation number.

Curves A and B are the forward and backward reactions for rhodopsin to acid metarhodopsin.

Curves C and D are the forward and backward reactions for rhodopsin and bathorhodopsin.

Table 2.1 : Measured enthalpies of reaction.

Reaction	Measured Enthalpy (KJ/mole)	Ave. ΔH	S.D.
rhodopsin to bathorhodopsin	130.50 130 42 130.62	130.51	0.13
rhodopsin to lumirhodopsin	49.04 51.71 58.99	53.25	5.15
rhodopsin to mesorhodopsin	18		10
rhodopsin to acid meta-rhodopsin (a)Phosphate buffer	20.29* 16.25* 20.77* 22.26 28.51 13.89* 15.15	19.59	3.97

* All enthalpies marked with an asterix were measured in membrane samples. The other enthalpies were obtained from detergent-extracted rhodopsin.

Table 2.1 continued:-

Reaction	Measured Enthalpy (KJ/mole)	Ave. ΔH	S.D.
rhodopsin to	27.64*		
acid meta-	21.95*		
rhodopsin	19.16*		
(b)Ethylene	14.60	17.3	5.15
diamine buffer	17.95		
	10.33		
	13.93		
	12.82		
rhodopsin to	14.73*		
acid meta-	15.69*	18.38	7.45
rhodopsin	24.71		
(c) Imidazole			
buffer			
rhodopsin to	57.03*		
alkaline meta-	62.72*	53.78	7.99
rhodopsin	46.78*		
(a)Borate	48.58*		
buffer			

Table 2.1 continued:-

Reaction	Measured Enthalpy (KJ/mole)	Ave. ΔH	S.D.
rhodopsin to alkaline meta (b)Ethylene diamine buffer	31.13* 23.97*	27.55	5.06
rhodopsin to alkaline meta (c)Tris buffer	10.92 5.61	34.58	3.77
rhodopsin to alkaline meta (d)Butylamine buffer	12.43		5
bathorhodopsin to rhodopsin	147.72 117.57 119.59	128.29	16.85
acid meta to rhodopsin	37.24 27.91 30.42	31.86	4.83

Table 2.2. Summarised results of calorimetrically determined enthalpies of formation of octopus rhodopsin photoproducts.

Rhodopsin to:	Temperature °C	ΔH (S.D.) KJ/mole
Bathorhodopsin	-195	130.5 (8.4)
Lumirhodopsin	-115	53.3 (5.2)
Mesorhodopsin	- 65	18 (10)
Acid Metarhodopsin	5	17.4 (7.8)
	5 - 20	19.6 (7.0)
Alkaline Metarhodopsin	5 - 20	68.9 (4.1)

Bathorhodopsin to:		
Rhodopsin	-195	128.3 (4.83)

Acid Metarhodopsin to:		
Rhodopsin	5	31.8 (4.8)

As can be seen from the results, variation of buffer showed that the reaction rhodopsin to acid metarhodopsin was independent of buffer used whereas in contrast, rhodopsin to alkaline metarhodopsin depended markedly on the heat of protonation of the buffer used. This indicated that no change of protonation was involved in the former reaction but that some protonation change was involved in the latter.

The variations observed in the enthalpies of the rhodopsin to alkaline metarhodopsin reaction are due to the fact that in a well buffered system, any protonation changes in the reaction leads to protonation changes in the buffer with subsequent secondary heat effects. The energy detected by the calorimeter is the sum of the reaction enthalpy plus buffer effects. It is possible to calculate the enthalpy of the rhodopsin to alkaline metarhodopsin reaction in the absence of buffer effects by plotting a graph of $\Delta H_{observed}$ versus $\Delta H_{protonation}$ of buffer and extrapolating the line to $\Delta H_p = 0$. The gradient of the line gives an indication of the number of protons (n), abstracted from the buffer in the reaction (equation 2.1):-

$$\Delta H_{obs.} = \Delta H_{reaction} + n \Delta H_p \quad \text{----------2.1}$$

From the graph Fig.(2.11), the enthalpy of the reaction can be seen to be 68 ± 4 KJ/mole with $n = -0.91 \pm 0.09$

ie. Approximately one hydrogen ion is released by the

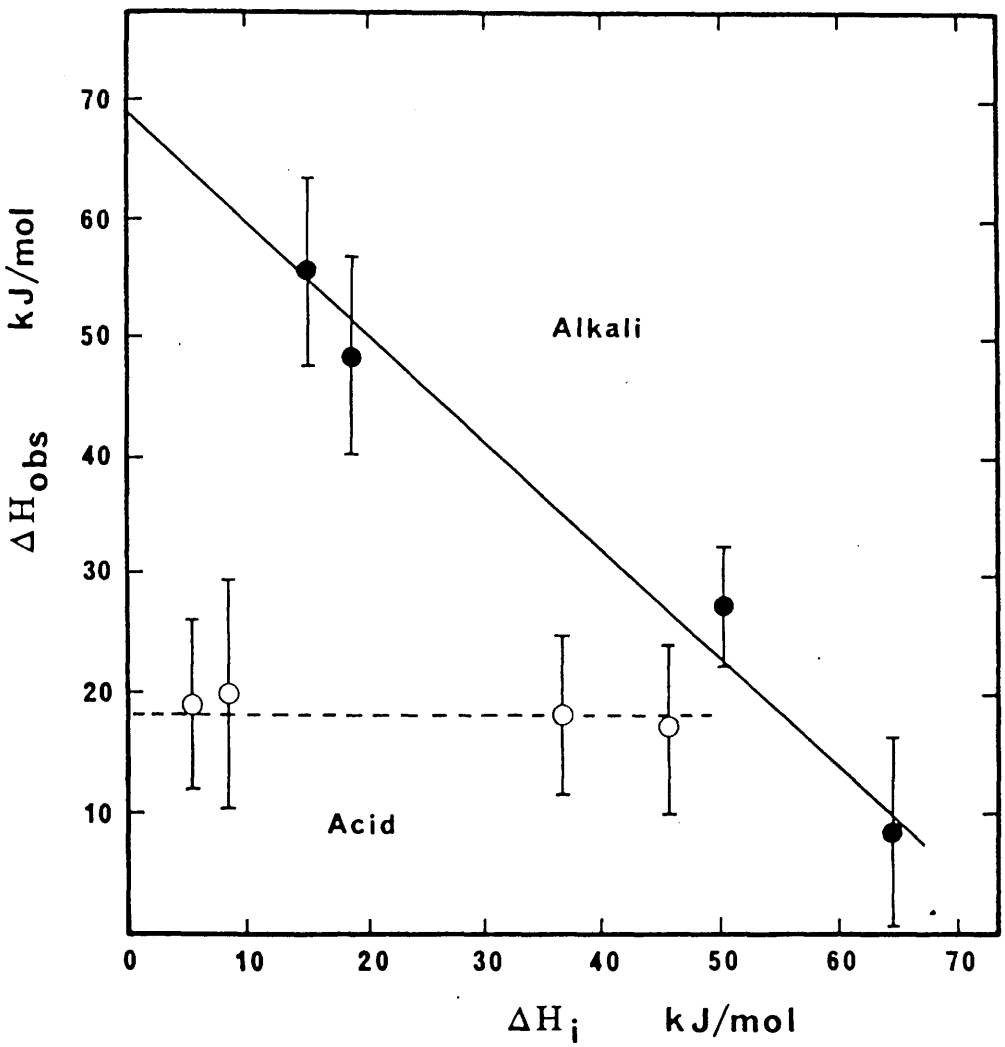

Fig.(2.11). Effect of differing buffer ionization heats (ΔH_i) on the observed enthalpies of acid or alkali metarhodopsin formation.

rhodopsin system in this reaction.

2.7 Measurement of the enthalpy of the acid to alkaline metarhodopsin reaction by another method.

The acid $\rightleftharpoons$ alkaline metarhodopsin equilibrium is temperature and pH dependent, both high temperature and pH favouring the alkaline metarhodopsin. This makes it possible to estimate the enthalpy for the acid to alkaline transition in a non-calorimetric way.

A sample of bleached rhodopsin at its pK_a (pH 9.5) in borate buffer was taken and placed in a cuvette in a temperature controlled block in the SP 1800 spectrophotometer. The temperature was monitored using a Comark thermocouple thermometer and the compartment was flushed with Argon gas to prevent condensation forming on the walls of the cuvette, and a series of spectra were run as the temperature was varied between 4°C and 30°C. A temperature profile of the type shown in Fig.(2.12) was obtained. The curves all cross at a single wavelength (430nm), the isosbestic point, indicating that the reaction involves only the two substances acid and alkaline metarhodopsin. Since the proportion of acid and alkaline metarhodopsin and hence the equilibrium constant varies with temperature, it is possible to apply the Van't Hoff relationship equation(2.2):-

$$\ln K = -\frac{\Delta H}{RT} + \frac{\Delta S}{R} \qquad \text{----------2.2}$$

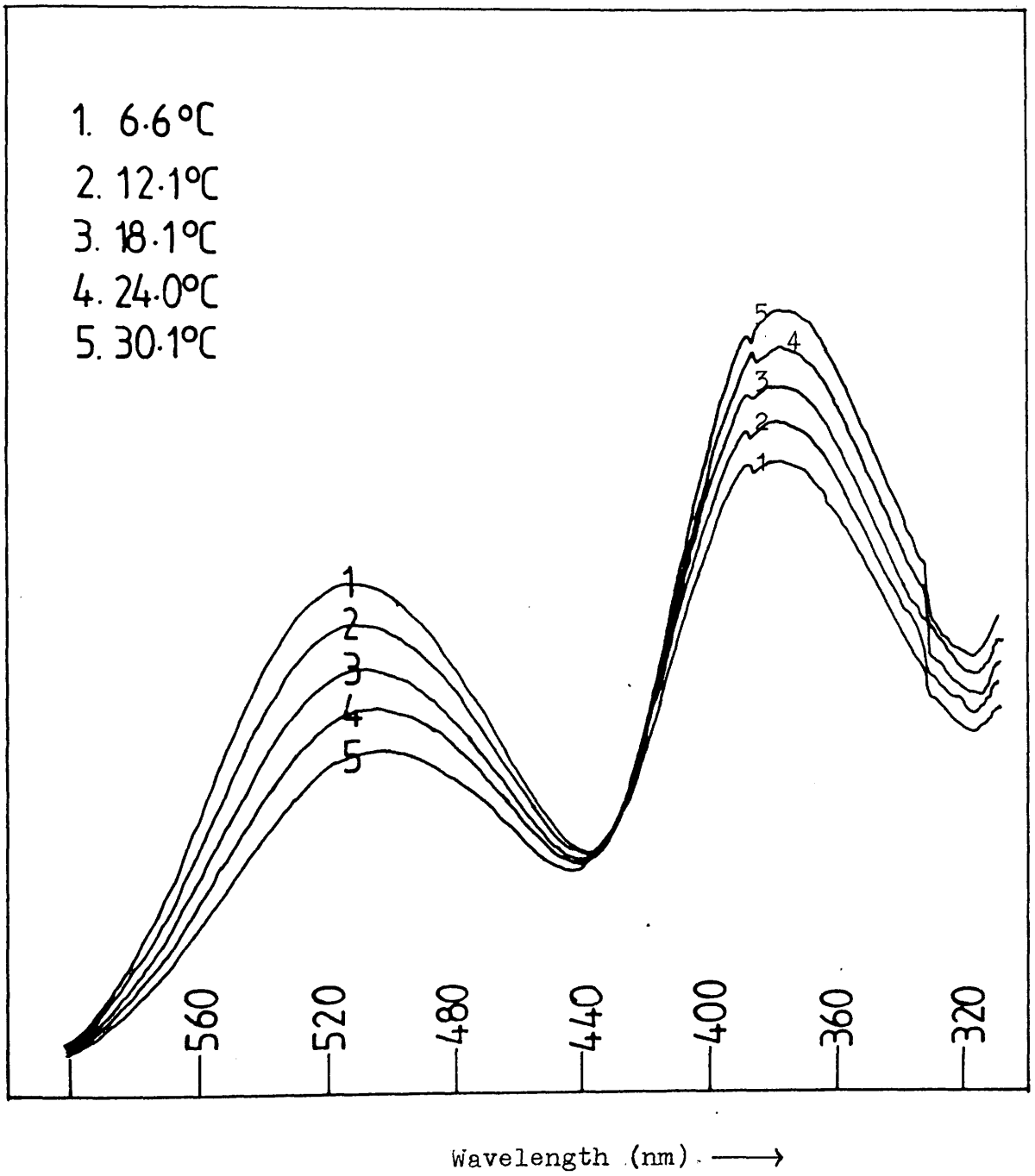

Fig.(2.12). Temperature profile of octopus metarhodopsin.

where K = the equilibrium constant for the reaction and is equal to $M_{alk.} / M_{acid}$.

ΔH = the enthalpy of the reaction.

ΔS = the entropy for the reaction.

R = the gas constant.

Thus a graph of ln K versus 1/T gives a line of gradient - $\Delta H/R$. For the temperature profile shown in Fig.(2.12), the following values were obtained:-

Curve No.	A_{370}	A_{510}	$M_{alk.}$	M_{acid}	$K = \frac{M_{alk.}}{M_{acid}}$
1	0.1175	0.0813	3.29×10^{-6}	2.61×10^{-6}	1.26
2	0.1325	0.0688	3.71×10^{-6}	2.21×10^{-6}	1.68
3	0.1438	0.0550	4.02×10^{-6}	1.77×10^{-6}	2.27
4	0.1563	0.0425	4.37×10^{-6}	1.37×10^{-6}	3.19
5	0.1688	0.0290	4.72×10^{-6}	0.93×10^{-6}	5.08

The absorbances for both acid and alkaline metarhodopsin were measured relative to the isosbestic to reduce any possible

contributions from scattering effects. The extinction coefficients for each of the species relative to the isosbestic point were calculated from the relative absorbance spectra by Tsuda et al (1982). The values used were:-

ε_{acid} (relative to the isosbestic)= 31149 $M^{-1}cm^{-1}$

$\varepsilon_{alk.}$ (relative to the isosbestic)= 35714 $M^{-1}cm^{-1}$

Curve No.	T(°C)	T(K)	1/T	K	lnK
1	6.6	279.6	3.58×10^{-3}	1.26	0.23
2	12.1	285.1	3.51×10^{-3}	1.68	0.52
3	18.1	291.1	3.44×10^{-3}	2.27	0.82
4	24.0	297.0	3.37×10^{-3}	3.19	1.16
5	30.1	303.1	3.30×10^{-3}	5.08	1.62

The graph of lnK versus 1/T is shown in Fig.(2.13b). The gradient of the line was calculated using a linear regression analysis program, from which :-

$$\text{gradient} = m = -4886 = \frac{-\triangle H}{R}$$

from which it may be estimated that $\triangle H = 40.62$ KJ/mole. ($\pm$ 2.33 KJ/mole)

Just as in the calorimetric experiments, this enthalpy will include any contributions from proton transfer to or from the buffer ions.

ie. $$\triangle H_{obs.} = \triangle H_{reaction} + \triangle H_{buffer\ ionisation} \quad \text{------2.3}$$

If it is assumed that the transition of acid to alkaline metarhodopsin involves the release of one proton per molecule, then the buffer contribution to the enthalpy change per mole is the heat of protonation for one mole. This value for buffer protonation varies somewhat with temperature, ranging from 18.8 KJ/mole at 5 °C to 13.1 KJ/mole at 30 °C. (Christensen et al 1976).The average value of $\triangle H_p$ over the range is used.

$$\triangle H_p \text{ (borate)} = -15.48 \text{ KJ/mole}$$

From equation (2.3) :-

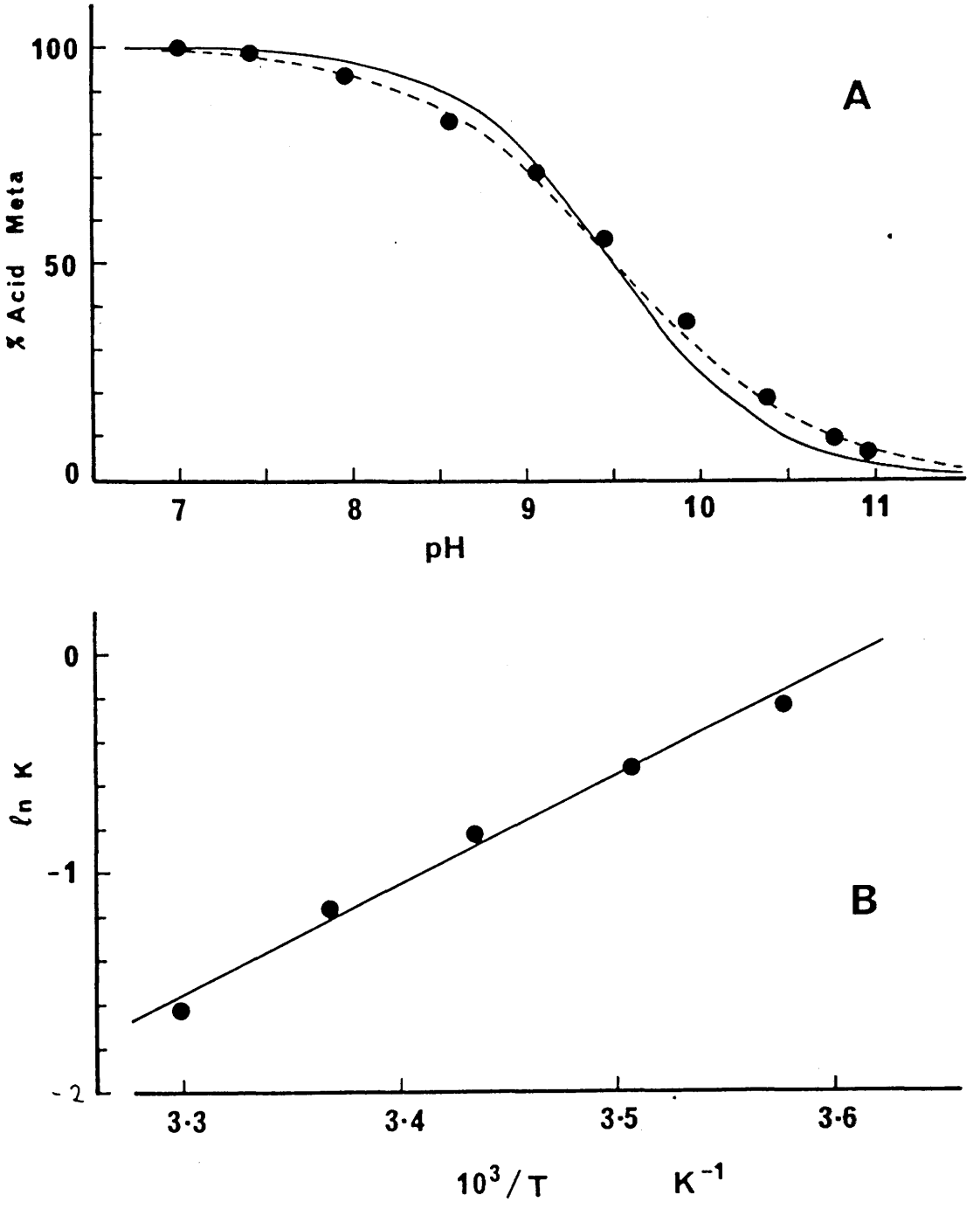

Fig.(2.13 A). pH titration plot of octopus metarhodopsin. The solid line gives the theoretical behaviour for simple titration of a single acidic group with pK_a = 9.5, whereas the dashed line is the best empirical fit for experimental data.

Fig.(2.13 B). Van't Hoff plot of the temperature dependence of the octopus metarhodopsin equilibrium.

$$40.62 = \Delta H_{reaction} - 15.48$$

$$\Delta H_{reaction} = 56.10 \text{ KJ/mole}$$

From the intercept of the line it is also possible to calculate the entropy of the reaction.

From equation (2.2), the intercept $= \frac{\Delta S}{R}$

$$\therefore \frac{\Delta S}{R} = 17.67 \quad ; \quad \therefore \Delta S = 146.97 \text{ JK}^{-1}\text{mole}^{-1}$$

2.8 pH titration profile :- an independent estimation of protonation changes.

The pH dependence of the metarhodopsin equilibrium allows the number of protons in the acid ⇌ alkaline metarhodopsin equilibrium to be investigated spectroscopically. This was done by making up a series of samples of detergent-extracted octopus metarhodopsin at different pH. A series of spectra were obtained giving a pH profile of the type shown in Fig.(2.14). A titration curve showing the observed fraction of metarhodopsin in the acid form versus pH, Fig.(2.13a) was roughly sigmoidal in shape with an apparent mid-point pK_a of 9.5 .

Taking the pK_a as 9.5, and assuming that the number of protons titrated was one, a theoretical titration curve was plotted Fig.(2.13a). The percentage acid metarhodopsin was calculated using the relationship derived below:-

$$M + H^+ = MH^+ \quad ; \quad K_a = \frac{[M]\,[H^+]}{[MH^+]}$$

$$[M] + [MH^+] = c_{total} \quad ; \text{ where } c_{total} = \text{total meta concentration.}$$

$$\frac{c_{total}}{[M]} = 1 + \frac{[MH^+]}{[M]}$$

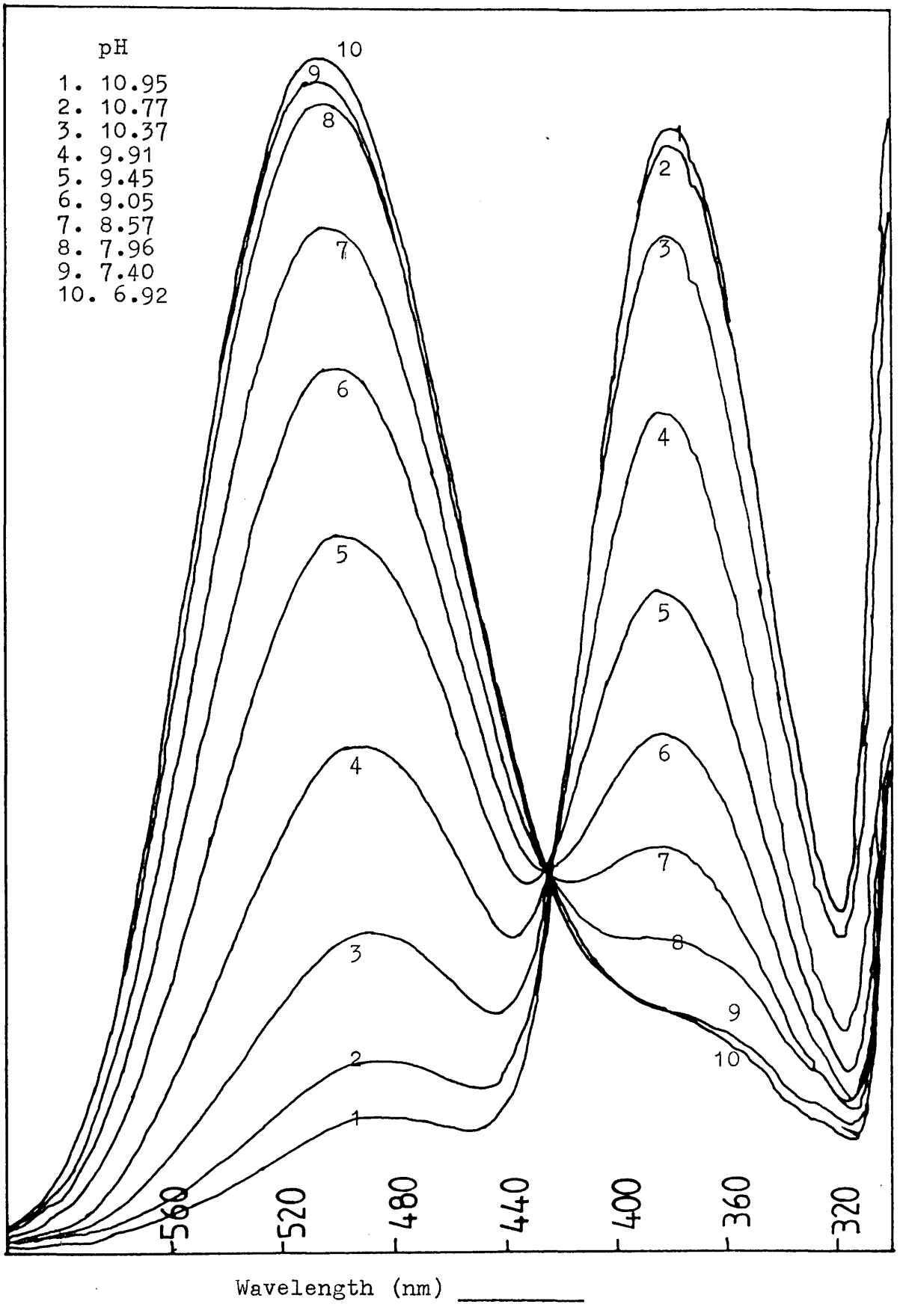

Fig.(2.14). Spectral titration of octopus metarhodopsin, showing the transition from alkaline to acid metarhodopsin.

$$= 1 + [H^+] / K_a$$

$$\text{fraction of } M = \frac{1}{1 + [H^+]/K_a}$$

$$\text{fraction of } MH^+ = \frac{1}{1 + K / [H^+]}$$

It is clear however, that this ideal titration curve is only a rough approximation to the observed data. A better fit, indicated by the dashed curve in Fig.(2.13a), was obtained using the empirical expression :-

$$\text{fraction } MH^+ = \frac{1}{1 + K / [H^+]^n}$$

where n = number of protons = 0.8.

Similar non-ideal behaviour has been observed in the vertebrate metarhodopsins (Matthews et al 1963, Abrahamson and Fager 1973, Parkes and Liebman 1984), but the reason for this remains unclear.

2.9 Direct measurement of protonation changes.

If hydrogen ions are indeed released during the formation of alkaline metarhodopsin, it should be possible to measure pH changes taking place directly in the absence of buffer and with suitable calibration, compare the protonation changes with calorimetrically determined values. Buffer removal was achieved by sedimentation of the octopus microvilli membranes in an MSE 18 centrifuge at 18,000 rpm at 5°C. The supernatant was removed and the membranes resuspended in 0.4 M sodium chloride. The process was repeated at least four times.

The sample was placed in a transparent thermostatted vessel and allowed to equilibrate to 6°C. A combined glass electrode and Radiometer pH meter connected to a sensitive linear recorder were used to monitor pH changes. The sample was flushed with nitrogen or Argon gas throughout the experiment since this seemed to reduce baseline drift possibly due to absorption of CO_2 from the atmosphere.

Irradiation of unbuffered rhodopsin at pH 7 (producing acid metarhodopsin) produced no observable deflection. Fig.(2.15). Irradiation of rhodopsin at high pH resulted in a reproducible pH drop accompanying alkaline metarhodopsin formation. Later irradiation on totally bleached samples showed no pH changes. The pH drop can be calibrated by comparison to the chart deflection caused by addition of a known quantity of 0.001 M HCl. This gave a value of 1.08 ± 0.16 protons per rhodopsin molecule.

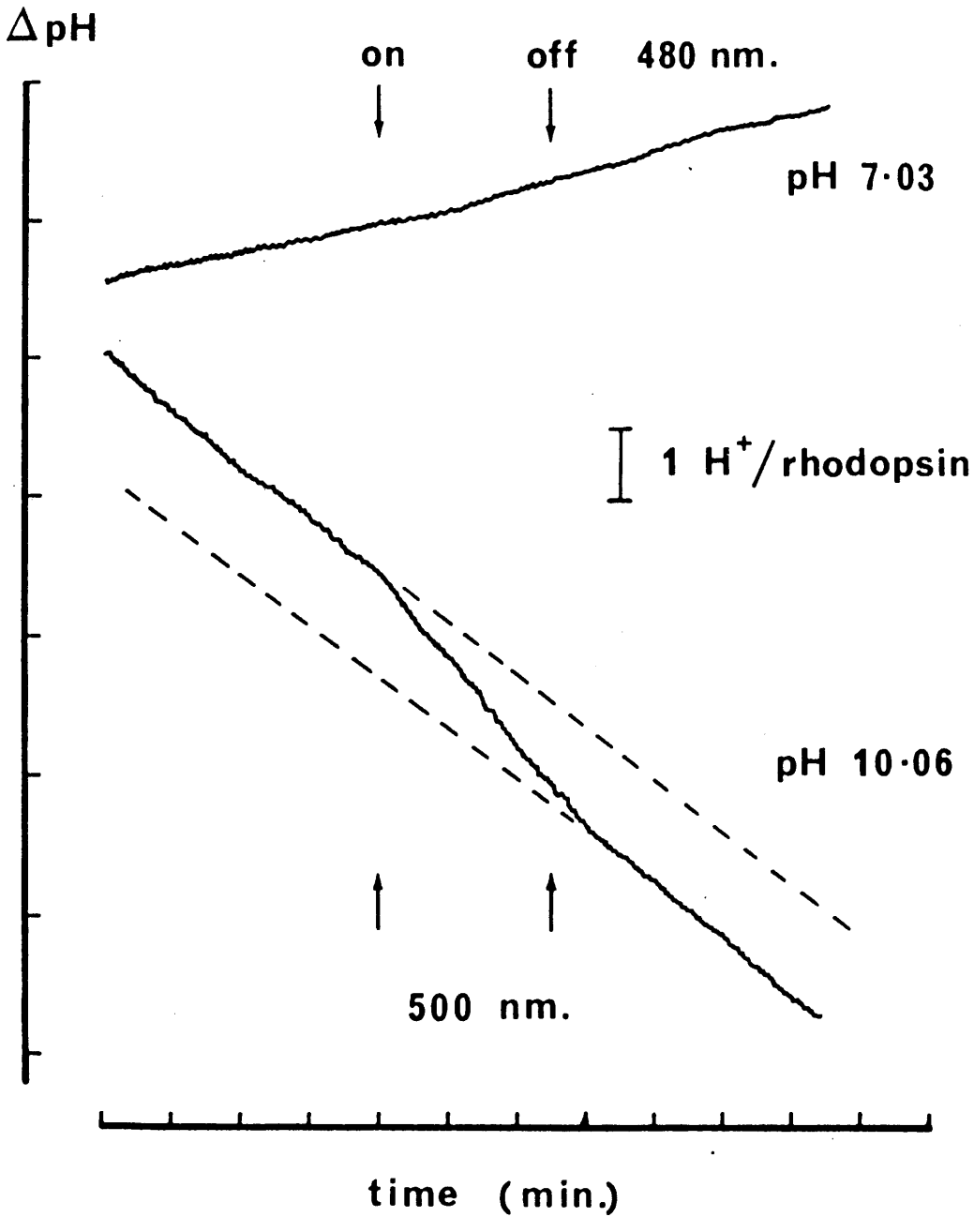

Fig.(2.15) Tracings of light-induced pH effects on unbuffered suspensions of octopus microvilli membranes in 0.4M NaCl at 6 °C. The dashed lines are linear extrapolations of pre- and post- illumination drift.

under these conditions.

Rhodopsin to alkaline metarhodopsin:-

1. Deflection due to addition of 25μl of 0.001 M HCl = 2.3cm

   Deflection due to bleach = 2.2cm

   $\triangle$ moles for reaction = 2.01×10^{-8}

   $\therefore$ $\triangle$moles H^+/ mole rhodopsin = 1.19

2. Deflection due to addition of 25μl of 0.001 M HCl = 1.6cm

   Deflection due to bleach = 1.8 cm

   $\triangle$ moles for reaction = 2.90×10^{-8}

   $\therefore$ $\triangle$moles H^+ / moles rhodopsin = 0.97

Average response = 1.08 $\pm$ 0.16 moles H^+/mole rhodopsin.

2.10 Discussion

Comparison of the light activated changes which occur for bovine and octopus rhodopsin reveals a remarkable similarity Fig.(2.16). Both exhibit high energy uptake as the primary step in visual excitation. This could suggest that photon energy storage is a common if not obligatory feature of all rhodopsins.

The first step in visual excitation is believed to be isomerisation of the 11-cis double bond (Hubbard and Kropf 1958). If this is so, an important consideration is suppression of thermal noise since retinal in organic solvents freely isomerises at room temperature (Hubbard et al 1965). In a laboratory device such as a photomultiplier, thermal noise could be suppressed by cooling the system. This of course is not a biologically viable solution and it seems that nature's solution to the problem has been to trap the chromophore in a protein matrix such that isomerisation is an energetically expensive step. This reduces the extent of thermal noise. If this is true, it could explain why the value of the octopus bathorhodopsin enthalpy is slightly lower at 50% of the exciting photon energy compared to 60% for cattle. Considering that octopuses live in a colder environment and have a much lower body temperature compared to mammals, 12 °C versus 37 °C, the barrier to thermal noise can afford to be lower while just as efficient.

The way in which energy is stored in the primary reaction step is still unclear. One possible model is that steric constraints force the chromophore in the bathorhodopsin

Fig(2.16). Comparison of the energy levels of the various octopus rhodopsin photoproducts with the equivalent bovine intermediates.

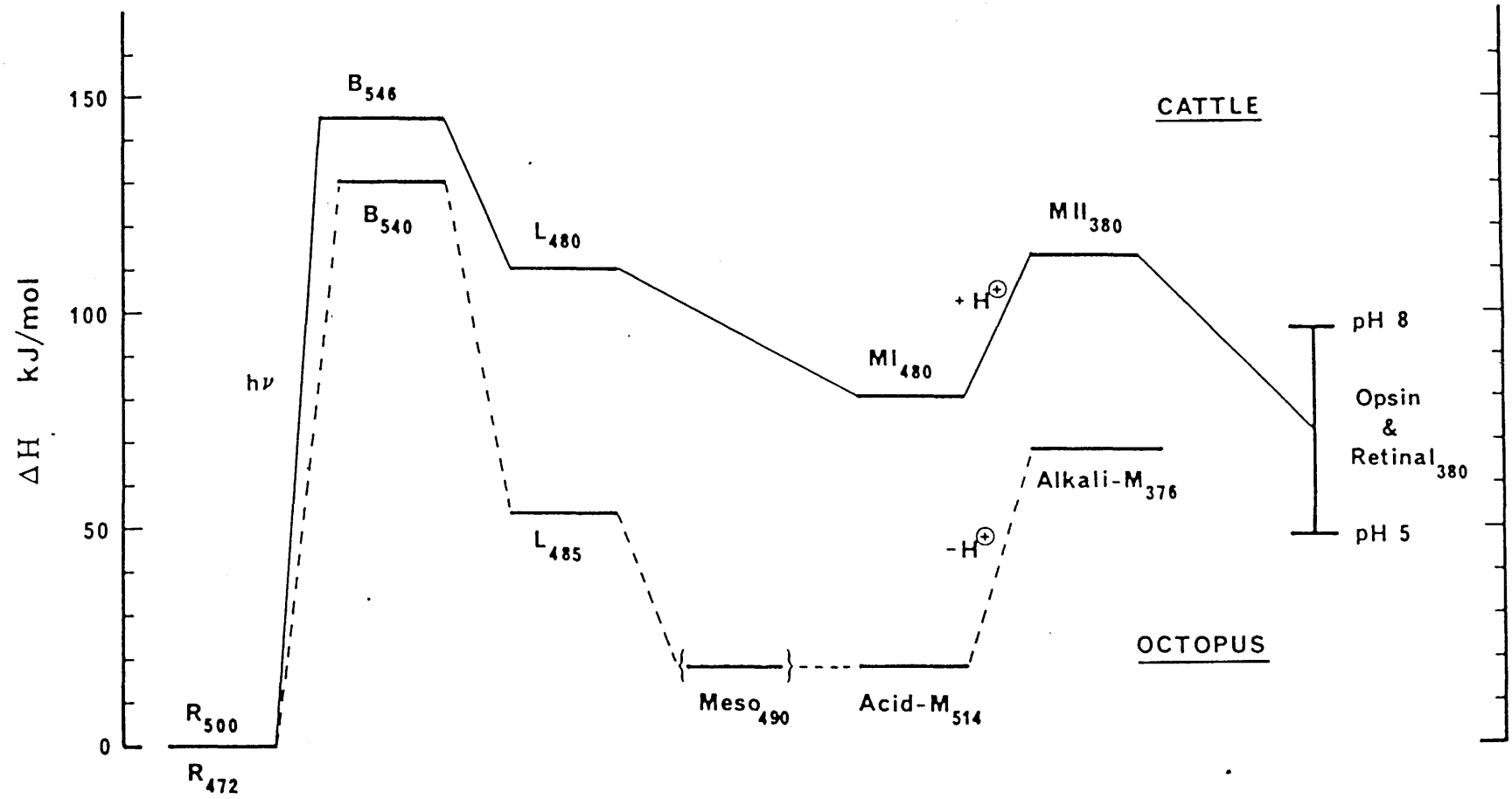

product in to a strained geometry. Since the barrier to isomerisation about double bonds is of the order of 100 KJ/mole, a twisted conformation about one or more of these bonds might account for the considerable destabilisation in bathorhodopsin. (Rosenfeld et al 1977).

An alternative possibility may involve isomerisation affecting the electrostatic interaction between the chromophore and the protein eg. by moving the protonated Schiff base away from its counterion. (Rosenfeld et al 1977). Both models also account for the red shift in wavelength.

The later intermediates show a similar trend although the absolute values of the enthalpies are not the same. The bathorhodopsin to lumirhodopsin and lumirhodopsin to metarhodopsin transitions in vertebrates and the bathorhodopsin to lumirhodopsin, lumirhodopsin to mesorhodopsin and mesorhodopsin to metarhodopsin transitions in invertebrates have been attributed to protein configurational changes and as such, the values of the enthalpies do not impart a great deal of information.

The values of the metarhodopsin transition in both species is however very interesting. It has been thought that the cattle meta I to meta II transition was complex, involving the deprotonation of the Schiff base with exposure of two titrating groups (Matthews et al 1963, Emrich and Reich 1974), or even possibly hydrolysis of the Schiff base bond (Cooper and Converse 1976). In invertebrates, the acid metarhodopsin to alkaline metarhodopsin transition was believed to be due to simple deprotonation of the Schiff

base bond. Hubbard and St.George (1957-58) studied the acid to alkaline transition in squid rhodopsin. They obtained an enthalpy of 32.84 $KJmol^{-1}$ and an entropy of -33.47 $JK^{-1}mol^{-1}$ for the transition which proceeds with the release of ~1 proton/rhodopsin molecule. They also noted that the equilibrium was temperature dependent, higher temperatures favouring alkaline metarhodopsin. Since nearly all acid groups have positive heats of dissociation ie. warming favours the release of protons and since the reaction parallels studies by Ball et al (1948) on model Schiff bases, they proposed the reaction acid to alkaline metarhodopsin to be simple deprotonation of the chromophore-protein Schiff base bond.

In contrast to this, the vertebrate meta I to meta II transition involves the uptake of ~1 proton/rhodopsin molecule and proceeds with an enthalpy of 54.81 $KJmol^{-1}$, and an entropy of 194.56 $JK^{-1}mol^{-1}$, which prompted Matthews et al (1963) on comparison with the enthalpy and entropy of squid rhodopsin to propose a mechanism for the meta I to meta II transition :- deprotonation of the Schiff base linkage accompanied by binding of two protons per rhodopsin molecule.

The results presented in this work for the octopus acid to alkaline metarhodopsin transition show the situation to be more complex . There is not such an obvious distinction between the octopus and cattle rhodopsins and neither octopus nor squid rhodopsins exactly match the enthalpy and entropy results obtained for simple Schiff

base deprotonation in model compounds (Table 2.3). It has to be said that Hubbard and St.George used only two points to calculate their results which cannot be as accurate as a linear regression analysis on five points. Also they did not take the buffer ionisation enthalpy in to account when presenting their results. In addition, their measurements were made on digitonin extracted squid rhodopsin whereas L1690 detergent was used to extract the octopus rhodopsin used here. L1690 detergent obviously mimics membrane conditions since temperature profile results are supported by calorimetrically determined enthalpies on membrane samples. Finally the octopus and squid metarhodopsins in question have a different pK_a, 9.5 for octopus versus 7.7 for squid, so perhaps subtle electrostatic effects contribute to the enthalpy and entropy of the transition.

The other difference at the metarhodopsin stage is the respective energies of the cattle and octopus metarhodopsins. In cattle, the meta II is at a fairly high energy which may be the driving force for the hydrolysis of the Schiff base bond while the octopus acid metarhodopsin is at a much lower energy and is the end product in the octopus photocycle, at which point the chromophore and protein are still attached. The alkaline metarhodopsin is much higher in energy and indeed is not a major physiological intermediate.

Could these results point to convergent evolution between vertebrates and molluscs at the molecular level?

Table 2.3. Comparison of ΔH and ΔS for the meta I to meta II transition in cattle rhodopsin, the acid to alkaline transition for squid and octopus rhodopsin and simple Schiff base deprotonation for a model compound.

	ΔH (KJ/mole)	$\Delta S(JK^{-1}mol^{-1})$
Cattle	54.81 (a)	194.56
	47.68 (b)	
Squid	32.84 (c)	-33.47
	25.71 (d)	
Octopus	56.10 (e)	146.97
Model Compound	41.42 (f)	165.06

(a) Taken from Matthews et al (1963).

(b) Value (a) corrected for buffer ionisation.

(c) Taken from Hubbard and St.George (1957-58).

(d) Value (c) corrected for buffer ionisation.

(e) Value measured in this work by temperature profile.

(f) For the reaction $Ret\text{-}CH=\overset{+}{\underset{H}{N}}(CH_2)_3CH_3 \rightarrow Ret\text{-}CH=N(CH_2)CH_3 + H^+$ in emulphogene. ΔH value taken from Cooper and Converse (1976). ΔS calculated assuming a pK_a of 6.1 (Cooper unpublished observations).

In view of this evidence, it is very tempting to suggest that this is so although it is very possible that both have simply conserved a vital function which had already developed before branching in the evolutionary tree took place.

It is interesting to consider why the two mechanisms are not identical. Both have an 11-cis chromophore and a large protein component opsin. The opsins although not identical (they have different molecular weights), must be similar since there is evidence that octopus opsin can activate vertebrate cGMP (Saibil and Michel-Villaz 1984), although simple antibody cross-reactivity tests carried out in this work with vertebrate antiserum and octopus rhodopsin in Ouchterlony gels failed to show a positive test. (Appendix two).

The fact remains however that both pigments perform the same function in a different way. It has been shown that vertebrate and cephalopod eyes have a different structure and that the retinas have developed from different tissues (Packard 1972), so it could be that rhodopsins developed in a different way in the course of evolution were striving towards the same goal. The alternative is that the differences developed deliberately to suit the needs and environment of each species. The problem then is to discover what the advantages are in each mechanism.

As mentioned already, vertebrate rhodopsins bleach and release their chromophore, while the invertebrate

pigments retain their chromophore-protein link. This difference can be reconciled theoretically by attributing it to the degree of protection of the Schiff base bond by the protein. In cattle rhodopsin it is assumed that the Schiff base is exposed to water at some point during the course of the reaction and that this coupled with a high energy strained conformation is the driving force for hydrolysis.

The octopus rhodopsin chromophore is believed to remain buried within the protein. If the sole function of rhodopsin is to activate cGMP (Reviews: Zurer 1983, Knowles 1984, Kuhne 1984, Vines 1985) as is believed, then in both cases this will have happened at or before the metarhodopsin stage. Hydrolysis or otherwise then would seem to be irrelevant.

The real value of the differences at the metarhodopsin stage may be due to different regeneration processes. In cattle, free all trans retinal diffuses from the rod outer segments, is oxidised to retinol and is carried by liposomes to the pigment epithelium where it is converted to the 11-cis chromophore again by enzymes (Hubbard and Wald 1952).

In cephalopods it is not yet clear what happens. There seems to be two regenerative reactions (Schwemer 1969):- 1. photoregeneration, 2. a slow dark reaction. It has been postulated that cephalopod regeneration is connected with another pigment, retinochrome , which is found in tissues behind the rhodopsin-containing rhabdomes (Hara and Hara 1972). Retinochrome has an all trans chromophore

which in the course of its photocycle is converted to 11-cis retinal. It was thus postulated that the two photocycles were cooperative and supplied each other with a suitable chromophore for regeneration.

The main problem with this theory is that:-

1. The chromophore of each is attached to the protein.
2. Retinochrome is not in direct contact with rhodopsin.

It was postulated (Hara and Hara 1972) that the retinochrome migrated with the black screening pigments during the visual process to bring the two pigments together. This theory however is inconclusive since mixing bleached rhodopsin and retinochrome with incubation did not result in appreciable rhodopsin regeneration.

It was later shown (Seki 1982) that retinochrome in the presence of opsin would generate rhodopsin and the scheme shown in Fig.(2.17) was proposed. Seki (1984) maintained that some of the metaretinochrome is present as aporetinochrome + free 11-cis retinal. This free retinal can recombine with opsin to give rhodopsin, or it can be isomerised thermally to all-trans retinal to recombine with aporetinochrome to yield retinochrome. This may suggest that the rhodopsin and retinochrome photocycles are not directly linked and that retinochrome only serves as a source of 11-cis retinal for newly synthesised opsin.

What then is this dark reaction? It has been observed (Schwemer 1969) that in vivo, metarhodopsin is slowly reconverted to rhodopsin. Also it is possible to prepare rhodopsin without any metarhodopsin present. This shows

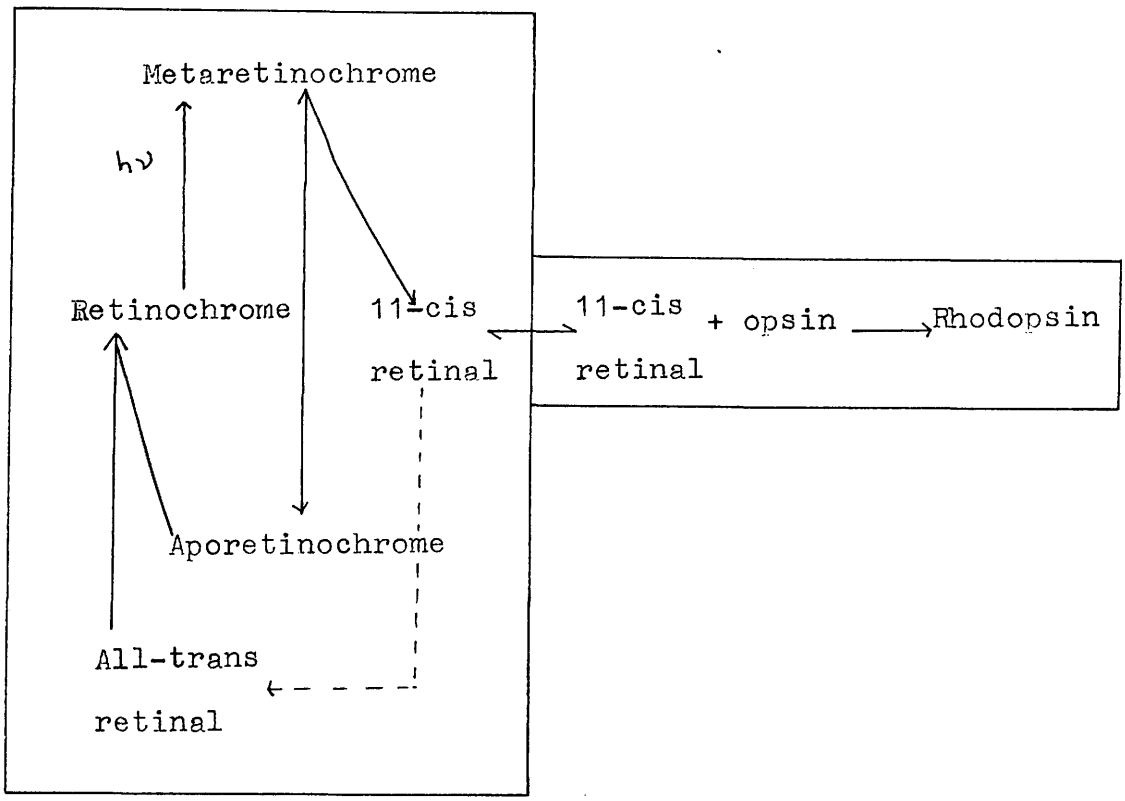

Fig.(2.17). Schematic representation of the relationship between metaretinochrome in a membrane and opsin in the other membrane.

(Taken from Seki 1984).

that the retina is capable of transforming metarhodopsin to rhodopsin. If retinochrome is not implicated then it is possible that a metabolic pathway exists to regenerate rhodopsin in situ without the need to remove the chromophore from the protein. The enthalpy difference between rhodopsin and acid metarhodopsin is small ($\sim$32 KJmol^{-1}) and exothermic for the regeneration process. Perhaps metabolic activity serves to reduce the activation energy for this process. It is of interest to note that Hamdorf (1979) postulated the participation of metabolic energy in the photoregeneration. Fig.(2.18).

The reason why vertebrates and invertebrates have different regeneration processes may be due to the different arrangement and mobility of the rhodopsin in the two species. In the discs of the outer segments of vertebrates, the axes of the pigments lie parallel to the surface of the discs (Liebman 1962) but not parallel to one another (Cone 1972) and within the discs the rhodopsin molecules can actually diffuse freely (Liebman and Entine 1974, Poo and Cone 1974).In invertebrates, the rhodopsin can neither freely diffuse nor freely rotate (Wehner and Goldsmith 1975) a property which enabled them to detect polarisation of light (Waterman 1979) which is postulated to be used by them as a method of navigation and for detecting food. Thus one rhodopsin is mobile, the other is relatively fixed.

For vertebrate rhodopsins it may be to its advantage to hydrolyse its used chromophore to allow it to diffuse to the pigment epithelium for reconversion to 11-cis retinal.

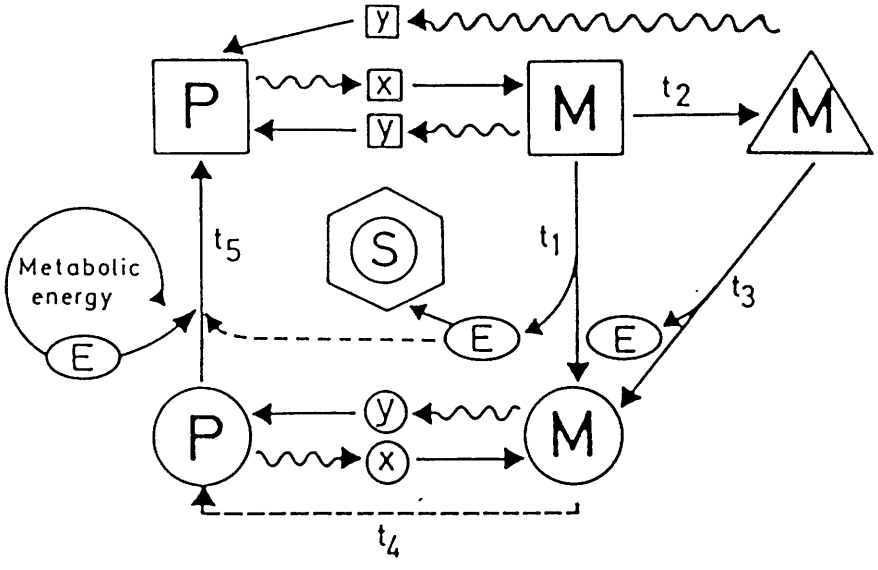

Fig(2-18) A scheme of pigment reactions in the microvillus membrane of invertebrate rhabdomeric photoreceptors. Appropriate quantum absorption by dark-adapted visual pigment [P] converts this to energy-rich metarhodopsin [M] which can activate membrane sites (S) by the release of energy (E), through which conversion it becomes inactivated, (M). Further appropriate quantum absorption can change the latter to (P), which needs metabolic energy to resume the activated form [P]. This cycle is dominant during normal physiological light levels, but intense, extraphysiologic illuminations increase the [P]⇝[M] transitions, and the rate t_1, limited by the rate of the membrane utilization of the energy, forces some [M] molecules into a storing form [M*], the latter releasing energy through a much slower decay to (M). The intermediate states of the forward and the backward reactions are symbolized by [x] and [y]; *dashed arrows* denote the possibility of energy by-pass from [M] and [M*] directly to (P); $t_1 - t_5$ are thermally controlled rates of the dark reactions, and t_4 indicates the possibility of a very slow metabolic dark regeneration of the visual pigment (STAVENGA, 1974), so that $t_4 \ll t_5$, $t_3 \ll t_1$.

(Taken from Hamdorf 1979).

Since the protein is free to move, it has a high probability of meeting new chromophore and since the reaction between opsin and 11-cis retinal to give rhodopsin is spontaneous, fresh rhodopsin will ensue.

The mechanism would not work well for invertebrates since a fixed protein would not readily capture a fresh chromophore. A method for regeneration in situ e.g. photoregeneration and metabolic conversion would be much more efficient.

The difference in the two mechanisms ie. hydrolysis of chromophore for vertebrates and preservation of chromophore for invertebrates also conveniently explains the protonation differences obtained at the metarhodopsin stage. The invertebrate metarhodopsin equilibrium simply corresponds to protonation and deprotonation of the Schiff base bond whereas in the vertebrate case the situation is more complex involving hydrolysis of the chromophore with subsequent titration of an exposed amino group.

It would seem that both pigments have maintained the same purpose in the forward reaction in vision but have evolved different regeneration mechanisms to suit the different membrane structures (rod outer segment discs versus microvilli) which in turn is connected with their respective environments.

Chapter 3

Determination Of The Quantum Yield Of Octopus Rhodopsin.

Introduction

A photochemical reaction can be regarded as taking place in two stages. The first is the absorbance of a single quantum of light by an individual chromophore. The molecule is excited to one of its singlet electronic states (here called S_1 and S_2) Fig.(3.1), in which one electron is in an orbital of higher energy than it was in the ground state. If the excited molecule is in state S_2 (or any higher S state), it drops back to the singlet excited state of lowest energy S_1, from which it has several options open to it:

1. It may give up energy and go back to the ground state by emitting radiation of the appropriate wavelength, a process called fluorescence.
2. It may give up energy as heat (thermal deactivation).
3. It may undergo radiationless crossover requiring spin-flipping to T_1 (intersystem crossing) where it may then undergo phosphorescence.
4. It may react or rearrange to give a different chemical species.

Thus not every quantum of light absorbed necessarily gives rise to products. The overall quantum efficiency then, as measured by some permanent change is :-

$$\text{Quantum Efficiency} = \frac{\text{Number of chromophores affected}}{\text{Number of quanta absorbed}}$$

The visual pigment rhodopsin contains the 11-cis isomer of retinal Fig.(1.3a) as the photochemically active chromophore linked to the surrounding apoprotein opsin by a protonated

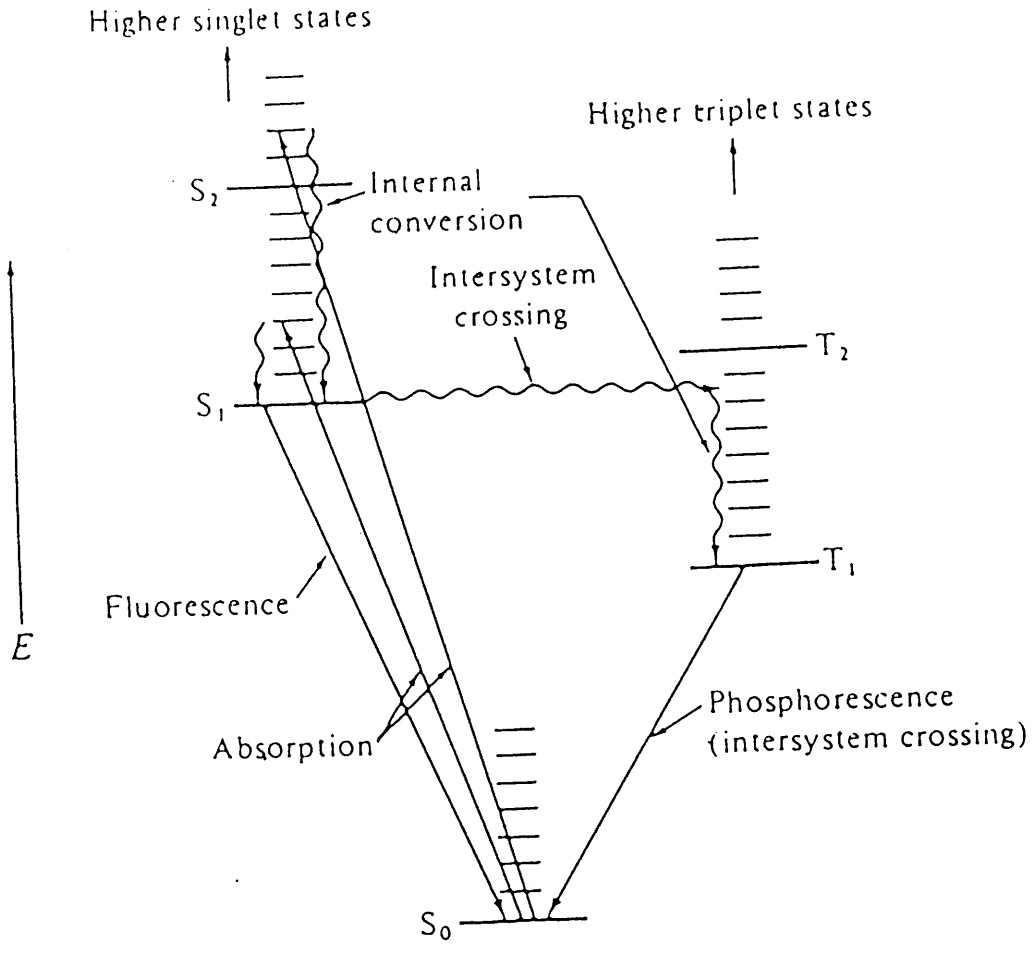

Fig.(3.1). Possible energy transformations on absorption of a photon of light.

Schiff base Fig.(1.3b).

The primary photochemical event in visual pigments has been a matter of considerable controversy. This is believed to correspond to the rhodopsin to bathorhodopsin transition although an earlier intermediate, hypsorhodopsin has been detected which may be a precursor (Yoshizawa and Horiuchi 1969) or a branching reaction (Abrahamson and Fager 1973) to bathorhodopsin. It may not be a genuine intermediate at all (Cooper 1983).

Various models for the photoreaction have been proposed: (Reviews: Abrahamson and Ostroy 1967, Rosenfeld et al 1977, Honig 1978, Ottolenghi 1980, Balogh-Nair and Nakanishi 1982).
(a) The classical picture involving a cis-trans isomerisation about the 11-12 bond. (Hubbard and Kropf 1958).
(b) A mechanism involving deprotonation of the Schiff base nitrogen. (Thomson 1975).
(c) Proton transfer from the methyl group to a protein heteroatom. (Fransen et al 1976).
(d) A photoinduced electron transfer from the chromophore to an appropriate acceptor group on the protein. (Rosenfeld et al 1977).

Resonance Raman experiments (Oseroff and Callender 1974) have shown that the Schiff base nitrogen in bathorhodopsin is protonated. This rules out mechanism (b). Mechanism (c) may be discounted since it has been shown that desmethyretinals bleach via a batho intermediate. (Rosenfeld et al 1977). Finally (d) cannot account for the fact that in bovine rhodopsin, the change may be photochemically but not thermally

reverted throughout the bleaching sequence. (Rosenfeld et al 1977).

Accumulated evidence would seem to favour mechanism (a) which was based on the fact that at low temperatures, irradiation of rhodopsin results in a photoequilibrium between rhodopsin, bathorhodopsin and isorhodopsin (pigment containing 9-cis as oppose to 11-cis retinal):

i.e. rhodopsin $\underset{\gamma_2}{\overset{\gamma_1}{\rightleftharpoons}}$ bathorhodopsin $\underset{\gamma_4}{\overset{\gamma_3}{\rightleftharpoons}}$ isorhodopsin

The model assumes that isomerisation of both rhodopsin and isorhodopsin occurs via a common trans configuration.

The values of the quantum yields for each of the above processes $\gamma_1, \gamma_2, \gamma_3, \gamma_4$ have important consequences concerning the mechanism of the photoisomerisation in the primary process of visual pigments and several investigations have been carried out.

The first measurements of the quantum yield of the photochemical bleaching of visual pigments were made by Dartnall (Dartnall 1936,1938). His most recent measurements on a variety of rhodopsins show the quantum yield for the forward reaction to be essentially the same for all visual pigments, ranging between 0.65 and 0.70.(Dartnall 1968, 1972).

Hubbard and Kropf (1958) studied the equilibrium established between rhodopsin, metarhodopsin and isorhodopsin:

i.e. rhodopsin $\underset{\gamma_2'}{\overset{\gamma_1'}{\rightleftharpoons}}$ metarhodopsin $\underset{\gamma_4'}{\overset{\gamma_3'}{\rightleftharpoons}}$ isorhodopsin

on irradiation of bovine rhodopsin at -20°C. They concluded that the ratio of the quantum yields, taking rhodopsin to metarhodopsin as unity, was 1 : 0.5 : 0.09 : 0.3 for $\gamma_1' : \gamma_2' : \gamma_3' : \gamma_4'$. If Dartnalls value of 0.67 is used for rhodopsin to metarhodopsin, then values of 0.670, 0.330, 0.067, 0.200 are obtained for $\gamma_1', \gamma_2', \gamma_3', \gamma_4'$ respectively.

Yoshizawa and Wald (1963) performed low temperature studies on the rhodopsin $\overset{\gamma_1}{\rightleftharpoons}$ bathorhodopsin $\overset{\gamma_3}{\rightleftharpoons}$ isorhodopsin equilibrium and obtained a value of 5 for the ratio $\gamma_{B-R}/\gamma_{B-I}$ which is almost identical to the value $\gamma_{M-R}/\gamma_{M-I}$ in the metarhodopsin equilibrium. From this, Rosenfeld et al (1977) concluded that although meta I and bathorhodopsin are different trans species, their photochemical behaviour appears to be essentially identical. They also observed that $\gamma_1 + \gamma_2 = 1$ from which it was postulated that a single potential minimum was populated by exciting bathorhodopsin and rhodopsin. Furthermore, the values of the quantum yields were found to be independent of temperature and wavelength of irradiation (Hurley et al 1977) which suggested that cis to trans isomerisation took place after complete thermal relaxation in the excited state, and required no activation energy.

A more detailed analysis of the quantum yields was carried out by Rosenfeld et al (1977), taking in to account formation of isorhodopsin. They considered that the quantum yield γ_1, was a product of ϕ_1, the probability of reaching the single potential minimum along the 11-12 coordinate, and a, the yield of crossing from this minimum to the ground state

conformation Fig.(3.2). Similarly, $Y_2 = \phi_2 b$ etc. This analysis gave values of 0.67, 0.33, 0.80, 0.20 for a,b,c,d respectively and 1.0, 0.9, 0.1, 1.0 for $\phi_1, \phi_2, \phi_3, \phi_4$. The value $\phi = 1$ is based on the assumption that upon excitation of rhodopsin, all excess vibrational energy relaxes in to the 11-12 torsional coordinate. ϕ_2 is calculated to be 0.9. The fact that it is less than 1 is due to leakage (ϕ_3) of bathorhodopsin in to the 9-10 torsional coordinate, leading to formation of isorhodopsin.

The most striking implication of the model is the complete channeling ($\phi = 1$) in to the common minimum from excited rhodopsin molecules and almost complete channeling of excited batho ($\phi_2 = 0.9$) in to the 11-12 torsional coordinate.

The behaviour of the protein bound chromophore can be contrasted sharply to that of free retinal. The quantum yield of retinal and model compounds are strongly wavelength dependent and can be 1-2 orders of magnitude less than those of pigments. Kropf and Hubbard (1970) measured the quantum yield for isomerisation of 11-cis to trans retinal at 25 °C in hexane and obtained a value of 0.2 which is much lower than the equivalent isomerisation in rhodopsin (0.67).

Thus it seems that the protein facilitates isomerisation in the chromophore by altering the excited state potential energy surfaces and / or by modifying rates of radiationless deactivation.

Apparently contradictory effects observed by Peters et al (1977) i.e. deuterium isotope effects and non-Arrhenius

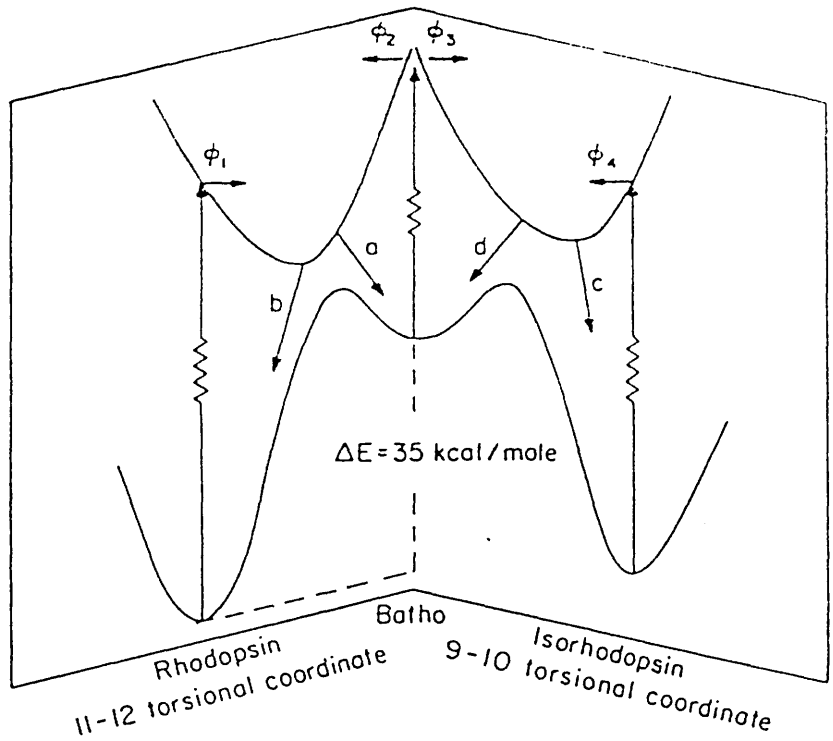

Fig.(3.2). Potential energy diagrams for rhodopsin, bathorhodopsin, and isorhodopsin. The quantum yield for rhodopsin isomerisation γ_1, involves the product of ϕ_1, the probability of reaching the single potential minimum along the 11-12 coordinate , and a, the yield of crossing from this minimum to the ground state conformation.

(Taken from Suzuki and Callender 1981).

kinetic behaviour can also be resolved by the cis-trans isomerisation mechanism. Cooper (1979) postulated an overlap of the ground state and excited state surfaces. Fig.(3.3).

This would mean that at very low temperatures, some excited molecules may be trapped at the bottom of the potential energy well where a barrier would have to be overcome to give bathorhodopsin formation. This would explain the temperature dependence observed in picosecond studies (Peters et al 1977). However, even at very low temperatures, some crossing over to the ground state surface might be expected before complete thermal relaxation after excitation , and non-Arrhenius kinetic behaviour might be seen.

Deuterium isotope effects would arise from changes in the vibrational energy levels of modes involving exchangeable hydrogens in the protein and chromophore.

Measurement of quantum yield values then, have given valuable insight in to the mechanism of action of light on rhodopsin. The work carried out here involves investigation of the quantum yield of octopus rhodopsin and its photo-regeneration. It will be interesting to see if the same arguments hold for the reaction of invertebrate visual pigments.

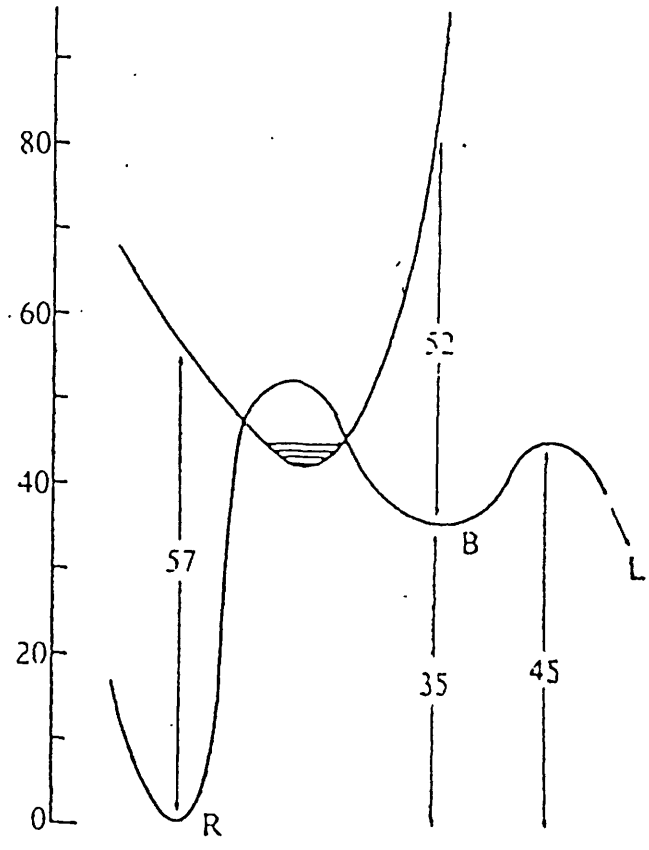

Fig.(3.3). Two dimensional projection of the possible ground and excited-state potential energy surfaces for the primary step in rhodopsin photolysis. The ground state energy of bathorhodopsin (B) with respect to rhodopsin (R) is from direct measurement. Vertical excitation energies to the electronically excited state are from absorbance maxima (500nm and 548nm for R and B respectively). The B → L (lumirhodopsin) barrier is from kinetic data, and suggests a lower limit to the R → B barrier in the ground state. The possible overlap (in projection) of the two surfaces is, probably, exaggerated for clarity. The hatched region indicates possible trapping in lower vibrational levels of the excited state minimum at low temperatures.

(Taken from Cooper 1979).

3.1 Materials and methods

Octopus rhodopsin was supplied by Professor M. Tsuda as in chapter 2. To obtain a sample suitable for use, a sample of octopus rhodopsin was extracted with L1690 detergent to give a final concentration of 5% detergent and spun down at 18,000 r.p.m. for 30 minutes on an MSE 18 centrifuge. The supernatant in each case had a final O.D. of between 0.2 and 2 at its absorbance maximum λ= 480nm.

Cattle rhodopsin was prepared by the method of Papermaster and Dreyer (1974) (Appendix 3), and was extracted with cetyltrimethylammoniumbromide (CTAB) detergent to a final concentration of 2% CTAB and spun down at 18,000r.p.m. for 30 minutes. The supernatant as before had a final O.D. of between 0.2 and 2 at its absorbance maximum λ = 500nm. Before irradiating cattle rhodopsin, solid hydroxylamine hydrochloride was added to a final concentration of 10mM. This was used to convert intermediates to retinal oxime and thus prevent any photoregeneration.

Potassium ferrioxalate was prepared and used as discussed in section (2.4). L1690 detergent was a gift from the Ryoto Chemical Company. CTAB detergent was supplied from Sigma and hydroxylamine hydrochloride was from Hopkins and Williams.

Extinction coefficients for cattle rhodopsin at various wavelengths were calculated from Dartnalls nomogram (Dartnall 1953). Extinction coefficients for octopus rhodopsin at various wavelengths were calculated by proportion

to the extinction coefficient and absorbance at $\lambda_{max.}$ using spectra from Tsuda et al (1982). Concentration changes for octopus rhodopsin were calculated using absorbance changes at λ=580nm with the appropriate extinction coefficient since it is one of the few wavelengths where only acid metarhodopsin absorbs. i.e. there should be no contribution to any absorbance changes from octopus rhodopsin.

Absorbance measurements were made as before on a Pye-Unicam SP 1800 spectrophotometer with an appropriate detergent reference. Baseline absorbances were obtained by running a spectrum with water in both sample and reference cells.

3.2 Theory

Two different methods were used to calculate the quantum yield for octopus rhodopsin.

1. Method one : Dartnall's Method.

The first method is based on theory developed by Dartnall (1957). This method is based on analysis of transmission versus time curves, and was used originally to determine the quantum yield of frog rhodopsin. (Dartnall 1936). The equations have to be modified since octopus metarhodopsin is photoreversible to rhodopsin.

Consider a beam of monochromatic light falling on a solution. For the general case of a solution with absorbing impurities and photoproducts as well as rhodopsin, and assuming that the Beer-Lambert law holds, the intensity of light absorbed by the solution may be expressed as:-

$$A = \log_e \frac{I}{I_t} = \alpha_r cl + \alpha_m(c_o - c)l + di \quad \text{-------(1)}$$

where I= intensity of light incident on the solution.

I_t= intensity of light transmitted by the solution at any given time t.

α_r= the extinction coefficient of the rhodopsin chromophore, expressed in $1M^{-1}cm^{-1}$.

c= the concentration of chromophores.

l= cell pathlength in cm.

α_m= the extinction coefficient of the products.

di= the density of impurities.

c_o=the concentration of chromophores when t=0.

Differentiating (1) with respect to time and rearranging the result gives:-

$$-\frac{1}{I_t}\frac{dI}{dt} = (\alpha_r l - \alpha_m l)\frac{dc}{dt} \qquad \text{----------(2)}$$

From the definition of quantum efficiency, γ, the rate of decrease in the number of rhodopsin chromophores, -dn/dt, is equal to the product of the quantum efficiency and the intensity of light absorbed by the rhodopsin. This latter quantity is related to the total light absorbed $(I-I_t)$ by the ratio of $\alpha_r cl$ to the total density. We have therefore:-

$$-\frac{dn}{dt} = -V\frac{dc}{dt} = \frac{\gamma \alpha_r cl}{\alpha_r cl + \alpha_m(c_o-c)l + di} \cdot (I-I_t) \qquad \text{----(3)}$$

where V = volume in litres.

Whence by eliminating dc/dt between (2) and (3) and rearranging the result:-

$$\frac{dI_t}{I_t dt} = \frac{\alpha_r cl - \alpha_m cl}{\alpha_r cl + \alpha_m(c_o-c)l + di} \cdot \frac{I-I_t}{I} \cdot \frac{\alpha_r \gamma Il}{V} \qquad \text{--(4)}$$

Now the density of the completely bleached solution is:-

$$\log_e \frac{I}{I_f} = \alpha_r c_o + di \qquad \text{----------(5)}$$

and subtracting equation (5) from equation (1) gives:-

$$\log_e \frac{I_f}{I_t} = \alpha_r cl - \alpha_m cl \qquad \text{----------(6)}$$

whence by substituting equations (1) and (6) in to equation (4) gives:-

$$\frac{dI_t}{I_t dt} = \frac{\log_e I_f/I_t}{\log_e I/I_t} \cdot \frac{I-I_t}{I} \cdot \frac{\alpha_r \gamma I l}{V} \qquad \text{----(7)}$$

On multiplying both sides by $I_f/(I_f-I_t)$, we have:-

$$\frac{I_f}{I_f-I_t} \cdot \frac{dI_t}{I_t dt} = \frac{\phi \alpha_r \gamma I l}{V} \qquad \text{----------(8)}$$

where $$\phi = \frac{I_f}{I_f-I_t} \cdot \frac{I-I_t}{I} \cdot \frac{\log_e I_f/I_t}{\log_e I/I_t} \qquad \text{------(9)}$$

Dartnall showed that ϕ may be treated as a constant in any one experiment (Dartnall 1957). Thus equation (8) may be integrated to give:-

$$\log_e \frac{I_t}{I_f-I_t} = \frac{\phi \alpha_r \gamma I lt}{V} + \text{constant} \qquad \text{--------(10)}$$

This is the general equation derived by Dartnall (1957) for use with vertebrate rhodopsins. It is not however directly applicable to octopus rhodopsin due to photoreversal of octopus acid metarhodopsin to rhodopsin. The equation was modified in the following way:-

As before: $A = \log_e I/I_t = \alpha_r cl + \alpha_m(c_o - c)l + di$ ----(11)

and $$\frac{-dI_t}{I_t dt} = (\alpha_r l - \alpha_m l)\frac{dc}{dt}$$ ----------(12)

but: $$-\frac{dn}{dt} = -V\frac{dc}{dt} = \alpha_r \gamma_r - \alpha_m \gamma_m$$ ----------(13)

where γ_r = quantum efficiency of rhodopsin to acid metarhodopsin.

α_r = extinction coefficient of rhodopsin at λ irradiation.

γ_m = quantum efficiency of acid metarhodopsin to rhodopsin.

α_m = extinction coefficient of acid metarhodopsin at λ irradiation.

Equation (13) may be expressed in terms of transmitted light as :-

$$-\frac{dc}{dt} = \frac{1}{V}\left\{\frac{\gamma_r\alpha_r cl - \gamma_m\alpha_m(c_o-c)l}{\alpha_r cl + \alpha_m(c_o-c)l + di}\right\} \times (I-I_t) \qquad ---(14)$$

Eliminating dc/dt between equations (12) and (14) gives:-

$$\frac{-dI_t}{I_t dt} = \frac{(I-I_t)\, l(\alpha_r-\alpha_m)}{(\alpha_r cl + \alpha_m(c_o-c)l + di)\, V}\left\{\frac{\gamma_r\alpha_r c - \gamma_r\alpha_r c_\infty \alpha_m(c_o-c)}{\alpha_m(c_o-c_\infty)}\right\} \qquad --(15)$$

Since $\gamma_m = \gamma_r\alpha_r c_\infty/\alpha_m(c_o-c_\infty)$ at equilibrium.

$$\therefore \frac{-dI_t}{I_t dt} = \frac{(I-I_t)\; I\; l(\alpha_r-\alpha_m)\gamma_r\alpha_r}{(\alpha_r cl+\alpha_m(c_o-c)l+di)\; VI(c_o-c_\infty)}\left\{c(c_o-c_\infty) - c_\infty(c_o-c)\right\} \qquad --(16)$$

$$= \frac{(I-I_t)\; I\; l(\alpha_r-\alpha_m)\gamma_r\alpha_r}{IV\,(\alpha_r cl+\alpha_m(c_o-c)l+di)(c_o-c_\infty)}\left\{c_o(c-c_\infty)\right\} \qquad -----(17)$$

The density of the completely bleached solution is :-

$$\log_e I/I_f = \alpha_r c_\infty l + \alpha_m (c_o - c_\infty) l + di \quad \text{----------(18)}$$

and subtracting (18) from (11) :-

$$\log_e I_f/I_t = (\alpha_r - \alpha_m)(c - c_\infty) \quad \text{----------(19)}$$

Whence by substituting (11) and (19) in to (17) :-

$$\frac{-dI_t}{I_t dt} = \frac{I-I_t}{I} \quad \frac{\log_e I_f/I_t}{\log_e I/I_t} \quad \frac{I\, l\, \gamma_r \alpha_r\, c_o}{V(c_o - c_\infty)} \quad \text{---------(20)}$$

$$\text{since} \quad c_o/(c_o - c) = 1 + \frac{\gamma_m \alpha_m}{\gamma_r \alpha_r} \quad \text{----------(21)}$$

$$\frac{-dI}{I_t dt} = \frac{I-I_t}{I} \cdot \log_e I_f/I_t \quad \frac{I\, l\, (\gamma_r \alpha_r + \gamma_m \alpha_m)}{V} \quad \text{------(22)}$$

Multipying both sides by $I_f/I_f - I_t$ gives :-

$$\frac{I_f}{I_f - I_t} \cdot \frac{dI_t}{I_t dt} = \frac{\phi\, (\gamma_r \alpha_r + \gamma_m \alpha_m)\, I\, l}{V} \quad \text{----------(23)}$$

which on integration gives :-

$$\log_e = \frac{I_t}{I_f - I_t} = \frac{\phi(\gamma_r\alpha_r + \gamma_m\alpha_m)\ I\ tl}{V} + \text{constant} \quad \text{--------(24)}$$

Since absorbance of solution and not transmission was used, equation (3.24) was converted to absorbance as follows :-

$$I = 10^{-A}$$

$$\log_e(I_t/I_f - I_t) = \log_e\left(\frac{10^{-A_t}}{10^{-A_f} - 10^{-A_t}}\right) \quad \text{----------(25)}$$

$$= -\log_e\left(\frac{10^{-A_f} - 10^{-A_t}}{10^{-A_t}} \times \frac{10^{A_t}}{10^{A_t}}\right) \quad \text{--(26)}$$

$$= -\log_e\ (10^{-A_f + A_t} - 1) \quad \text{--------(27)}$$

$$\log_e(10^{A_t - A_f} - 1) = \frac{-\phi\ (\gamma_r\alpha_r + \gamma_m\alpha_m)\ I\ l\ t}{V} + \text{constant} \quad \text{---(28)}$$

Thus a graph of $\log_e(10^{A_t - A_f} - 1)$ versus t should give a line of gradient, $m = -\frac{\phi(\gamma_r \alpha_r + \gamma_m \alpha_m) I_o \, l}{V}$.

Before a value for $(\gamma_r \alpha_r + \gamma_m \alpha_m)$ can be calculated however, it is necessary to find a value for I_o. This can be achieved in two ways :-

1. By using potassium ferrioxalate as a chemical actinometer. (See section 2.4).
2. By using cattle rhodopsin as an actinometer.

Both options are used for irradiation at λ = 460 nm. For irradiation at λ = 520 nm and λ = 540 nm, only option (2) is used since potassium ferrioxalate does not operate at these wavelengths.

For each wavelength, a sum of the forward and backward photosensitivities will be obtained which are then separable by simultaneous equations.

When applying option (2), a value of I_o is not extracted directly. Instead a direct comparison of the gradient of the lines $\log_e(10^{A_t - A_f} - 1)$ versus t for cattle and octopus rhodopsin was used. (As performed by Becher and Ebrey (1977) on bacteriorhodopsin):-

$$(\varepsilon_r \gamma_r + \varepsilon_m \gamma_m) = \frac{m_{or}}{m_c} \times \varepsilon_{cattle} \times \frac{\phi \text{ cattle}}{\phi \text{ octopus}} \times \gamma_{cattle}$$

The value of ϕ varies slightly during the course of the reaction and an average value is used.

Method 2 : Kropf's Method.

Kropf (1967) used a different approach to the same problem. Consider the following:-

rhodopsin + hydroxylamine $\longrightarrow$ retinal oxime + opsin

Let the molar concentration of rhodopsin at time t $=[\alpha]$

the molar concentration of retinal oxime at time t $=[\beta]$

Then $$\frac{-d[\alpha]}{dt} = \frac{\gamma_r I_\lambda}{V}$$

where I_λ = number of Einsteins per second at wavelength λ absorbed by rhodopsin.

γ_r = the quantum efficiency of bleaching at wavelength λ .

V = volume of solution.

The intensity of light absorbed by rhodopsin I_λ is equal to :-

$$\frac{\text{rhodopsin density}}{\text{total density}} \times \text{total light absorbed}$$

ie. $$I_\lambda = \frac{\alpha\,[\alpha]\;l}{Dl} \times I_o(1-e^{-Dl}) \qquad \text{---------(31)}$$

where D = the total density (natural logs) of the solution and is defined as $\left[\alpha[\alpha] + \beta[\beta] + k\right]$

α = the absorption coefficient* of rhodopsin.

β = the absorption coefficient* of retinal oxime.

k = the absorption due to light stable impurities.

l = length of light path in the solution.

* $\alpha = \varepsilon/0.434$, where ε is the decadic molar extinction coefficient.

Equation (31) substituted in to equation (30) yields equation (32) :-

$$\frac{-d[\alpha]}{dt} = \frac{\gamma_r I_o \alpha [\alpha] (1-e^{-Dl})}{VD} \quad \text{----------(32)}$$

which can be rearranged to give :-

$$-\int \frac{D \; d[\alpha]}{(1-e^{-Dl})[\alpha]} = \int \frac{\gamma_r I_o \alpha \; dt}{V} \quad \text{-----(33)}$$

Using the approximation that :-

$$\frac{D}{(1-e^{-Dl})} = 1 + \frac{Dl}{2} + \frac{D^2 l^2}{12}$$

which is valid in the range $0.2 < D < 2$ (Zimmermann et al 1958).

Then (33) may be rewritten as :-

$$-\left\{ \int \frac{1 \; d[\alpha]}{[\alpha]} + \frac{1}{2}\int \frac{D \; d[\alpha]}{[\alpha]} + \frac{l^2}{12}\int \frac{D^2 \; d[\alpha]}{[\alpha]} \right\} = \int \frac{\gamma_r I_o \alpha \, dt}{V} \quad \text{---(34)}$$

which may be integrated to give :-

$$(1+\frac{E}{2}+\frac{E^2}{12})\log_e\frac{[\alpha]_o}{[\alpha]_t} + \frac{3+E}{6}(\alpha-\beta)[\beta]l + \frac{1}{24}(\alpha-\beta)^2 l^2(2[\alpha]_o[\beta]-[\beta]^2)$$

$$= \frac{\gamma_r\alpha}{V}\int_o^t I_o\, dt \qquad \text{----------(35)}$$

where $E = l\beta[\alpha]_o$

This is the basic equation describing the time rate of appearance of photoproduct as a function of the incident light intensity, the geometric constants of the solution being irradiated, the light absorbing properties of all the compounds in solution and the photosensitivity of rhodopsin.

For the experiments performed in this case, ie. irradiation of cattle rhodopsin at λ= 460 nm, 540 nm, 520 nm, equation (35) may be simplified since $\beta \simeq 0$ ie. retinal oxime does not absorb significantly at these wavelengths. Thus equation (35) may be expressed as :-

$$(1+\frac{E}{2}+\frac{E^2}{12})\log_e\frac{[\alpha]_o}{[\alpha]_t} + \frac{3+E}{6}l\alpha[\beta] + \frac{l^2\alpha^2}{24}(2[\alpha]_o[\beta]-[\beta]^2)$$

$$= \frac{\gamma_r\alpha}{V}\int_o^t I_o\, dt \qquad \text{----------(36)}$$

Let Ω = the left hand side of equation (36), then

$$\Omega = \frac{\gamma_r \alpha}{V} \int_0^t I_o \, dt$$

For octopus rhodopsin, the equation must be modified to allow for photoreversal:-

rhodopsin $\rightleftharpoons$ acid metarhodopsin

Let the molar concentration of rhodopsin at time t = [R]
the molar concentration of acid metarhodopsin at time t = [M]

then: $$\frac{d[R]}{dt} = \frac{-\gamma_r I_r}{V} + \frac{\gamma_m I_m}{V} \quad \text{---------(37)}$$

where γ_r = the quantum efficiency of rhodopsin to acid metarhodopsin.

γ_m = the quantum efficiency of acid metarhodopsin to rhodopsin.

I_r = the fraction of light absorbed by rhodopsin.

I_m = the fraction of light absorbed by acid metarhodopsin.

and $$I_r = \frac{\alpha_r [R] I_o (1-e^{-Dl})}{D} ;$$

$$I_m = \frac{\alpha_m [M] I_o (1-e^{-Dl})}{D} ;$$

where α_r = the extinction coefficient of rhodopsin at the wavelength of irradiation.

α_m = the extinction coefficient of acid metarhodopsin at the wavelength of irradiation.

Thus $$\frac{d[R]}{dt} = \frac{I_o (1-e^{-Dl})}{DV} \left\{ - \gamma_r \alpha_r [R] + \gamma_m \alpha_m [M] \right\} \quad ----(38)$$

at ∞ , $\frac{d[R]}{dt} = 0$; $\gamma_r \alpha_r [R]_\infty = \gamma_m \alpha_m [M]_\infty$ ----(39)

$$\gamma_m = \frac{\gamma_r \alpha_r [R]_\infty}{\alpha_m [M]_\infty}$$

where $[R]_\infty$ = the concentration of rhodopsin at $t = \infty$

$[M]_\infty$ = the concentration of acid metarhodopsin at $t = \infty$

Substituting equation (39) in to equation (38) gives :-

$$\frac{d[R]}{dt} = \frac{I_o(1-e^{-Dl})}{DV} \left\{ \frac{-\gamma_r \alpha_r [R] + [M] \gamma_r \alpha_r [R]_\infty}{[M]_\infty} \right\} \text{------(40)}$$

now, $[M] = [R]_{total} - [R]$

where $[R]_{total}$ = the total concentration of pigment present as both rhodopsin and acid metarhodopsin.

Thus:

$$\frac{d[R]}{dt} = \frac{-I_o(1-e^{-Dl})\gamma_r \alpha_r}{[M]_\infty DV} \left\{ ([M]_\infty + [R]_\infty)[R] - [R]_\infty [R]_{total} \right\}$$

------(41)

since $[M] + [R] = [R]_{total}$, rearranging (41) gives:-

$$-\int \frac{Dl \quad d[R]}{(1-e^{-Dl})([R]-[R]_\infty)} = \int \frac{I_o \gamma_r \alpha_r \quad l \quad [R]_{total} \quad dt}{V \quad [M]_\infty} \text{---(42)}$$

Assuming that :-

$$\frac{Dl}{(1-e^{-Dl})} = 1 + \frac{Dl}{2} + \frac{D^2l^2}{12}$$ as before gives :-

$$-\left\{\int \frac{d[R]}{([R]-[R]_\infty)} + \frac{l}{2}\int \frac{D\,d[R]}{([R]-[R]_\infty)} + \frac{l^2}{12}\int \frac{D^2\,d[R]}{([R]-[R]_\infty)}\right\}$$

$$= \int \frac{I_o \gamma_r \alpha_r l [R]_{total}\ dt}{V [M]_\infty} \qquad \text{--------(43)}$$

Integrating (43) and rearranging gives :-

$$\log\left[\frac{[R]_o - [R]_\infty}{[R]_t - [R]_\infty}\right] + \frac{l(\alpha_m [R]_{tot} + k)}{2} \log\left[\frac{[R]_o - [R]_\infty}{[R]_t - [R]_\infty}\right] + \frac{l(\alpha_r - \alpha_m)([R]_o - [R]_t)}{2}$$

$$+ \frac{l(\alpha_r - \alpha_m)[R]_\infty}{2} \log\left[\frac{[R]_o - [R]_\infty}{[R]_t - [R]_\infty}\right] + \frac{l^2(\alpha_m [R]_{tot} + k)^2}{12} \log\left[\frac{[R]_o - [R]_\infty}{[R]_t - [R]_\infty}\right]$$

$$+ \frac{l^2\left\{(\alpha_m\alpha_r - \alpha_m^2)[R]_{tot} + (\alpha_r - \alpha_m)\, k\right\}([R]_o - [R]_t)}{6}$$

$$+ \frac{[R]_{tot}\, l^2\left\{(\alpha_m\alpha_r - \alpha_m^2)[R]_{tot} + (\alpha_r - \alpha_m)\, k\right\}}{6} \log\left[\frac{[R]_o - [R]_\infty}{[R]_t - [R]_\infty}\right]$$

$$+ \frac{l^2(\alpha_r - \alpha_m)^2([R]_o^2 - [R]_t^2)}{24} + \frac{l^2(\alpha_r - \alpha_m)^2 [R]_{tot}([R]_o - [R]_t)}{12}$$

$$+ \frac{l^2(\alpha_r - \alpha_m)^2 [R]_{tot}^2}{12} \log\left[\frac{[R]_o - [R]_\infty}{[R]_t - [R]_\infty}\right] = \int \frac{I_o \gamma_r \alpha_r\, l\, [R]_{tot}\, dt}{V\, [M]_\infty}$$

------(44)

since $\dfrac{[R]_{tot}}{[M]_\infty} = \dfrac{1 + [R]_\infty}{[M]_\infty} = 1 + \dfrac{\gamma_m \alpha_m}{\gamma_r \alpha_r}$

and let Ψ = left hand side of equation (44), then:-

$$\Psi = \frac{(\gamma_r \alpha_r + \gamma_m \alpha_m)}{V} \int I_o \, dt$$

3.3 Experimental.

3.3.1 Irradiation at λ= 460 nm.

A 2ml sample of octopus rhodopsin was pipetted in to a cuvette with a mini magnetic stirring bar. The sample was placed in a cuvette holder which slotted in to a fixed position on top of a magnetic stirring plate, situated in front of a lamp fitted with a monochromator.

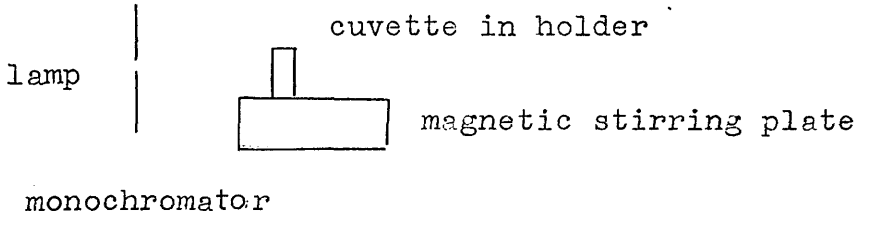

A spectrum of the unbleached sample was taken, then the sample was irradiated at λ= 460 nm for a period timed with a stopwatch. Absorbance changes were monitored spectroscopically at regular intervals throughout.

A 2ml sample of CTAB extracted cattle rhodopsin containing 10mM hydroxylamine was bleached immediately afterwards in identical conditions and this was used as an actinometer.

A 2ml sample of potassium ferrioxalate was irradiated immediately after the cattle rhodopsin and this too was used as an actinometer.

3.3.2 Irradiation at λ= 520 nm.

For λ= 520 nm, a 2ml sample od octopus rhodopsin was irradiated to give predominantly acid metarhodopsin. This was regenerated by irradiation at λ= 520 nm. Absorbance changes were monitored as before.

A 2ml sample of cattle rhodopsin was used as an actinometer.

3.3.3 Irradiation at λ= 540 nm.

This was identical to λ= 520 nm. Again cattle rhodopsin was used as an actinometer.

3.4 Results.

3.4.1 Determination of I_o from potassium ferrioxalate.

The use of potassium ferrioxalate as a chemical actinometer was discussed in section 2.4. A fresh calibration graph of A_{510} versus $\left[Fe^{2+}\right]$ was prepared before commencing the experiment.

A 0.15M potassium ferrioxalate solution in 0.1N H_2SO_4 was prepared. 2ml of this was pipetted in to a cuvette and irradiated at 460 nm for a period timed with a stopwatch. After irradiation, 1ml of the solution was removed and 1ml of 10% o-phenanthroline was added followed by 1.5ml of H_2SO_4 / sodium acetate buffer. The mixture

was made up to 10ml in a volumetric flask and after allowing it to develop for 30 minutes, its absorbance was measured relative to an identically prepared solution containing unexposed potassium ferrioxalate. From this the intensity of light was calculated as before:-

Absorbance of unexposed potassium ferrioxalate =0.032

Absorbance at 510 nm of solution irradiated for 30 minutes = 0.21

$\therefore A = 0.178$

From calibration graph, $\left[Fe^{2+}\right]$ produced = 1.30×10^{-4} M

In 2ml, number of moles of $\left[Fe^{2+}\right]$ produced = 2.60×10^{-7}

At 460 nm quantum efficiency of ferroixalate = 1.25

The number of photons incident = $\frac{\text{moles}}{\text{Q.E.}} = 2.08 \times 10^{-7}$ E

(1E = 6×10^{23} photons).

But not all light is absorbed by solution: $A_{460} = 0.928$

Total number of photons incident = 2.24×10^{-7} E in 30 mins.

Intensity of light = 7.47×10^{-9} E/min.

3.4.2 Analysis of results using Dartnall's method.

For irradiation at λ = 460 nm.

(a) With cattle rhodopsin as actinometer.

Octopus rhodopsin :- Spectrum of absorbance changes given in Fig.(3.4).

t(min)	A_{460}	$A_t - A_f$	$\ln(10^{A_t - A_f} - 1)$
0	0.3390	0.0400	-2.3384
2	0.3270	0.0280	-2.7091
4	0.3180	0.0190	-3.1073
6	0.3150	0.0160	-3.2827
8	0.3090	0.0100	-3.7596
11	0.3045	0.0055	-4.3626
14	0.3020	0.0030	-4.9716
∞	0.2990	0	———

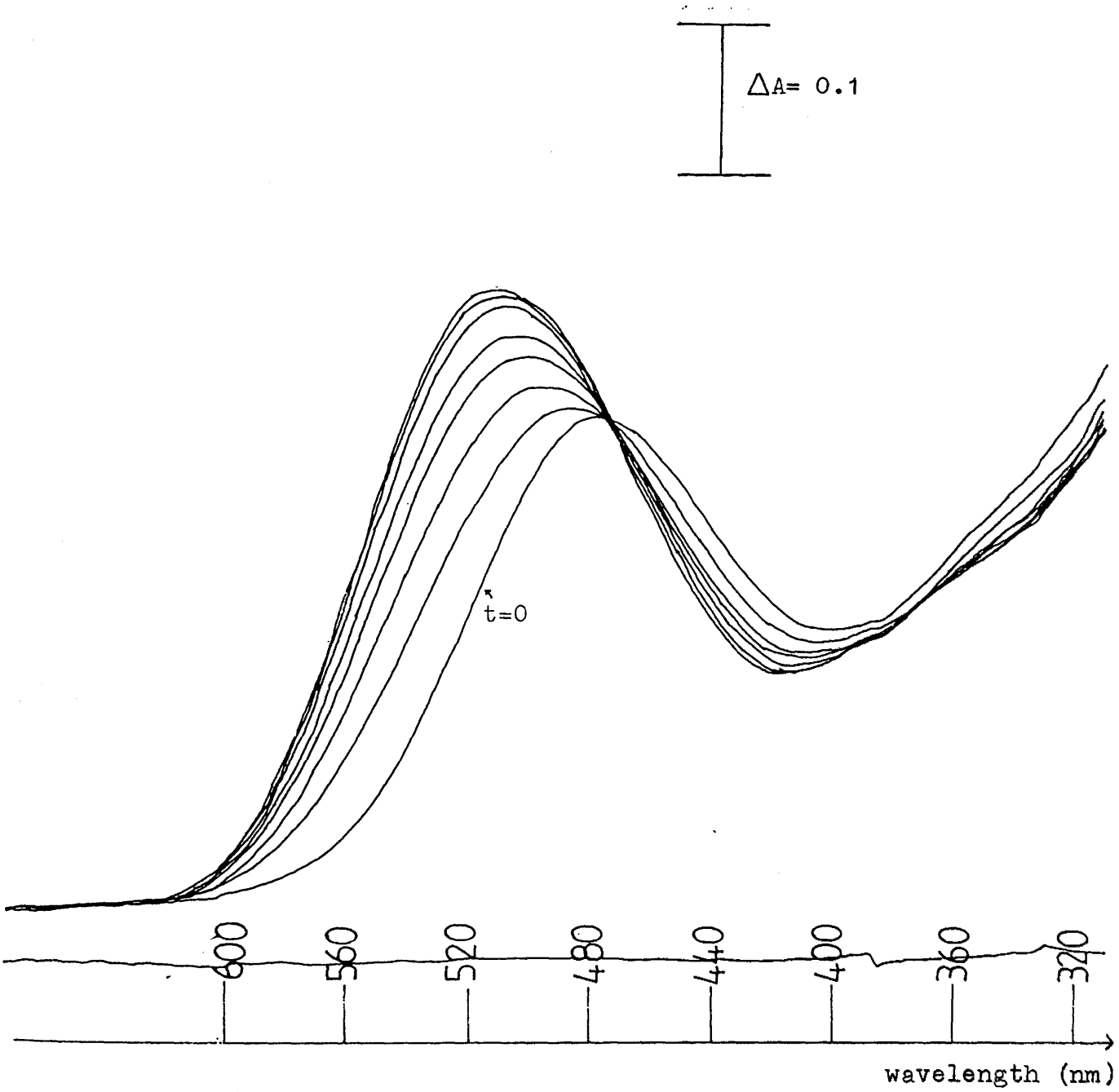

Fig.(3.4). Absorbance changes upon irradiation of octopus rhodopsin at λ= 460 nm.

Plotting $\ln(10^{A_t-A_f} - 1)$ versus t, Fig.(3.5a) gives a line with gradient, m = -0.1862.

Calculation of ϕ for octopus rhodopsin:-

$$\phi = \frac{I_f}{I_f - I_t} \times \frac{I - I_t}{I} \times \frac{\log I_f/I_t}{\log I/I_t}$$

t(min)	$-A_t+A_f$	$(1-10^{-A_t+A_f})^{-1}$	$1-10^{-A_t}$	$\frac{A_t-A_f}{A_t}$	
0	-0.040	11.3650	0.5419	0.1180	0.7267
2	-0.028	16.0159	0.5290	0.0856	0.7252
4	-0.019	23.3612	0.5192	0.0597	0.7241
6	-0.016	27.6465	0.5158	0.0508	0.7244
8	-0.010	43.9314	0.5091	0.0324	0.7246
11	-0.0055	79.4637	0.5040	0.0181	0.7249
14	-0.003	145.2654	0.5011	0.0099	0.7206

$\therefore$ average value of ϕ = 0.72

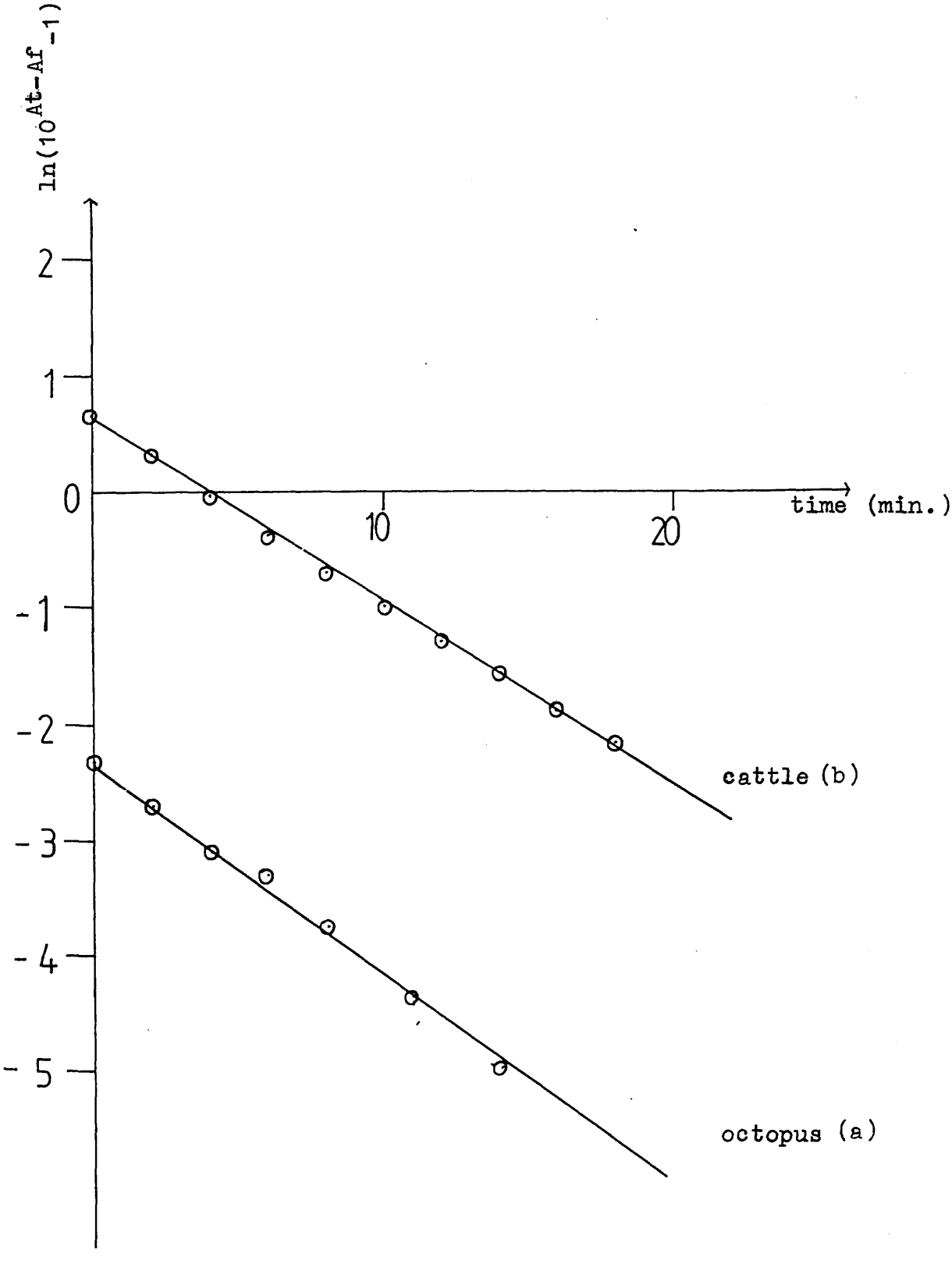

Fig.(3.5). Plot of $\ln(10^{At-Af}-1)$ versus time for cattle and octopus rhodopsin at λ= 460 nm.

Cattle rhodopsin :- Spectrum of absorbance changes given in Fig.(3.6).

t(min)	A_{460}	$A_t - A_f$	$\ln(10^{A_t - A_f} - 1)$
0	0.529	0.462	0.6405
2	0.440	0.373	0.3078
4	0.354	0.287	-0.0657
6	0.290	0.223	-0.3989
8	0.239	0.172	-0.7217
10	0.203	0.136	-1.0004
12	0.170	0.103	-1.3181
14	0.149	0.082	-1.5711
16	0.128	0.061	-1.8918
18	0.114	0.047	-2.1690
∞	0.067	0	——

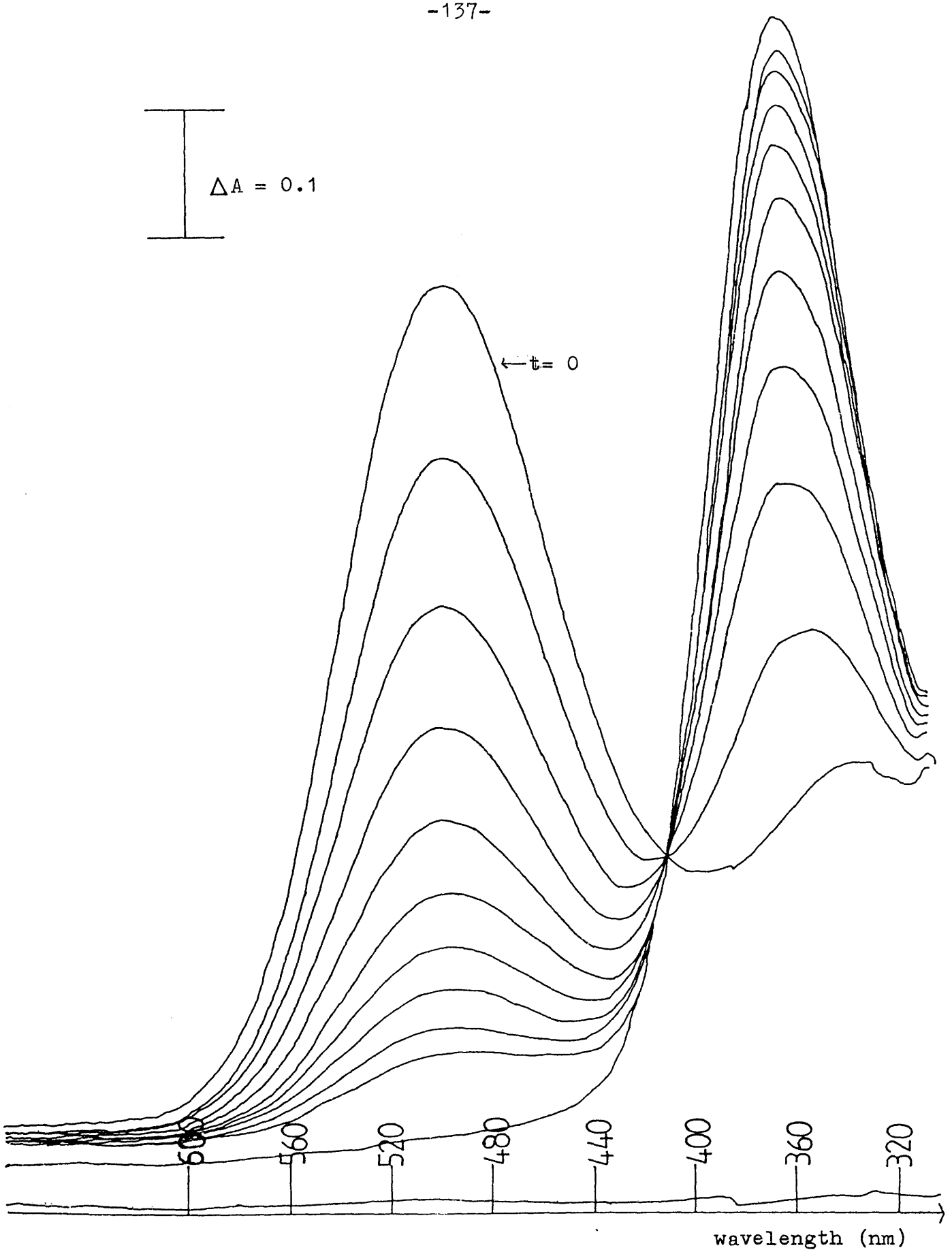

Fig.(3.6). Absorbance changes upon irradiation of cattle rhodopsin at λ= 460 nm.

Plotting $\ln(10^{A_t-A_f} - 1)$ versus t, Fig.(3.5b) gives a line with gradient, m = -0.1552.

Calculation of ϕ for cattle rhodopsin:-

t(min)	$-A_t+A_f$	$(1-10^{-A_t+A_f})^{-1}$	$1-10^{-A_t}$	$\frac{A_t-A_f}{A_t}$	ϕ
0	-0.462	1.5271	0.7042	0.8733	0.9391
2	-0.373	1.7350	0.6369	0.8477	0.9367
4	-0.287	2.0679	0.5574	0.8107	0.9345
6	-0.223	2.4901	0.4871	0.7690	0.9327
8	-0.172	3.0579	0.4232	0.7197	0.9314
10	-0.136	3.7194	0.3734	0.6699	0.9304
12	-0.103	4.7362	0.3239	0.6059	0.9295
14	-0.082	5.8120	0.2904	0.5503	0.9288
16	-0.061	7.6312	0.2553	0.4766	0.9285
18	-0.047	9.7493	0.2309	0.4123	0.9281

Average value of ϕ for cattle rhodopsin = 0.93.

Thus applying equation (3.29) :-

$$(\varepsilon_r\gamma_r + \varepsilon_m\gamma_m) = \frac{-0.1862}{-0.1552} \times 28000 \times \frac{0.93}{0.72} \times 0.67$$

$$= 29078$$

(b) Using potassium ferrioxalate as actinometer:-

From section (3.4.1), $I_o = 7.47\ 10^{-9}$ E/min.

Using equation (3.28) :-

$$\ln(10^{A_t - A_f} - 1) = \frac{-\phi(\varepsilon_r\gamma_r + \varepsilon_m\gamma_m)\ I\ l\ t}{0.434\ V} + \text{constant}$$

From section (3.4.2a), $\ln(10^{A_t - A_f} - 1)$ versus t has gradient:-

$$m = -0.1862$$

and ϕ was calculated to be 0.72.

Thus, $(\varepsilon_r\gamma_r + \varepsilon_m\gamma_m) = 30050$

Thus the results obtained using both cattle rhodopsin and potassium ferrioxalate as actinometer are identical within the limits of experimental error.

For irradiation at λ= 520 nm.
With cattle rhodopsin as actinometer.

Octopus rhodopsin:- Spectrum of absorbance changes given in Fig.(3.7).

t(min)	A_{520}	$A_t - A_f$	$\ln(10^{A_t - A_f} - 1)$
0	0.3535	0.079	-1.6119
1	0.3235	0.049	-2.1250
2	0.3095	0.035	-2.4778
4	0.2865	0.012	-3.5750
6	0.2815	0.007	-4.1199
11	0.2745	0	———

Plotting $\ln(10^{A_t - A_f} - 1)$ versus t, Fig.(3.8a) gives

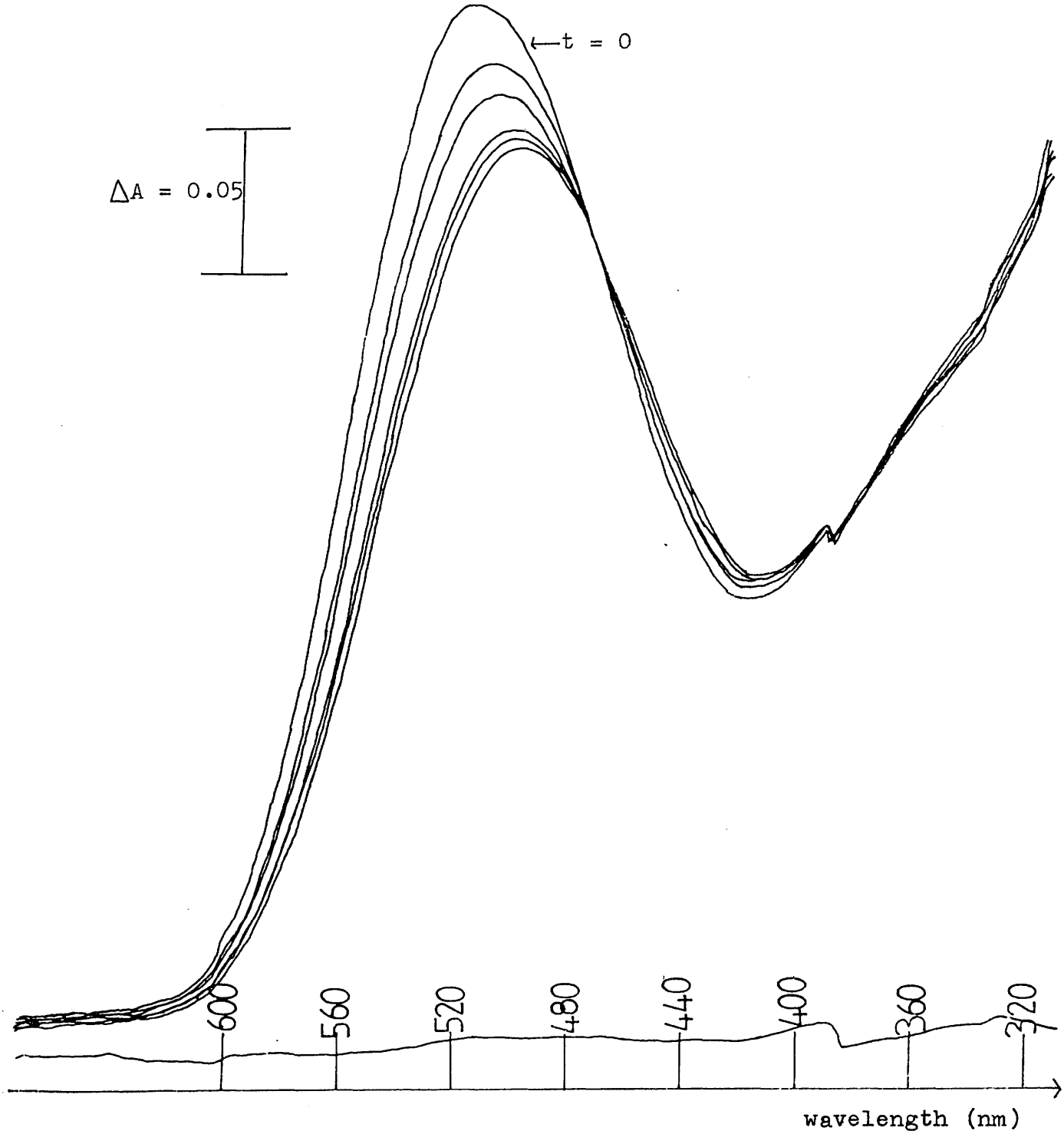

Fig.(3.7). Absorbance changes upon irradiation of octopus acid metarhodopsin at λ= 520 nm.

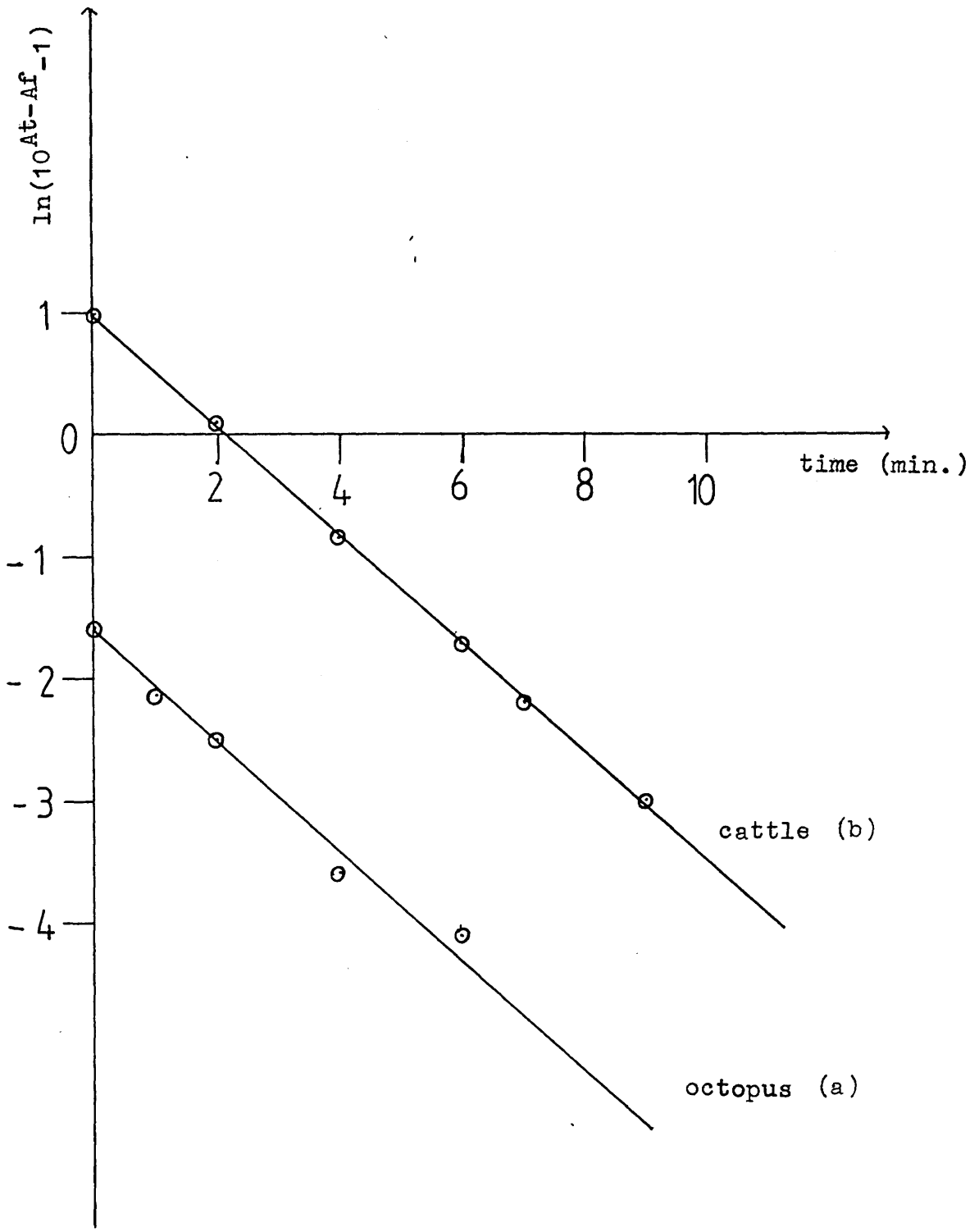

Fig.(3.8). Plot of $\ln(10^{At-Af}-1)$ versus time for irradiation of cattle and octopus rhodopsin at λ= 520 nm.

a line of gradient, m = -0.4282.

Calculation of ϕ for octopus rhodopsin:-

t(min)	$-A_t+A_f$	$(1-10^{-A_t+A_f})^{-1}$	$(1-10^{-A_t})$	$\frac{A_t-A_f}{A_t}$	ϕ
0	-0.079	6.0125	0.5569	0.2235	0.7484
1	-0.049	9.3726	0.5252	0.1515	0.7458
2	-0.035	12.9151	0.5097	0.1131	0.7445
4	-0.012	36.6935	0.4830	0.0419	0.7426
6	-0.007	62.5434	0.4770	0.0249	0.7428

Average value of ϕ = 0.75.

Cattle rhodopsin:- Spectrum of absorbance changes given in Fig.(3.9).

t(min)	A_{520}	$A_t - A_f$	$\ln(10^{A_t - A_f} - 1)$
0	0.655	0.562	0.9736
2	0.415	0.322	0.0943
4	0.245	0.152	-0.8697
5	0.200	0.107	-1.2753
6	0.164	0.071	-1.7282
7	0.139	0.046	-2.1917
9	0.114	0.021	-3.0049
14	0.093	0	

Plotting $\ln(10^{A_t - A_f} - 1)$ versus t Fig.(3.8b), gives a line of gradient, m = -0.4557.

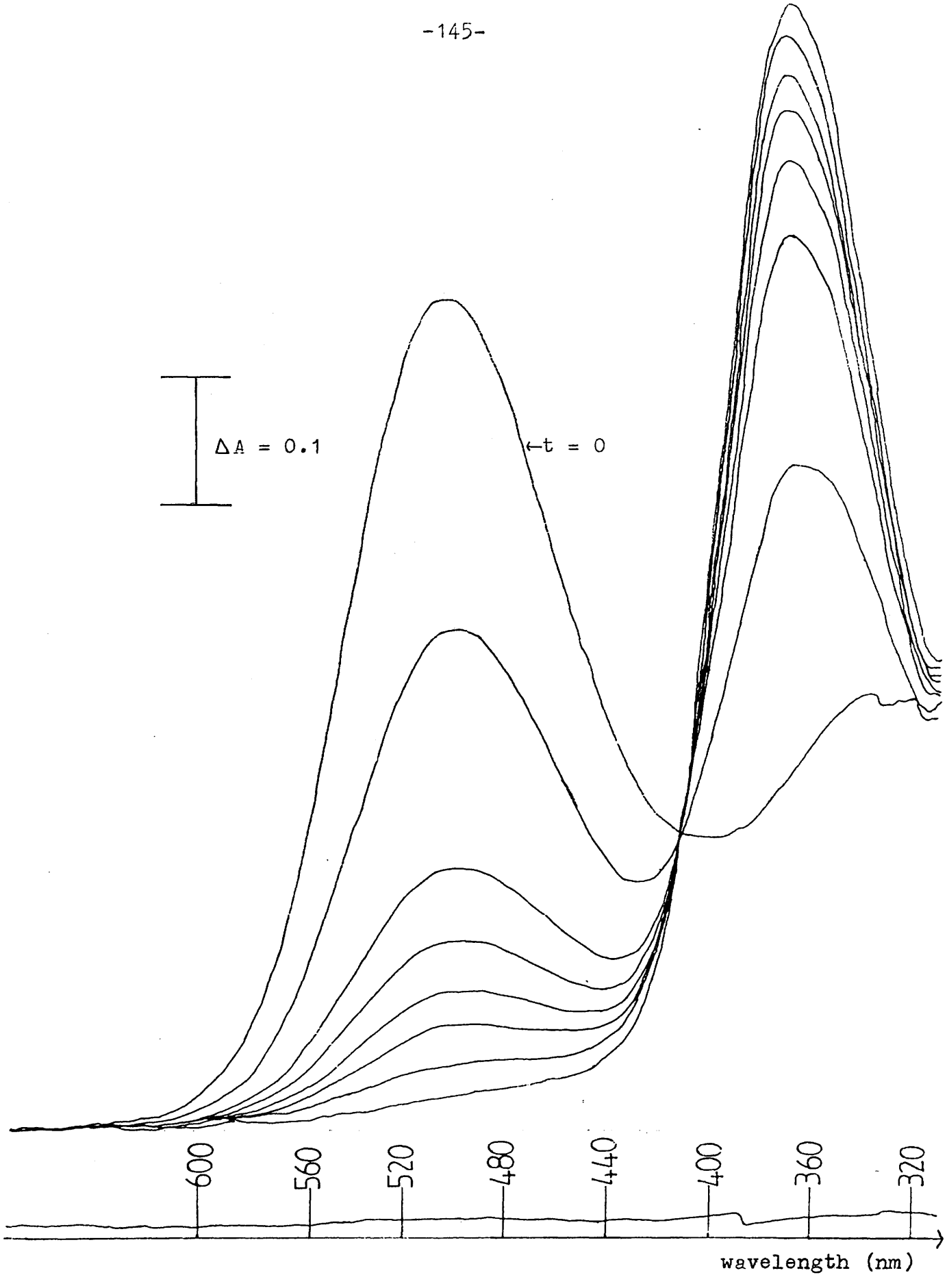

Fig.(3.9). Absorbance changes upon irradiation of cattle rhodopsin at λ= 520 nm.

Calculation of ϕ for cattle rhodopsin :-

t(min)	$-A_t+A_f$	$(1-10^{-A_t+A_f})^{-1}$	$1-10^{-A_t}$	$\frac{A_t-A_f}{A_t}$	ϕ
0	-0.562	1.3777	0.7787	0.8580	0.9205
2	-0.322	1.9099	0.6154	0.7759	0.9120
4	-0.152	3.3863	0.4311	0.6204	0.9057
5	-0.107	4.5793	0.3690	0.5350	0.9040
6	-0.071	6.6304	0.3145	0.4329	0.9027
7	-0.046	9.9500	0.2739	0.3309	0.9018
9	-0.021	21.1847	0.2309	0.1842	0.9010

Average value of ϕ = 0.91.

Thus applying equation (3.29):-

$$(\varepsilon_r\gamma_r + \varepsilon_m\gamma_m) = \frac{-0.4282}{-0.4557} \times 36700 \times \frac{0.91}{0.75} \times 0.67$$

$$= 28034$$

For irradiation at λ= 540 nm.

With cattle rhodopsin as actinometer.

Octopus rhodopsin:- Spectrum of absorbance changes given in Fig.(3.10).

t(sec.)	A_{540}	$A_t - A_f$	$\ln(10^{A_t-A_f} - 1)$
0	0.2690	0.1200	-1.1449
15	0.2400	0.0910	-1.4563
30	0.2210	0.0720	-1.7130
45	0.2065	0.0575	-1.9550
75	0.1835	0.0345	-2.4928
105	0.1705	0.0215	-2.9809
165	0.1605	0.0115	-3.6181
345	0.1490	0	

Plotting a graph of $\ln(10^{A_t-A_f} - 1)$ versus t Fig.(3.11a)

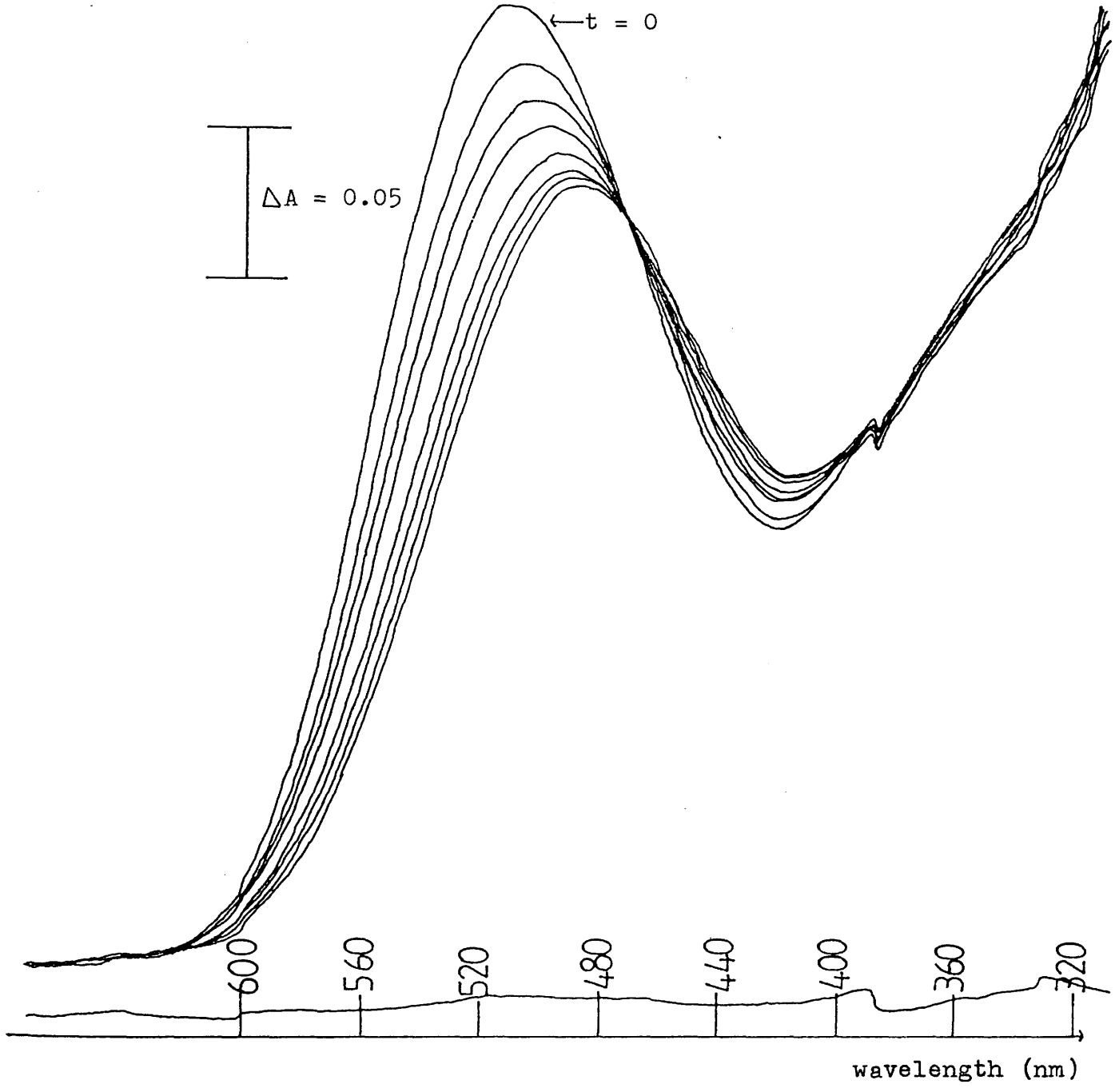

Fig.(3.10). Absorbance changes upon irradiation of octopus acid metarhodopsin at λ= 540 nm.

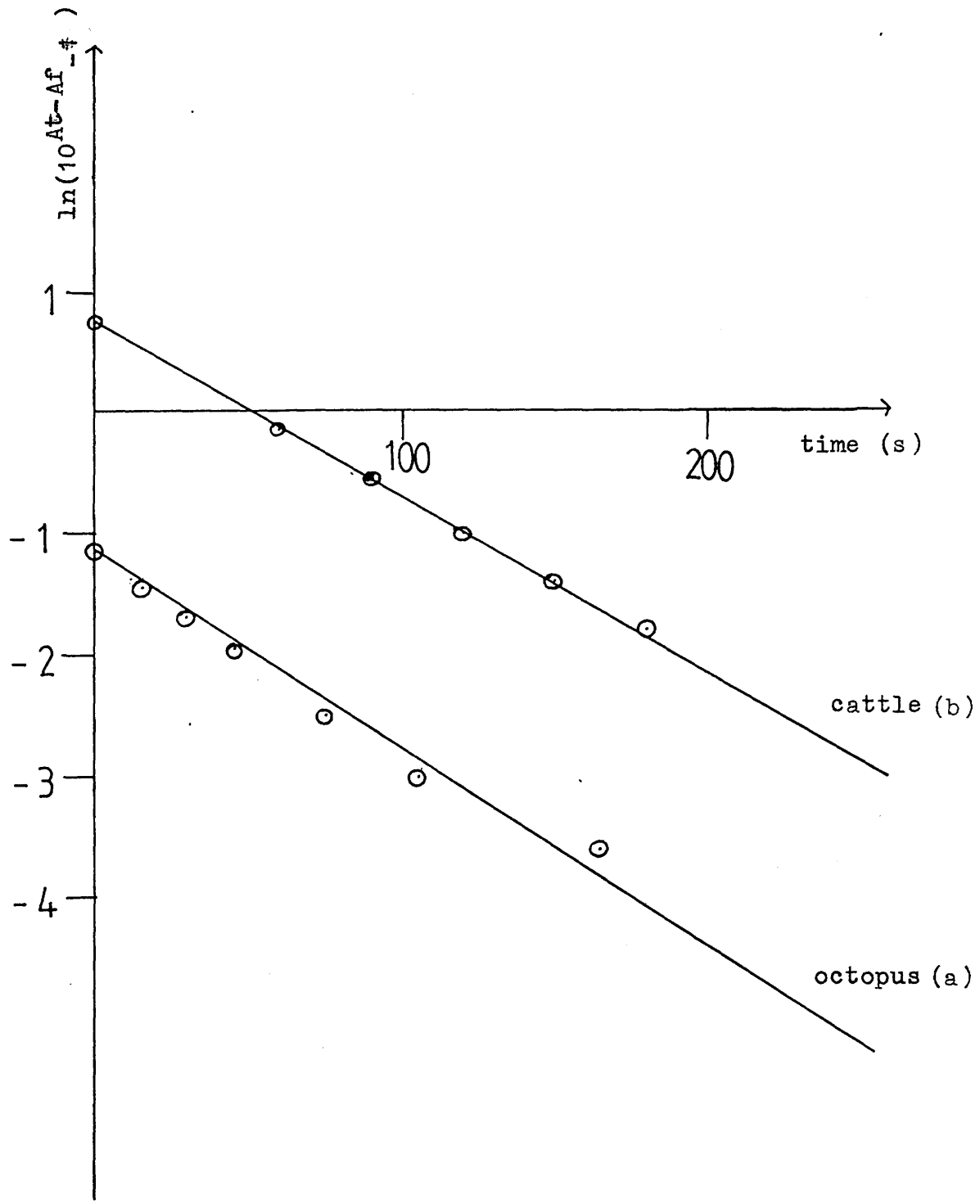

Fig.(3.11). Plot of $\ln(10^{At-Af}-1)$ versus time for irradiation of cattle and octopus rhodopsin at λ= 540 nm.

gives a line with gradient, m = -0.0152.

Calculation of ϕ for octopus rhodopsin :-

t(sec)	$-A_t+A_f$	$(1-10^{-A_t+A_f})^{-1}$	$1-10^{-A_t}$	$\frac{A_t-A_f}{A_t}$	ϕ
0	-0.1200	4.1421	0.4617	0.4461	0.8531
15	-0.0910	5.2899	0.4246	0.3791	0.8515
30	-0.0720	6.5457	0.3988	0.3258	0.8505
45	-0.0575	8.0640	0.3784	0.2785	0.8498
75	-0.0345	13.0949	0.3446	0.1880	0.8484
105	-0.0215	20.7039	0.3247	0.1261	0.8477
165	-0.0115	38.2669	0.3090	0.0717	0.8478

Average value of ϕ = 0.85

Cattle rhodopsin:- Spectrum of absorbance changes given in Fig.(3.12).

t(sec)	A_{540}	$A_t - A_f$	$\ln(10^{A_t - A_f} - 1)$
0	0.528	0.494	0.7509
60	0.304	0.270	-0.1484
90	0.230	0.196	-0.5615
120	0.168	0.134	-1.0176
150	0.130	0.096	-1.3968
180	0.100	0.066	-1.8071
420	0.034	0	———

Plotting a graph of $\ln(10^{A_t - A_f} - 1)$ versus t, Fig.(3.11b) gives a line of gradient, m = -0.0142.

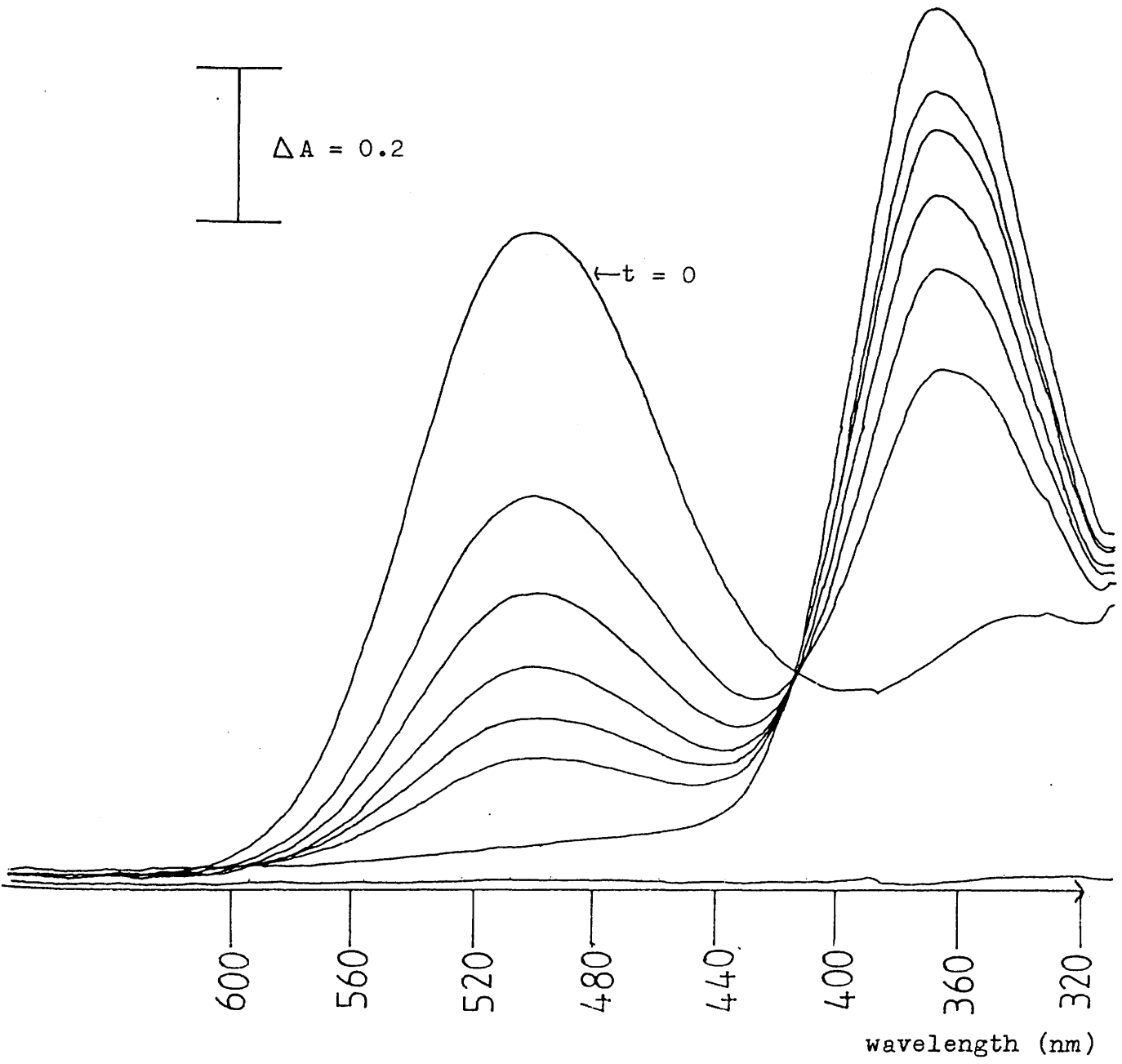

Fig.(3.12). Absorbance changes upon irradiation of cattle rhodopsin at λ= 540 nm.

Calculation of ϕ for cattle rhodopsin:-

t(s)	$-A_t+A_f$	$(1-10^{-A_t+A_f})^{-1}$	$1-10^{-A_t}$	$\frac{A_t-A_f}{A_t}$	ϕ
0	-0.494	1.4719	0.7035	0.9356	0.9688
60	-0.270	2.1599	0.5034	0.8881	0.9657
90	-0.196	2.7533	0.4112	0.8522	0.9648
120	-0.134	3.7663	0.3208	0.7976	0.9638
150	-0.096	5.0423	0.2587	0.7385	0.9633
180	-0.066	7.0929	0.2057	0.6600	0.9629

Average value of ϕ = 0.96

Thus applying equation (3.29) :-

$$(\varepsilon_r \gamma_r + \varepsilon_m \gamma_m) = \frac{-0.0152}{-0.0142} \times 25660 \times 0.67 \times \frac{0.96}{0.85}$$

$$= 20784$$

Summary of results from Dartnall's method.

λ irradiation	460	520	540
$\varepsilon_r\gamma_r + \varepsilon_m\gamma_m$ (a)	29078	28034	20784
$\varepsilon_r\gamma_r + \varepsilon_m\gamma_m$ (b)	30050	———	———

(a) Using cattle rhodopsin as actinometer.

(b) Using potassium ferrioxalate as actinometer.

Separation of quantum yields using simultaneous equations:-

With value (a) for λ=460.

1. $28300\,\gamma_r + 22600\,\gamma_m = 29078$; $\quad \gamma_m = \dfrac{29078 - 28300\gamma_r}{22600}$

2. $14850\,\gamma_r + 43500\,\gamma_m = 28034$; $\quad \gamma_m = \dfrac{28034 - 14850\gamma_r}{43500}$

3. $7425\,\gamma_r + 37300\,\gamma_m = 20784$; $\quad \gamma_m = \dfrac{20784 - 7425\gamma_r}{37300}$

Taking equations 1 and 2:-

$$28300\,\gamma_r - 7715\,\gamma_r = 14513$$

$$20585\,\gamma_r = 14513$$

$$\gamma_r = 0.705 \; ; \qquad \gamma_m = 0.404$$

Taking equations 1 and 3 :-

$$28300\,\gamma_r - 4499\,\gamma_r = 16485$$

$$23801\,\gamma_r = 16485$$

$$\gamma_r = 0.693 \; ; \qquad \gamma_m = 0.419$$

Taking equations 2 and 3 :-

$$14850\,\gamma_r - 8659\,\gamma_r = 3795$$

$$6191\,\gamma_r = 3795$$

$$\gamma_r = 0.613 \; ; \qquad \gamma_m = 0.435$$

average value for $\gamma_r = 0.670 \pm 0.050$

average value for $\gamma_m = 0.419 \pm 0.016$

With value (b) for $\lambda = 460$ nm.

1. $28300\,\gamma_r + 22600\,\gamma_m = 30050$; $\qquad \gamma_m = \dfrac{30050 - 28300\,\gamma_r}{22600}$

2. $14850\,\gamma_r + 43500\,\gamma_m = 28034$; $\qquad \gamma_m = \dfrac{28034 - 14850\,\gamma_r}{43500}$

3. $7425\,\gamma_r + 37300\,\gamma_m = 20784$; $\qquad \gamma_m = \dfrac{20784 - 7425\,\gamma_r}{37300}$

Taking equations 1 and 2 :-

$$28300\gamma_r - 7715\gamma_r = 15485$$

$$20585\gamma_r = 15485$$

$$\gamma_r = 0.752 \; ; \qquad \gamma_m = 0.388$$

Taking equations 1 and 3 :-

$$28300\,\gamma_r - 4499\,\gamma_r = 17457$$

$$23801\,\gamma_r = 17457$$

$$\gamma_r = 0.733 \; ; \qquad \gamma_m = 0.412$$

Taking equations 2 and 3 gives $\gamma_r = 0.613$ and $\gamma_m = 0.435$ as before.

average value for $\gamma_r = 0.699 \pm 0.062$

average value for $\gamma_m = 0.412 \pm 0.019$

3.4.3 Analysis of results using Kropf's method.

For irradiation at $\lambda = 460$ nm.

(a) Using cattle rhodopsin as actinometer:-

A value for I_o is obtained from application of equation (3.36) to changes in cattle rhodopsin absorbance Fig.(3.6). The product in the presence of hydroxylamine hydrochloride is retinal oxime. The results are tabulated on the following page.

t	A_{460}	$A_t - A_f$	A_{367}	$A_t - A_o$	Ω
0	0.529	0.462	0.298	0	0
2	0.440	0.373	0.438	0.140	0.3397
4	0.354	0.287	0.567	0.269	0.7206
6	0.290	0.223	0.661	0.363	1.0669
8	0.239	0.172	0.735	0.437	1.4015
10	0.203	0.136	0.792	0.494	1.6960
12	0.170	0.103	0.838	0.540	2.0288
14	0.149	0.082	0.868	0.570	2.2956
16	0.128	0.061	0.895	0.597	2.6341
18	0.114	0.047	0.910	0.612	2.9281
∞	0.067	0	0.940	0.642	———

Using equation (3.36):-

E = k l = absorbance due to impurities = 0.067

but, $k = \varepsilon_i c_i$; where ε_i = the decadic molar extinction coefficient of any impurities.

c_i = concentration of impurities.

Since equation (3.36) is derived in terms of α,

where $\alpha = \varepsilon / 0.434$,

absorbance due to impurities, $E = \frac{\varepsilon_i c_i}{0.434}$.

In this case E = 0.067/ 0.434 = 0.1544

$\varepsilon_r = 28014$; $\varepsilon_p = 51600$

A graph of Ω versus t, Fig.(3.13), gives a line zero weighted to pass through the origin of gradient,

$$m = \frac{\gamma_\lambda \varepsilon_\lambda I_o}{0.434\ V} = 0.1656$$

which gives a value of 7.66×10^{-9} E/min. for I_o.

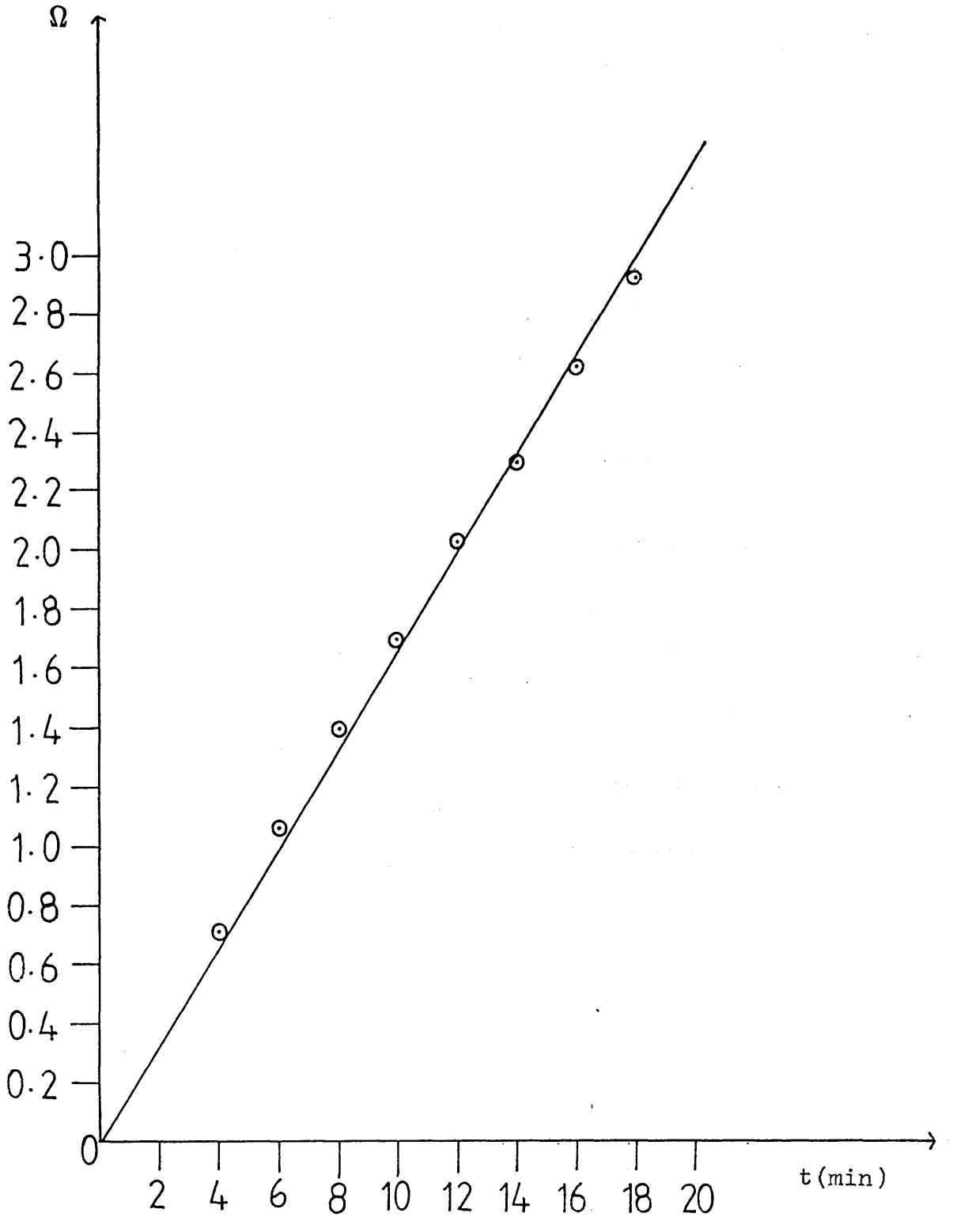

Fig.(3.13). Kropf plot for cattle rhodopsin at λ= 460 nm.

Using this value of I_o in equation (3.44) and using absorbance changes in octopus rhodopsin Fig.(3.4) :-

t(min)	A_{580}	$[R]$	$[M]$	Ψ	$\int I_o \, dt$
0	0.0585	1.1111×10^{-5}	0	0	0
2	0.0845	7.4490×10^{-6}	3.6620×10^{-6}	0.5843	1.532×10^{-8}
4	0.0990	5.4068×10^{-6}	5.7042×10^{-6}	1.0467	3.064×10^{-8}
6	0.1110	3.7166×10^{-6}	7.3944×10^{-6}	1.5832	4.596×10^{-8}
8	0.1170	2.8716×10^{-6}	8.2394×10^{-6}	1.9514	6.128×10^{-8}
11	0.1270	1.4631×10^{-6}	9.6497×10^{-6}	2.9182	8.426×10^{-8}
14	0.1310	8.9973×10^{-7}	10.2112×10^{-6}	3.6267	10.724×10^{-8}
∞	0.1370	5.4662×10^{-7}	11.0563×10^{-6}	____	____

A_{580} was used to calculate concentrations since only acid metarhodopsin should absorb here.

$\varepsilon_r = 28300$; $\varepsilon_m = 22600$; $E = 0.10$; ε_{580} acid M =7100

A graph of Ψ versus $\int I_o \, dt$ was plotted Fig.(3.14). According to equation (3.44), this should give a line zero weighted to pass through the origin of gradient :-

$$m = \frac{\varepsilon_r \gamma_r + \varepsilon_m \gamma_m}{0.434 \ V} = 3.3802 \times 10^7$$

$$(\varepsilon_r \gamma_r + \varepsilon_m \gamma_m) = 29340$$

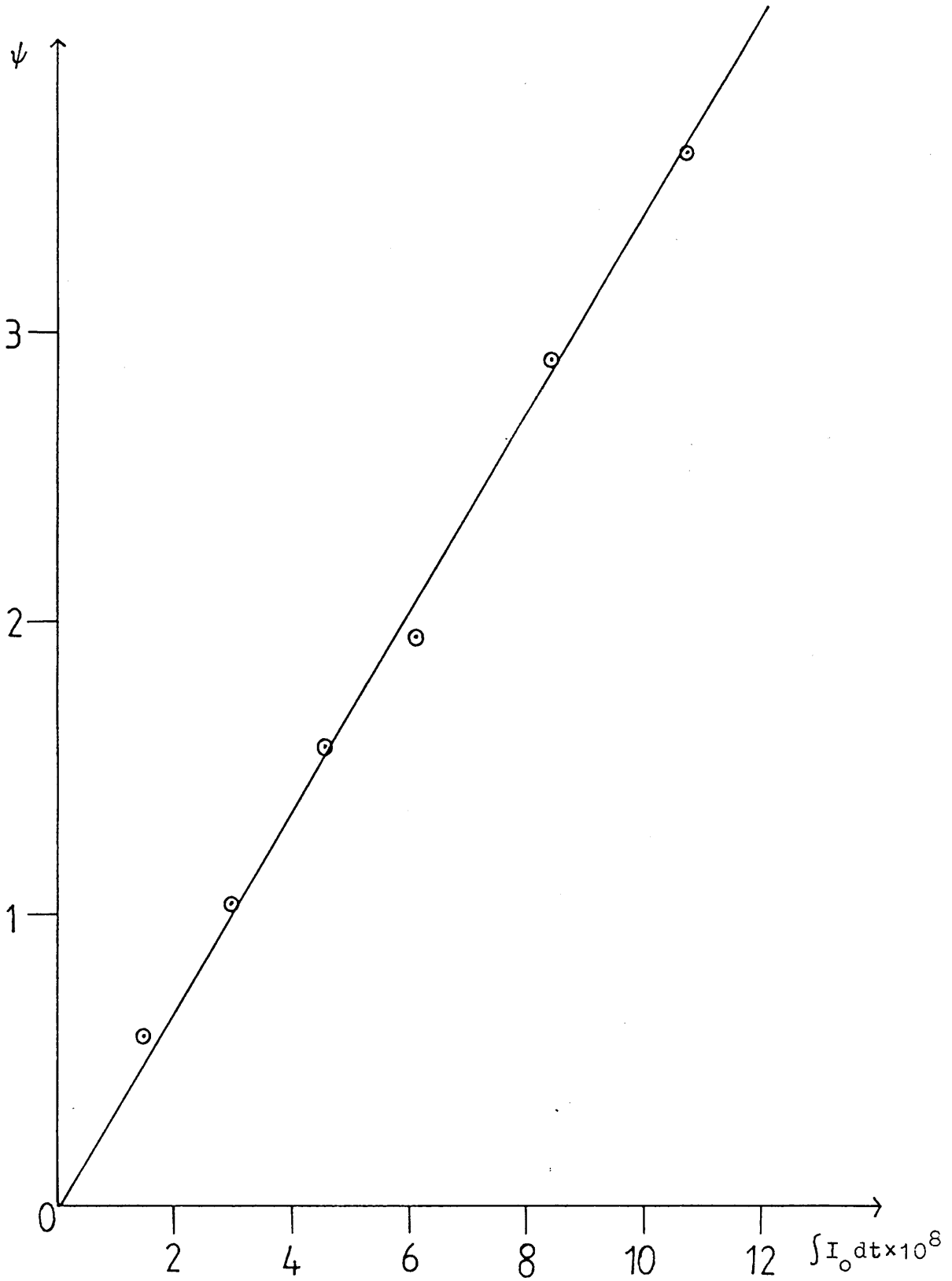

Fig.(3.14). Modified Kropf plot for octopus rhodopsin at λ = 460 nm.

(b) Using potassium ferrioxalate as chemical actinometer:-

t(min)	ψ	$\int I_o \, dt$
0	0	0
2	0.5843	1.494×10^{-8}
4	1.0467	2.988×10^{-8}
6	1.5832	4.482×10^{-8}
8	1.9514	5.976×10^{-8}
11	2.9182	8.217×10^{-8}
14	3.6267	10.458×10^{-8}

Plotting ψ versus $\int I_o \, dt$ (equation 3.44), gives a straight line zero weighted to pass through the origin of gradient :- Fig.(3.15)

$$m = \frac{\varepsilon_r \gamma_r + \varepsilon_m \gamma_m}{0.434 \; V} = 3.4655 \times 10^7$$

$$(\varepsilon_r \gamma_r + \varepsilon_m \gamma_m) = 30081$$

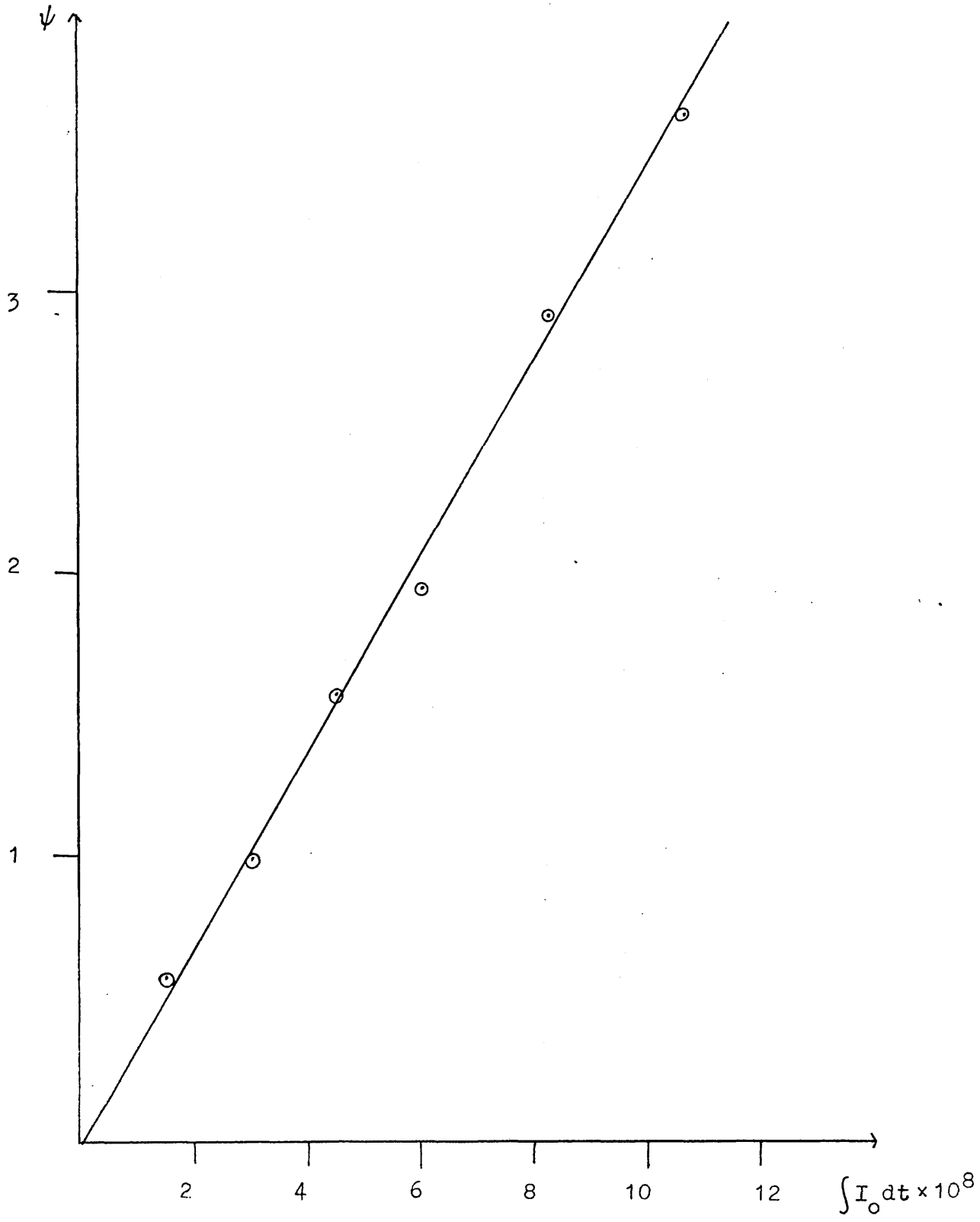

Fig.(3.15). Modified Kropf plot for octopus rhodopsin at λ = 460 nm using potassium ferrioxalate determined value for I_o.

For irradiation at λ= 520 nm.

As for λ= 460 nm, a value for I_o may be calculated from changes in cattle rhodopsin absorbance Fig.(3.9).

t(min)	A_{520}	$A_t - A_\infty$	A_{367}	$A_t - A_o$	Ω
0	0.655	0.562	0.340	0	0
2	0.415	0.322	0.593	0.253	0.9392
4	0.245	0.152	0.775	0.435	1.9945
5	0.200	0.107	0.834	0.494	2.4545
6	0.164	0.071	0.882	0.542	2.9664
7	0.139	0.046	0.900	0.560	3.4694
9	0.114	0.021	0.930	0.590	4.3747
14	0.093	0	0.959	0.619	——

$\varepsilon_{r\lambda}$ = 28014 ; $\varepsilon_{m\lambda}$ = 51600 ; E = 0.21 ;

Using equation (3.36) a graph of Ω versus t , Fig.(3.16), gives a line zero weighted to pass through the origin of gradient:-

$$m = \frac{\gamma, \varepsilon, I_o}{0.434\ V} = 0.4911$$

which gives a value of $1.73\ 10^{-8}$ E/min. for I_o.

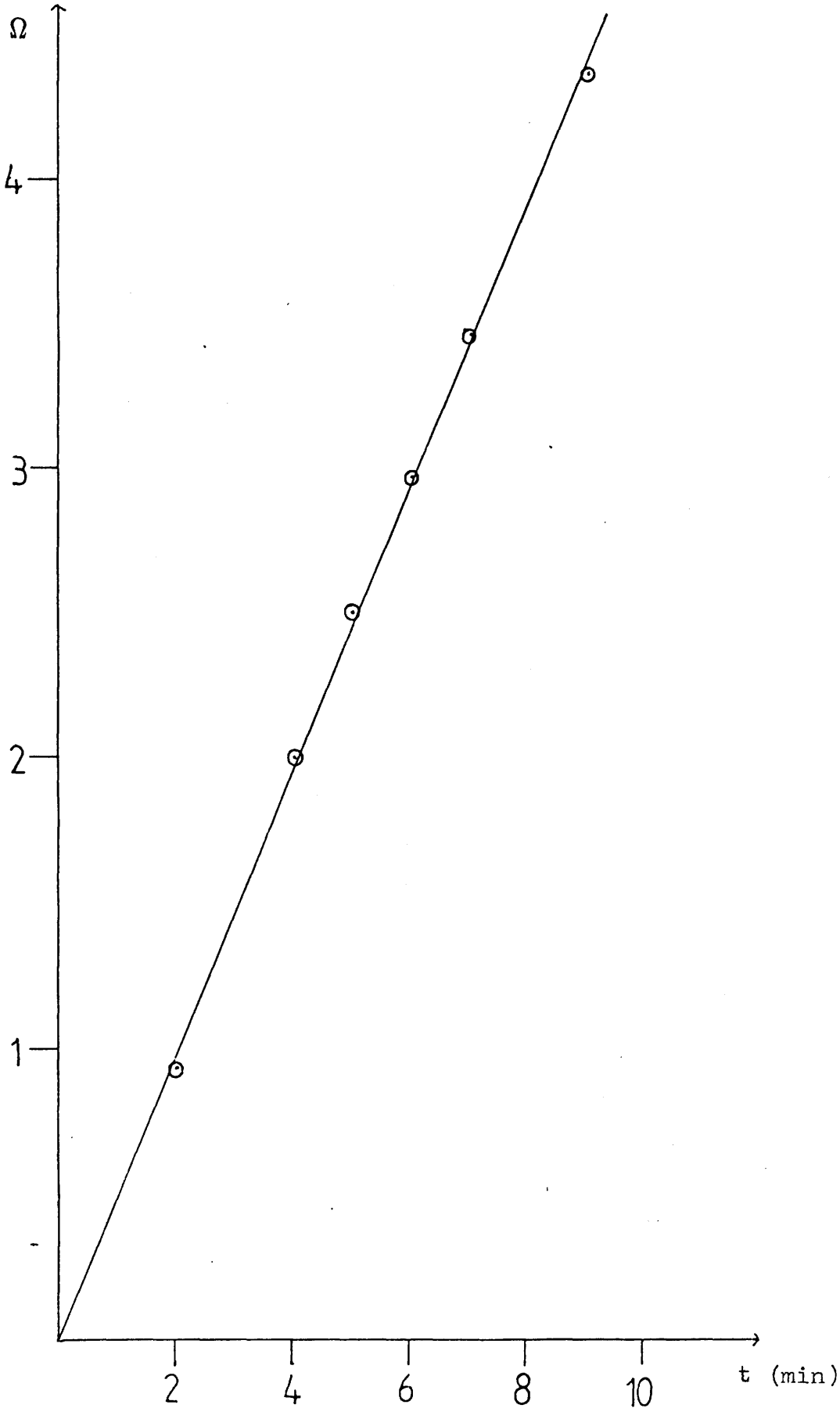

Fig.(3.16). Kropf plot for cattle rhodopsin at λ=520 nm.

Using this value of I_o in equation (3.44) and using absorbance changes in octopus rhodopsin Fig.(3.7) :-

t	A_{580}	[R]	[M]	ψ	$\int I_o dt$
0	0.0975	0	8.1609×10^{-6}	0	0
1	0.0850	1.7606×10^{-6}	6.4003×10^{-6}	0.7544	1.73×10^{-8}
2	0.0815	2.2535×10^{-6}	5.9074×10^{-6}	1.0517	3.46×10^{-8}
4	0.0720	3.5915×10^{-6}	4.5694×10^{-6}	2.4318	6.92×10^{-8}
6	0.0690	4.0141×10^{-6}	4.1468×10^{-6}	3.4916	10.38×10^{-8}
11	0.0665	4.3662×10^{-6}	3.7947×10^{-6}	———	———

Where $\varepsilon_{r\lambda} = 14850$; $\varepsilon_{m\lambda} = 43500$; $E = 0.0576$

A graph of ψ versus $\int I_o dt$ was plotted Fig.(3.17). According to equation (3.44), this should give a line weighted to pass through the origin of gradient:-

$$m = \frac{\varepsilon_r \gamma_r + \varepsilon_m \gamma_m}{0.434\ V} = 3.4032 \times 10^{7}$$

$$\underline{(\varepsilon_r \gamma_r + \varepsilon_m \gamma_m) = 29540}$$

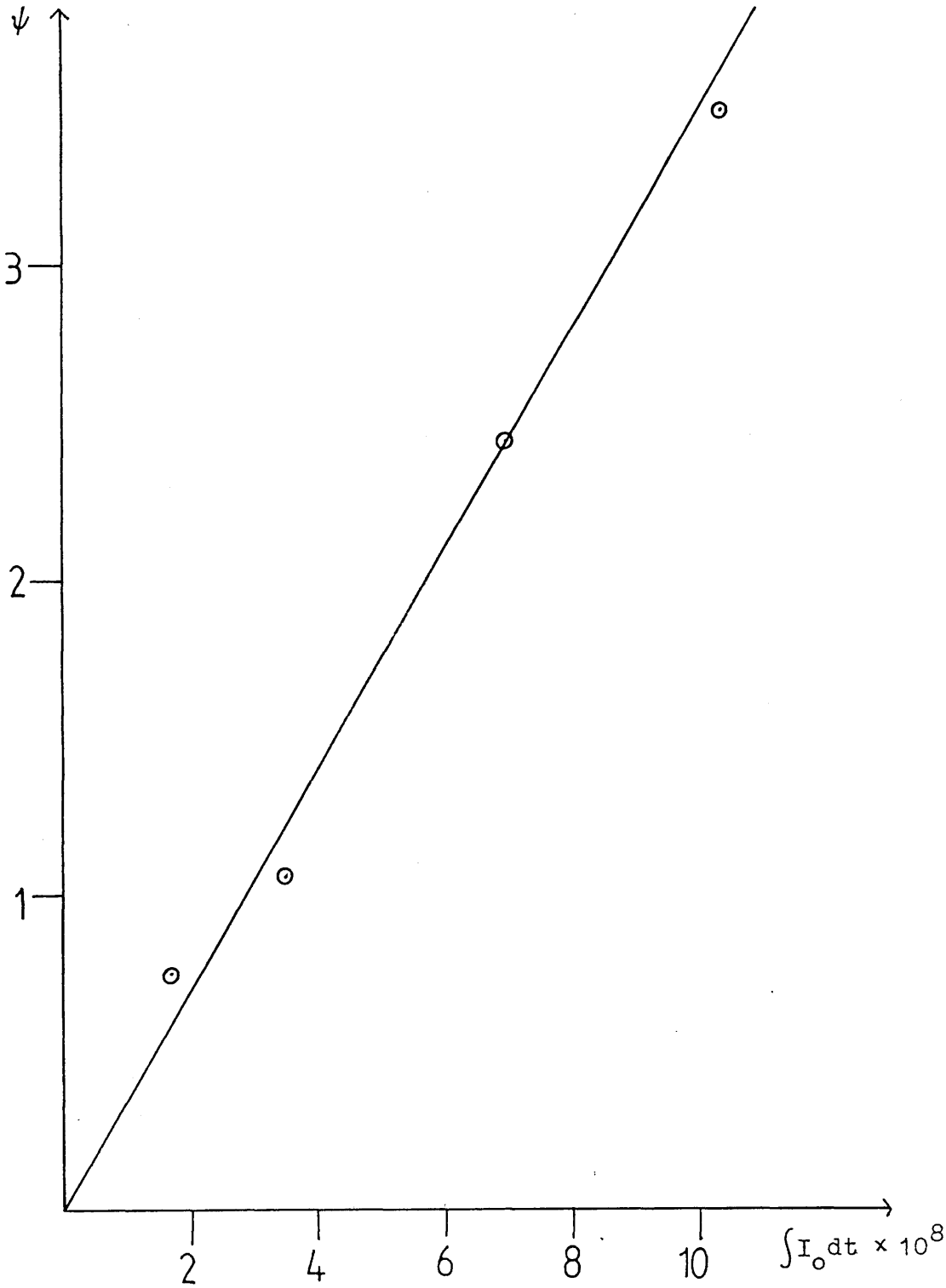

Fig.(3.17). Modified Kropf plot for octopus rhodopsin at λ= 520 nm.

For irradiation at λ= 540 nm.

As for λ= 520 nm, a value for I_o may be calculated from changes in cattle rhodopsin absorbance Fig.(3.9).

t(s)	A_{540}	$A_t - A_\infty$	A_{367}	$A_t - A_o$	Ω
0	0.528	0.494	0.300	0	0
60	0.304	0.270	0.684	0.384	0.8877
90	0.230	0.196	0.816	0.516	1.3063
120	0.168	0.134	0.912	0.612	1.7628
150	0.130	0.096	1.000	0.700	2.1646
180	0.100	0.066	1.050	0.750	2.5859
420	0.034	———	1.162	0.862	———

ε_{r_λ} = 25659 ; ε_{p_λ} = 51600 ; E = 0.0783

Using equation (3.36), a graph of Ω versus t, Fig.(3.17). gives a line zero weighted to pass through the origin of gradient :-

$$m = \frac{\gamma_\lambda \varepsilon_\lambda I_o}{0.434\ V} = 0.0145$$

which gives a value of 7.31×10^{-10} E/sec. for I_o.

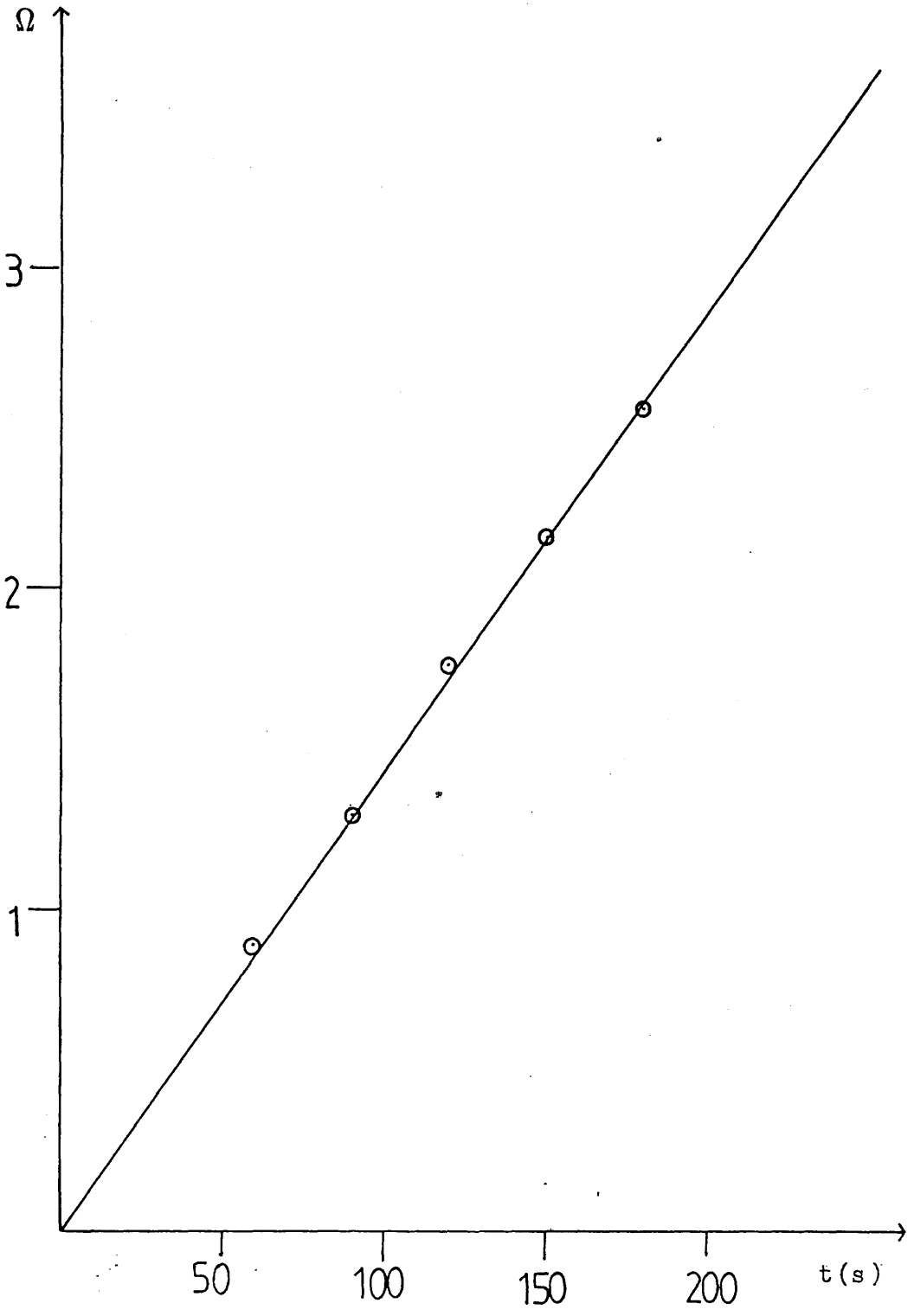

Fig.(3.18). Kropf plot for cattle rhodopsin at λ= 540 nm.

Using this value of I_o in equation (3.44) and using absorbance changes in octopus rhodopsin Fig.(3.10):-

t	A_{580}	[M]	[R]	ψ	$\int I_o dt$
0	0.0940	7.4713×10^{-6}	0	0	0
15	0.0840	6.0628×10^{-6}	1.4085×10^{-6}	0.3673	1.0965×10^{-8}
30	0.0800	5.4995×10^{-6}	1.9718×10^{-6}	0.5422	2.1930×10^{-8}
45	0.0735	4.5839×10^{-6}	2.8873×10^{-6}	0.8791	3.2895×10^{-8}
75	0.0650	3.3868×10^{-6}	4.0845×10^{-6}	1.4965	5.4825×10^{-8}
105	0.0600	2.6826×10^{-6}	4.7887×10^{-6}	2.0692	7.6725×10^{-8}
165	0.0565	2.1192×10^{-6}	5.3521×10^{-6}	2.8547	12.0620×10^{-8}
∞	0.0520	1.5206×10^{-6}	5.9507×10^{-6}	———	———

$\varepsilon_{r\lambda} = 7425$; $\varepsilon_{m\lambda} = 37300$; $E = 0.0576$

A graph of ψ versus $\int I_o dt$ was plotted Fig.(3.19). According to equation (3.44), this should give a line zero weighted to pass through the origin of gradient:-

$$m = \frac{\varepsilon_r \gamma_r + \varepsilon_m \gamma_m}{0.434\ V} = 2.5000 \times 10^7$$

$$(\varepsilon_r \gamma_r + \varepsilon_m \gamma_m) = 21700$$

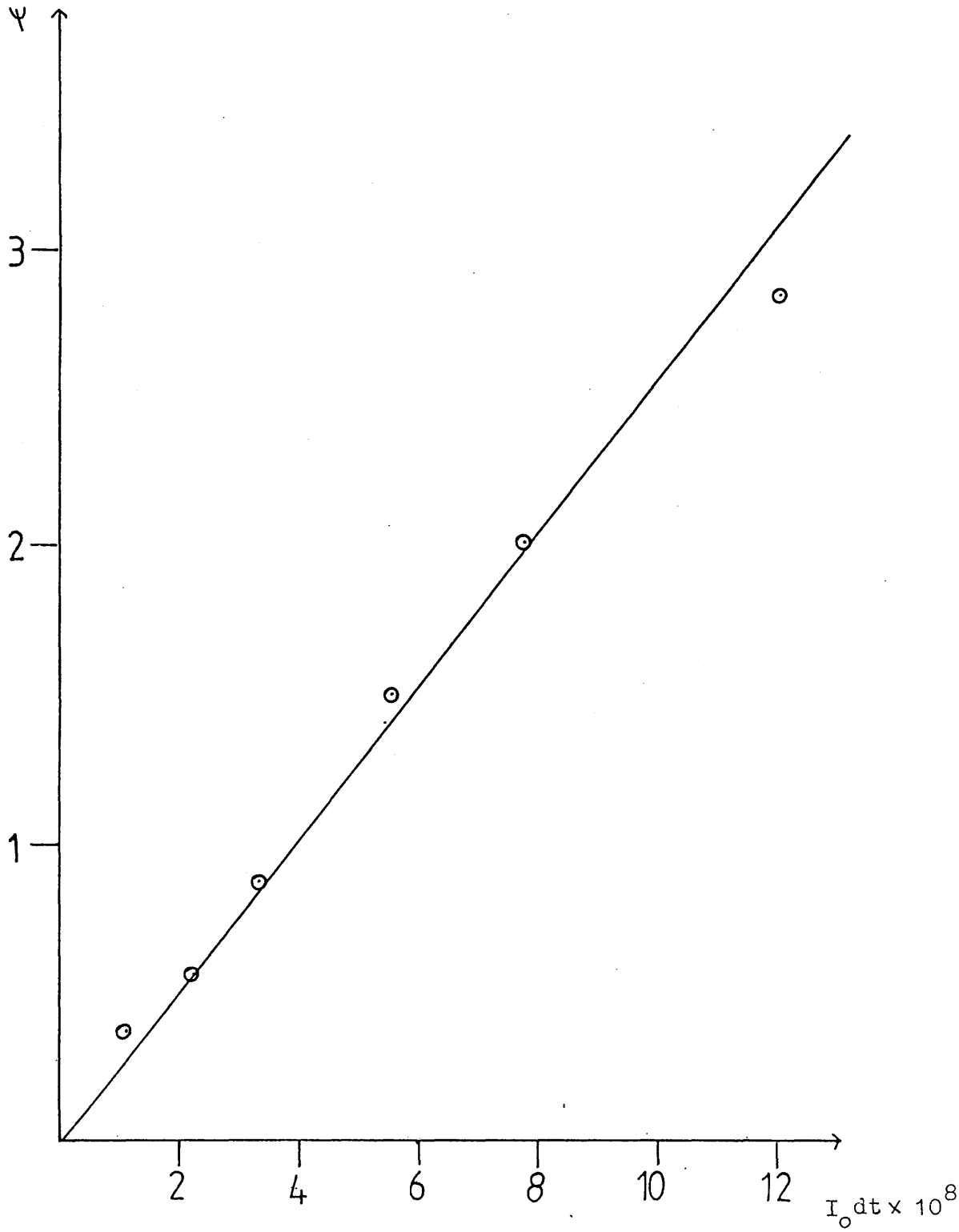

Fig.(3.19). Modified Kropf plot for octopus rhodopsin at λ= 540 nm.

Summary of results from Kropfs method :-

λ irradiation	460 nm	520 nm	540 nm
$\gamma_r\alpha_r + \gamma_m\alpha_m$ (a)	29340	29540	21700
$\gamma_r\alpha_r + \gamma_m\alpha_m$ (b)	30081	———	———

(a) Using cattle rhodopsin as actinometer.

(b) Using potassium ferrioxalate as actinometer.

Separation of quantum yields using simultaneous equations:-

With value (a) for λ = 460 nm.

1. $28300\,\gamma_r + 22600\gamma_m = 29340$; $\quad \gamma_m = \dfrac{29340 - 28300\gamma_r}{22600}$

2. $14850\,\gamma_r + 43500\gamma_m = 29540$; $\quad \gamma_m = \dfrac{29540 - 14850\gamma_r}{43500}$

3. $7425\,\gamma_r + 37300\gamma_m = 21700$; $\quad \gamma_m = \dfrac{21700 - 7425\gamma_r}{37300}$

Taking equations 1 and 2 :-

$$28300\gamma_r - 7715\gamma_r = 13993$$

$$20585\gamma_r = 13993$$

$$\gamma_r = 0.680 \; ; \qquad \gamma_m = 0.447$$

Taking equations 1 and 3 :-

$$28300\gamma_r - 4499\gamma_r = 16192$$

$$23801\gamma_r = 16192$$

$$\gamma_r = 0.680 \; ; \qquad \gamma_m = 0.447$$

Taking equations 2 and 3 :-

$$14850\gamma_r - 8659\gamma_r = 4233$$

$$6191\gamma_r = 4233$$

$$\gamma_r = 0.684 \; ; \qquad \gamma_m = 0.446$$

average value for $\gamma_r = 0.681 \pm 0.002$

average value for $\gamma_m = 0.447 \pm 0.0006$

With value (b) for = 460 nm.

1. $28300\gamma_r + 22600\gamma_m = 30081$; $\gamma_m = \dfrac{30081 - 28300\gamma_r}{22600}$

2. $14850\gamma_r + 43500\gamma_m = 29540$; $\gamma_m = \dfrac{29540 - 14850\gamma_r}{43500}$

3. $7425\gamma_r + 37300\gamma_m = 21700$; $\gamma_m = \dfrac{21700 - 7425\gamma_r}{37300}$

Taking equations 1 and 2 :-

$$28300\gamma_r - 7715\gamma_r = 14734$$

$$20585\gamma_r = 14734$$

$\gamma_r = 0.716$; $\gamma_m = 0.434$

Taking equations 1 and 3 :-

$$28300\gamma_r - 4499\gamma_r = 16933$$

$$23801\gamma_r = 16933$$

$\gamma_r = 0.711$; $\gamma_m = 0.441$

Taking equations 2 and 3 gives $\gamma_r = 0.684$ and $\gamma_m = 0.446$ as before.

average value for $\gamma_r = 0.704 \pm 0.014$

average value for $\gamma_m = 0.440 \pm 0.005$

Summary of Results

	ave. γ_r	ave. γ_m
Dartnall's method using cattle rhodopsin as actinometer.	0.670 ± 0.050	0.419 ± 0.016
Dartnall's method using potassium ferrioxalate as actinometer.	0.699 ± 0.062	0.412 ± 0.019
Kropf's method using cattle rhodopsin as actinometer.	0.681 ± 0.002	0.447 ± 0.001
Kropf's method using potassium ferrioxalate as actinometer.	0.704 ± 0.014	0.440 ± 0.005

average γ_r and γ_m quoted above are the average over all three wavelengths for each method.

Overall averages over three wavelengths and over all methods.	0.689 ± 0.016	0.430 ± 0.017

3.5 Discussion.

The quantum yield of the forward reaction ie. rhodopsin to acid metarhodopsin at 0.689 $\pm$ 0.016 agrees well with Dartnall's prediction that all forward reactions of visual pigments would have a quantum yield in the range 0.65 to 0.70. The value of the backward reaction at 0.430 $\pm$ 0.017 is higher than might have been expected.

From work done on the cattle rhodopsin equilibrium

$$\text{rhodopsin} \underset{\gamma_2}{\overset{\gamma_1}{\rightleftharpoons}} \text{bathorhodopsin} \underset{\gamma_4}{\overset{\gamma_3}{\rightleftharpoons}} \text{isorhodopsin}$$

it was found that $\gamma_r + \gamma_m = 1$ from which it was postulated that bathorhodopsin and rhodopsin populated a common barrierless excited state. Also since :-

$$\gamma_{\text{batho} \rightarrow \text{rhod}} / \gamma_{\text{batho} \rightarrow \text{iso}} \simeq \gamma_{\text{meta} \rightarrow \text{rhod.}} / \gamma_{\text{meta} \rightarrow \text{iso}}$$

it was presumed that bathorhodopsin and metarhodopsin shared a similar photochemistry.

This apparently does not hold for octopus rhodopsin since $\gamma_r + \gamma_m = 1.119$. This either means that the same principles do not hold for invertebrate pigments ie. rhodopsin and bathorhodopsin do not share a common excited state or else the bathorhodopsin and metarhodopsin species are not similar photochemically. ie. bathorhodopsin to rhodopsin may have a different quantum yield to that of metarhodopsin to rhodopsin. It is interesting to note that

Suzuki and Callender (1981) obtained a value of 0.36 for low temperature work on squid rhodopsin which is fairly close to the 0.33 obtained for cattle.

Perhaps bathorhodopsin has a quantum yield of 0.33 in octopus rhodopsin which increases to 0.43 for metarhodopsin to rhodopsin as a result of protein configurational changes. This difference compared to vertebrates may have evolved deliberately to give a higher value for the back reaction since the occurence of a photoregeneration reaction plays a significant role in invertebrate pigment regeneration.

Support for $\gamma_r + \gamma_m > 1$ in octopus rhodopsin comes from work done by Schwemer (1969) on the rhodopsin from octopus Eledone moschata. He found that the relative values of acid metarhodopsin to rhodopsin to be around 1 which would give $\gamma_r + \gamma_m = 1.34$ if $\gamma_r = 0.67$.

Thus it would seem that although vertebrates and invertebrates have a similar quantum yield for the forward reaction, they have evolved a different quantum yield for the back reaction presumably to suit their different regeneration requirements.

Chapter 4

Investigation Of The Metarhodopsin 1 to Metarhodopsin 11 Transition In Cattle Rhodopsin.

Introduction

The metarhodopsin intermediates in the photoreaction of visual pigments have received a lot of attention since they are relatively easy to study and are the last stage at which the neural impulse responsible for vision can occur. (Vision occurs within milliseconds.)

There have been conflicting views as to what the meta I → meta II reaction involves and it is not yet clear what the structural changes are which take place, or what significance these changes have on the visual process.

It is generally accepted that the reaction meta I → meta II involves an opening up of the structure as measured by a large increase in entropy (Matthews et al 1963) and exposure of approximately two sulphydryl groups (Wald and Brown 1951). It is also possible to extract more lipid from bleached rhodopsin than from unbleached rhodopsin, and since hydroxylamine and borohydride can react with the chromophore at meta II, the Schiff base cannot be so protected.

The position of the meta I ⇌ meta II equilibrium has also been shown to be dependent on the temperature, pH and ionic strength of the medium, meta II being favoured by higher temperature, low pH and higher ionic strength. Addition of glycerol and methanol will also favour meta II. (Matthews et al 1963).

The shift in equilibrium with pH corresponds to approximately one proton per molecule of rhodopsin, although conflicting views have been obtained. (Matthews et al 1963,

Abrahamson and Fager 1973, Emreich and Reich 1974, Bennet 1978, Parkes and Liebman 1984).

Originally, the step was postulated to be simple deprotonation of the Schiff base linkage. Yet the reaction proceeds with proton uptake. This apparent inconsistency forced postulations that two titrating groups on opsin are exposed during the reaction.(Matthews et al 1963).

This result seems somewhat clumsy and another approach was taken by Cooper and Converse (1976):- that hydrolysis of the Schiff base bond occurred during the meta I to meta II transition, releasing an amino group for proton titration. The pK_a for the titration would fit this result.

The only inconsistency is the result for reduction of meta II with sodium borohydride. This suggests that at meta II, the chromophore and protein are still attached.

In a bid to resolve this apparent inconsistency, it was decided to follow the meta I to meta II transition in the presence of labelled water to determine whether or not hydrolysis of the Schiff base occurs during the meta I to meta II transition.

The planned experiment was to bleach freeze-dried rhodopsin. This should give meta I, since formation of meta II will not occur in the absence of water.(Wald et al 1950). Labelled H_2O^{18} at 0°C with sufficient phosphate buffer to give a pH of 5.5 was added to the rhodopsin, which should then result in the formation of meta II, since lowering the pH favours meta II. The resulting solution was again freeze-dried before any later intermediates could

form and the retinal was extracted and analysed for the presence of label.

4.1 Materials and methods.

4.1.1 Materials.

Cattle rod outer segments were prepared by the method of Papermaster and Dreyer (1974), Appendix 3. All operations with rod outer segments were performed in the dark unless otherwise specified.

The retinal was obtained from Sigma and all operations involving retinal were performed in an Argon-flushed box. The H_2O came from Amersham International as either 20% enriched or 70% enriched samples. Butylamine from Koch-Light was redistilled before use. All solvents were of Analar quality. Temperature was checked using a Comark thermocouple with a digital display. Sodium ortho phosphate and sodium dihydrogen phosphate were from May and Baker.

4.1.2 Freeze drying.

Water was removed from the rhodopsin solutions by the technique of freeze drying :- An acetone-dry ice slush bath was prepared by slowly dropping small pieces of solid CO_2 in to an acetone bath. The aqueous rod outer segment suspension was placed in a round bottomed flask and a frozen shell of the sample was formed round the walls of the flask by rotating the vessel as it dipped in the slush bath. Once all the rhodopsin was frozen, the flask was quickly transferred to a vacuum line and the water was pumped off over a period of hours. The dried rod outer segments were stored under vacuum.

4.1.3 Extraction of retinal.

Five to ten millilitres of methylene chloride were added to the freeze dried rod outer segments and the solution was thoroughly mixed using a glass syringe. The mixture was transferred to a glass centrifuge tube and spun down at 3500 rpm for 15 minutes on an MSE Centaur 2 centrifuge. The methylene chloride extracted retinal was removed and the pellet was resuspended in a further 10ml of solvent. The process was repeated and the two supernatants were pooled and reduced in volume by evaporation in a stream of Argon.

The resulting solution was loaded on to a 5×20 cm silica TLC plate and developed in a solvent bath containing 25% ethyl acetate, 75% cyclohexane. After 45 minutes, the plate was removed and dried and the retinal band which was clearly visible, was scraped off. A band of impurities remained at the baseline.

The retinal was recovered by elution with methylene chloride. The solvent volume was reduced as before and the sample was analysed immediately by mass spectroscopy.

4.2 Mass spectroscopy.

The aim of the experiment was to determine the point of Schiff base hydrolysis in the bleaching of rhodopsin using an isotope of oxygen. Two isotopes of oxygen are possible :- O^{17} and O^{18}.

For the use of mass spectroscopy, it is better to use O^{18} since this results in a bigger shift in molecular weight relative to the unlabelled molecule.

In order to see if retinal was suitable for analysis by mass spectroscopy, a sample of commercial retinal (Sigma) was run in the mass spectrometer Fig.(4.1). This showed a straightforward mass spectrum with no impurities above the molecular ion.

To check the feasibility of detecting a label in retinal, it was decided to label a sample of commercial retinal via formation and hydrolysis of a Schiff base. This was achieved in the following way:- Redistilled butylamine and methylene chloride were dried for three days over activated 4 Å molecular sieves. A sample of retinal was added to butylamine over sieves and left until the Schiff base formed . This was detected by monitoring the wavelength shift from 380nm to 364 nm using a Pye-Unicam 1800 UV spectrometer. The butylamine was removed under vacuum and the Schiff base was taken up in ethanol. 1ml of the Schiff base was mixed with one ml of 20% enriched H_2O and an amount of sodium dihydrogen phosphate and sodium orthophosphate was added which had been predetermined to give a pH of 7 in the sample which was conducive to hydrolysis.

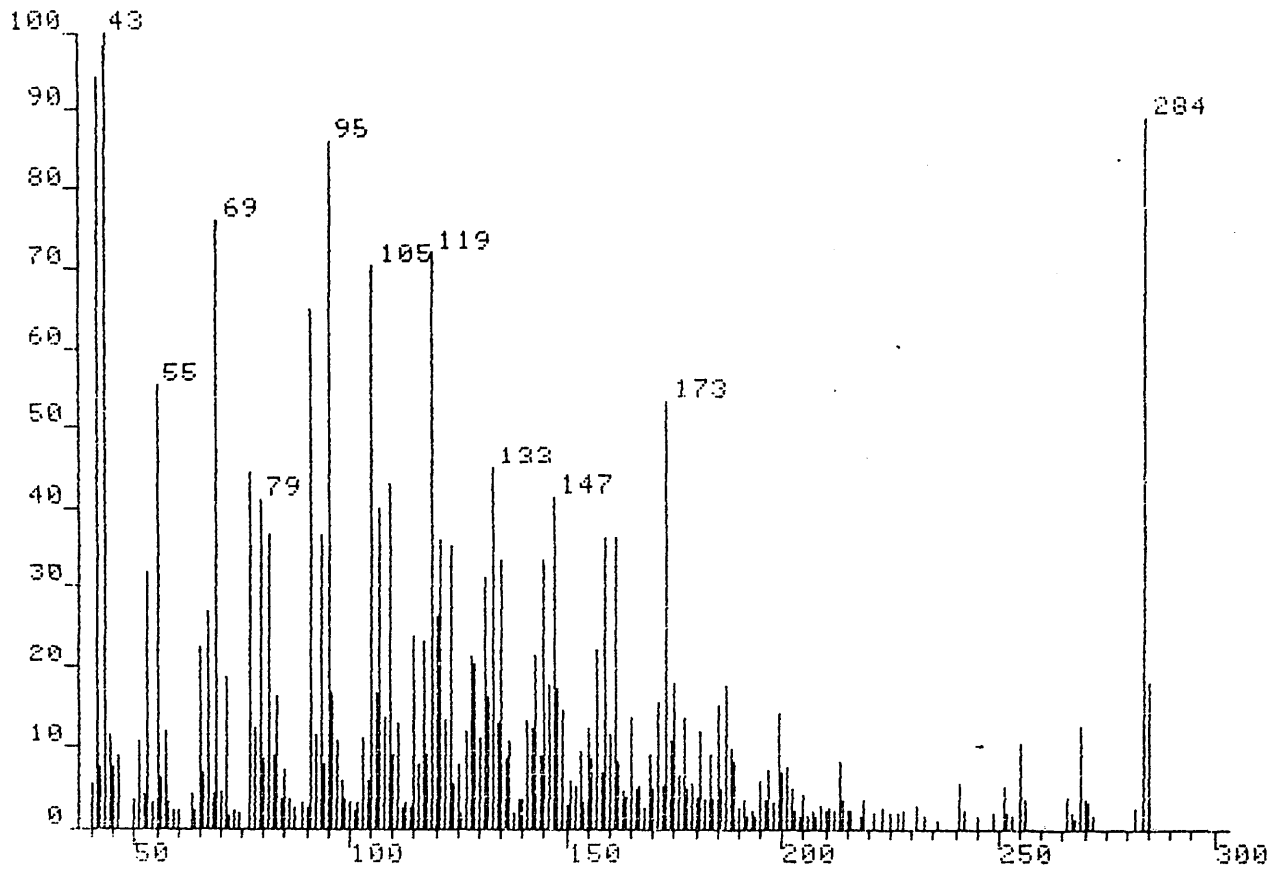

Fig.(4.1). Mass spectrum of pure retinal.

Once complete hydrolysis had occured, as monitored by a shift in wavelength, an equal volume of methylene chloride was added. The mixture was forced through a syringe to form an emulsion which gradually separated in to two layers. The bottom layer containing the methylene chloride extracted retinal was carefully removed, reduced in volume and submitted for immediate mass spectroscopic analysis. The mass spectrum of the sample Fig.(4.2) showed O^{18} label incorporation from the appearance of a peak at 286 AMU.

Thus it seemed that the technique of mass spectroscopy was suitable for the detection of O^{18} label incorporation in retinal.

4.3 O^{17} NMR :- A feasibilty study.

The possibility of using O^{17} NMR to follow the reaction was considered. An experiment was devised to follow the position of an O^{17} label as a sample of rhodopsin bleached. The planned experiment involved bleaching a rhodopsin sample containing H_2O^{17} in an NMR spectrometer at 0°C to produce meta I, and following the appearance of a signal corresonding to a carbonyl group. By observing the temperature at which the carbonyl signal appears, it should be possible to determine at which intermediate hydrolysis of the protein-chromophore bond occurs.

To determine how feasible this experiment would be, a trial sample was run on the Brüker NMR spectrometer. 150μl of acetone in 3ml of D_2O was used as the sample and the

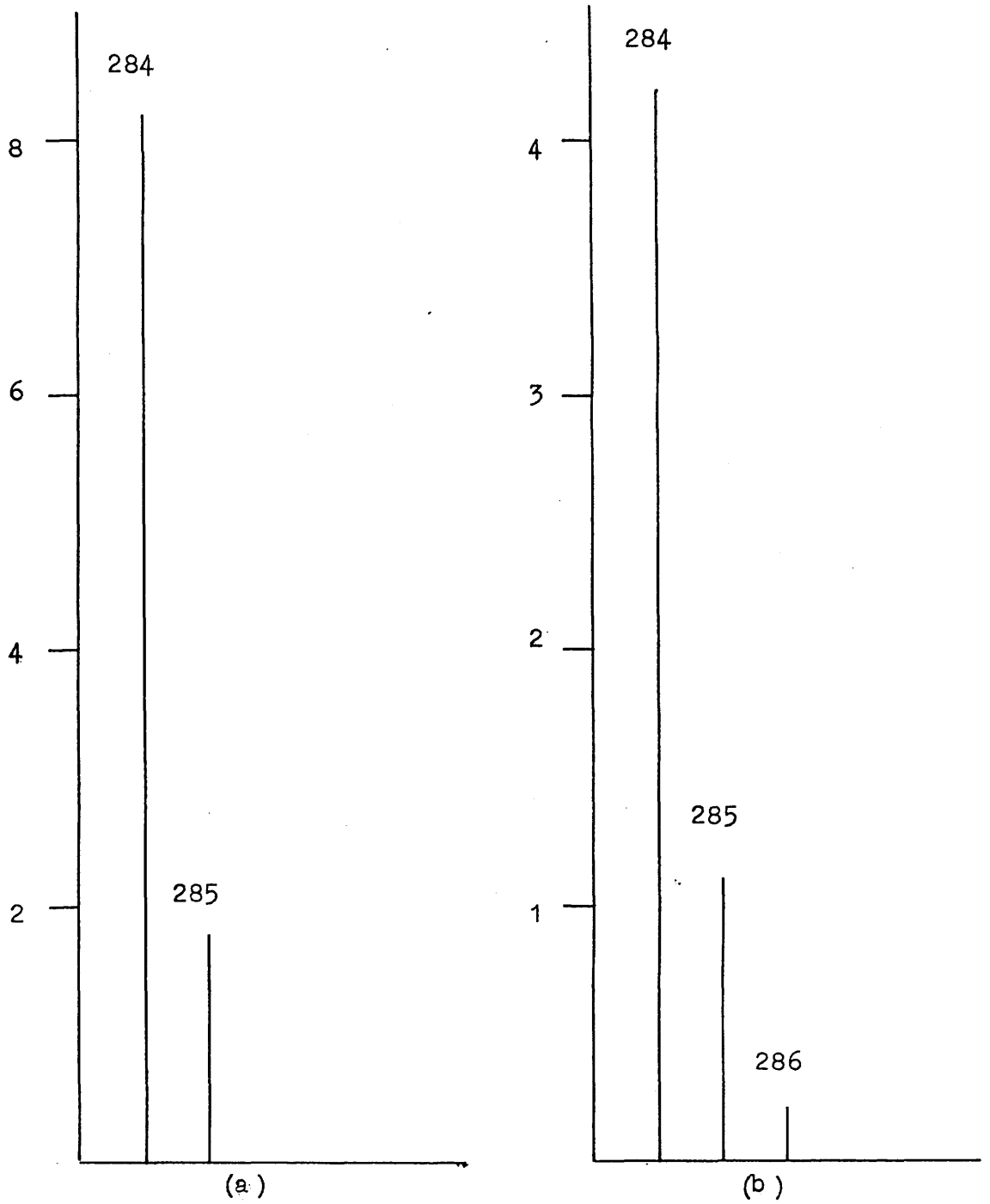

Fig.(4.2). Mass spectra of (b) retinal extracted from Schiff base hydrolysis and (a) reference retinal (Sigma). Both samples were run in the same solvent, under the same conditions.

signal detected was due to the natural abundance of O^{17}. A very small signal was obtained after collecting the data for one hour at room temperature. Fig.(4.3). Fig.(4.4) is the spectrum magnified and corrected for background noise and baseline drift.

The reason that the signal is so low is due to the low natural abundance of O^{17} :- 0.037 %. However, since a signal had been detected, it was decided to run a sample of retinal to observe the effect of increased molecular size on the signal. An 80 mM sample of retinal (Sigma) in ethanol was used and the spectrum in Fig.(4.5) was obtained. The upper spectrum is a magnification of the lower spectrum. The arrow shows the position of the signal. In this case, the signal is barely visible above the noise. The problem is that as the molecular size increases, the tumbling rate decreases and the linewidth increases. Added to this is the fact that the experiment would have to be run at lower temperatures ~0°C, which again would decrease tumbling, increase linewidth and further reduce signal. Also the sample would be in membranes which to obtain a high enough concentration would have to be very viscous, which would again reduce tumbling and increase linewidth. A detergent extract would be less viscous but unfortunately the lifetimes of the intermediates would be much reduced.

In principle then, it was possible that an O^{17} label might be detectable but there would be a lot of problems with no guarantee of picking up a signal. In view of the expense of the labelled water and the number of eyes required

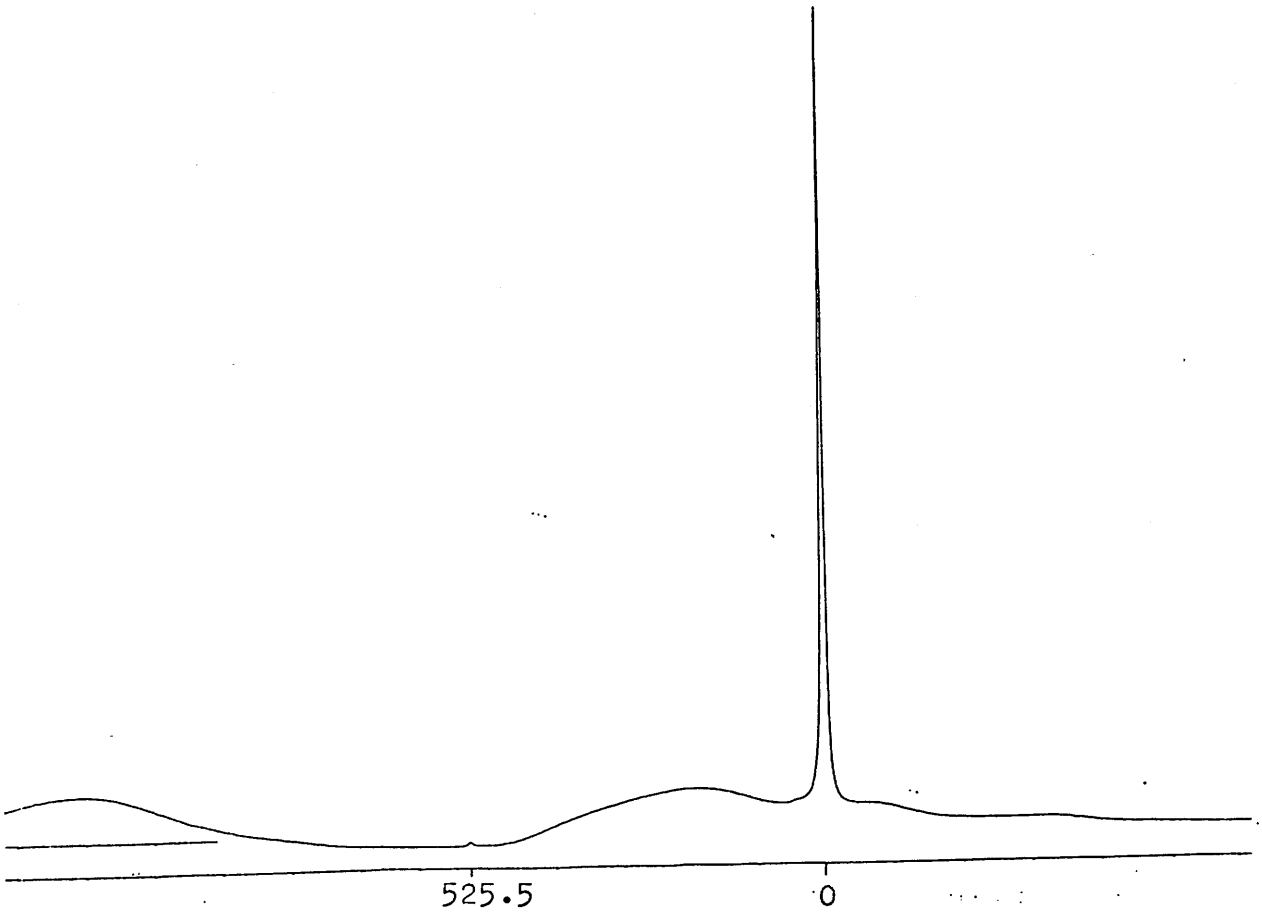

Fig.(4.3). O^{17} NMR of acetone in D_2O.

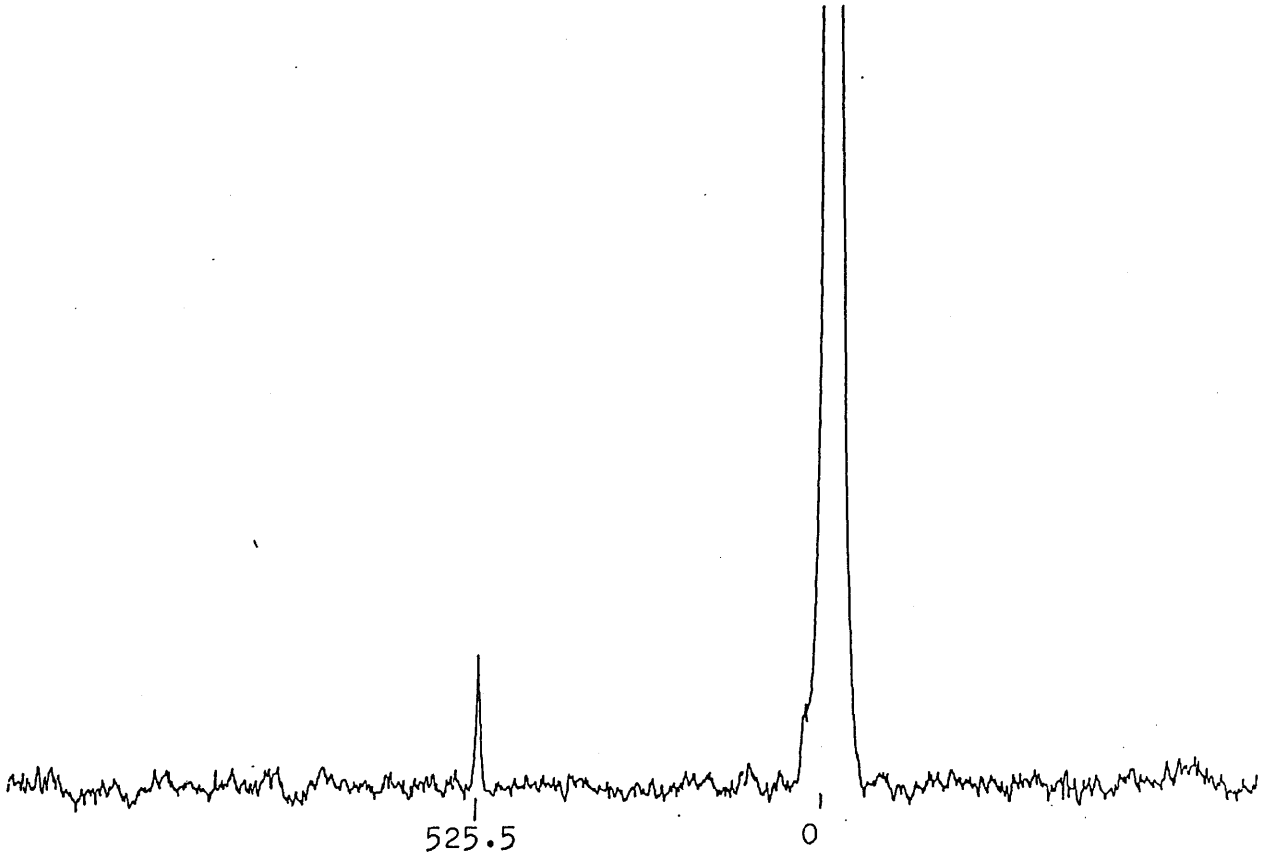

Fig.(4.4). Acetone O^{17} NMR spectrum magnified 32 times and corrected for background and baseline drift.

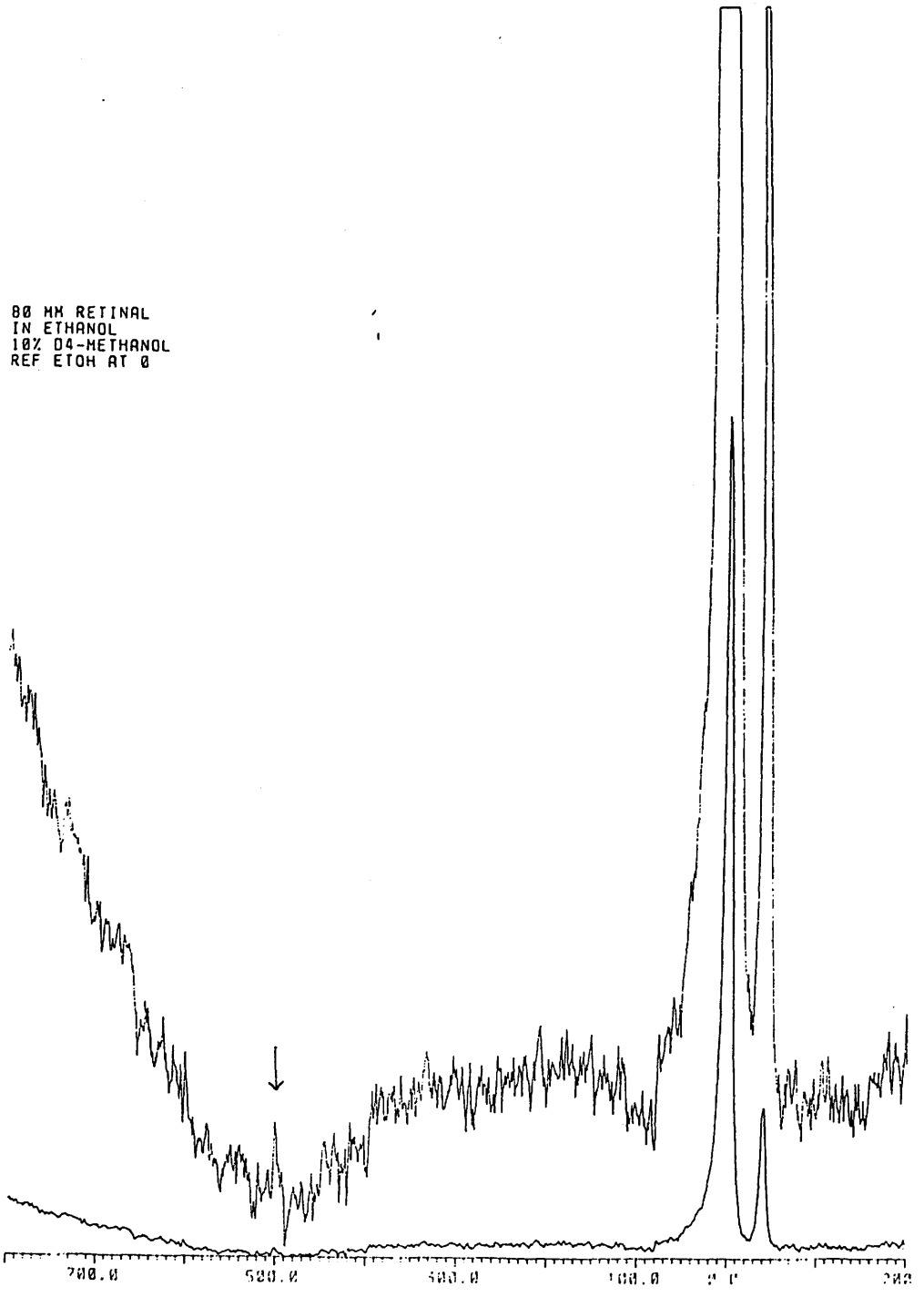

Fig.(4.5). O^{17} NMR spectrum of retinal in ethanol.

to give an adequate concentration for the NMR spectrometer, and the long data aquisition time required, it was decided to try out the technique of mass spectroscopy first.

4.4 Labelling of retinal in rhodopsin.

With the technique of mass spectroscopy characterised for retinal, it was possible to commence on rhodopsin experiments. The first step was to check that retinal extracted from rhodopsin was pure enough to detect a label. This caused considerable problems, but the method of extraction given in section (4.1.3) was found to give a suitable mass spectrum ie. one with no impurities appearing above the molecular ion peak.

The first experiment planned was to add labelled water at meta 1, allow the reaction to proceed to meta 11, then remove the water and extract the retinal.

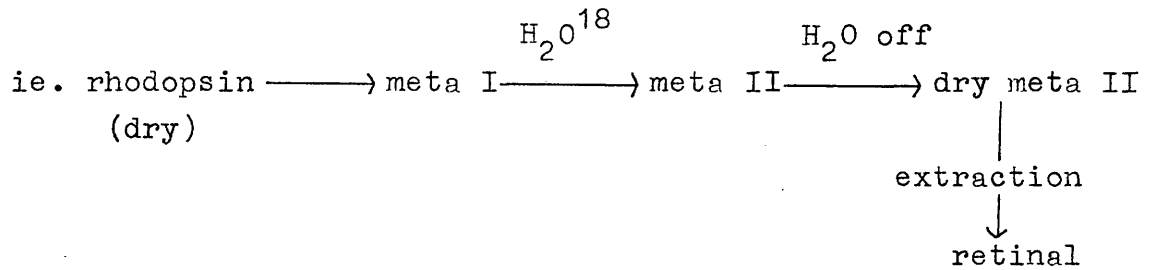

This was achieved by freeze drying a sample of rhodopsin (see section 4.1.2) in the dark, then bleaching it. According to Wald (1950), this should result in the formation of meta I since meta II will not form in the absence of water.

0.5 ml of 70% enriched H_2O^{18} was added to a glass cell cooled by a refrigerator unit circulating 15% methanol in water at 0°C. Sufficient sodium dihydrogen phosphate buffer was added to give a pH of 5.5.

The freeze dried meta I was added to the cell with stirring and the colour changed from red to orange. The temperature of the suspension was monitored throughout. After 10 minutes , the rhodopsin solution was transferred to a pre-cooled round bottomed flask using a syringe which had been kept in ice. The sample was immediately freeze-dried and the water removed under vacuum. The retinal was extracted as in section (4.1.3) giving a mass spectrum shown in Fig.(4.6b). Comparison with a reference mass spectrum of commercial retinal in the same solvent, Fig.(4.6a), run immediately afterwards under the same conditions showed a definite increase in signal at 286 AMU in the sample retinal. This showed incorporation of label.

The label incorporation was less than that predicted however, possibly due to condensation of water on the walls of the cell during cooling of the cell and throughout the reaction.

To reduce this effect, the experiment was repeated. This time the H_2O^{18} and buffer were kept at 0°C by suspending a round bottomed flask directly in to the refrigeration tank. This cut out the 2-3 hours required to pre-cool the glass cell and thus any condensation which appeared during this time. Also the top of the flask was sealed with parafilm to reduce the possibility of condensation

Reaction: Meta 1 (dried) $\xrightarrow[\text{pH drop}]{H_2O^{18}}$ Meta 11

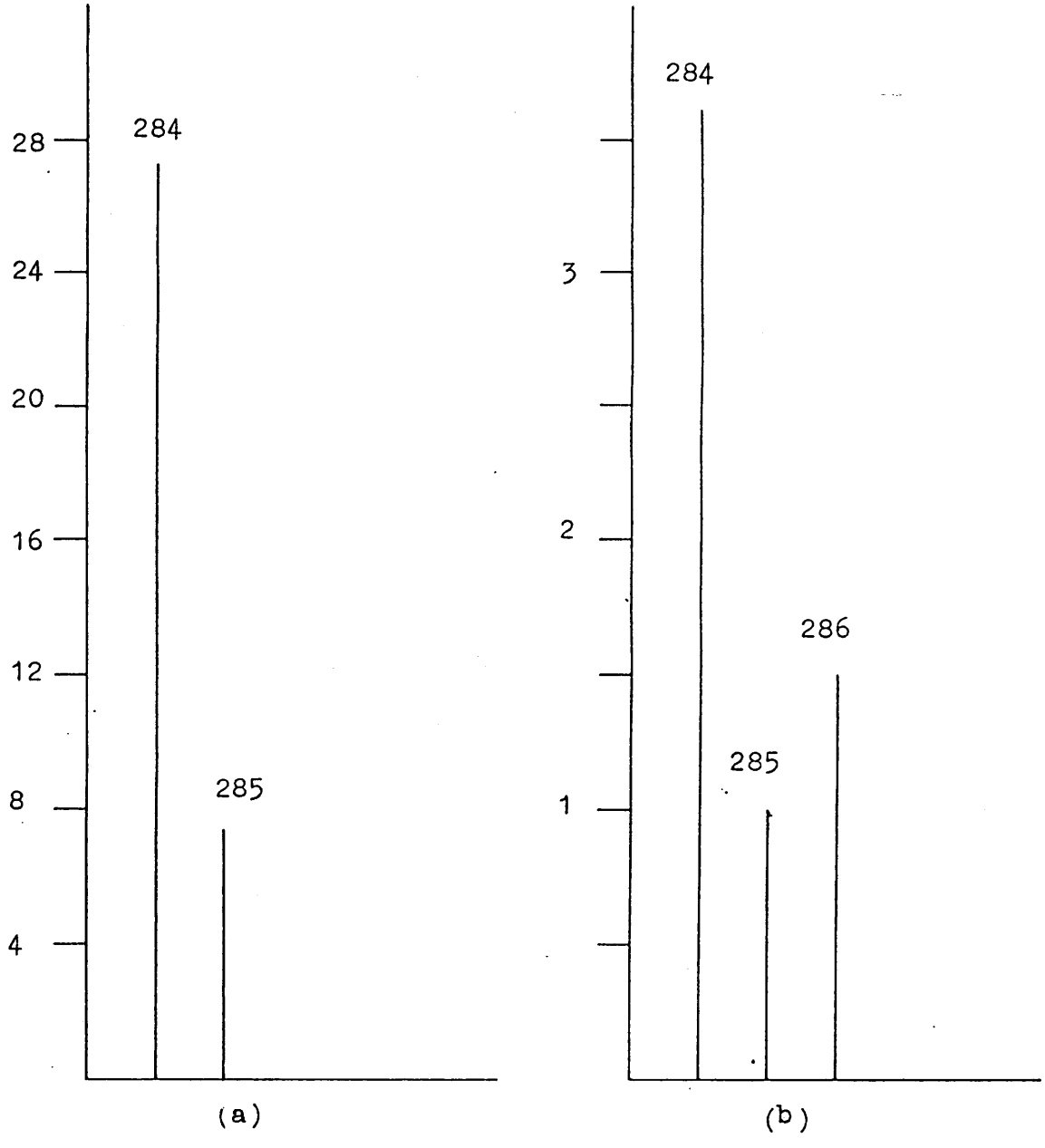

Fig.(4.6). Mass spectra of retinal extracted from meta 11 (b) and (a) reference retinal (Sigma). Both samples were run under the same conditions in the same solvent.

in the flask.

The meta I was added directly to the round bottomed flask and this method also cut out the intermediate step of transferring the rhodopsin from the cell to the flask, which in turn reduced the duration of the experiment and hence the possibility of formation of any of the later intermediates.

The retinal was extracted as before giving a mass spectrum shown in Fig.(4.7b). Comparison with commercial retinal, Fig.(4.7a) showed a higher incorporation of label.

4.5 Control experiments.

Two control experiments were performed. In the first, H_2O^{18} was added at meta I and removed again after $\sim$ 15 minutes without the pH jump. This gave a mass spectrum as shown in Fig.(4.8b). On comparison with a sample of commercial retinal Fig.(4.8a), there seemed to be no obvious uptake of label which ruled out incorporation of label via oxygen exchange.

The second experiment involved pre-equilibration of H_2O^{18} with unbleached rhodopsin. The sample was bleached at $0^{\circ}C$, pH 8 and the H_2O^{18} was again removed. The retinal was extracted as before, giving a mass spectrum shown in Fig.(4.9b). Again on comparison with a sample of commercial retinal Fig.(4.9a), there did not appear to be any label incorporation.

Reaction: meta 1 (dried) $\xrightarrow[\text{pH drop}]{H_2O^{18}}$ meta 11

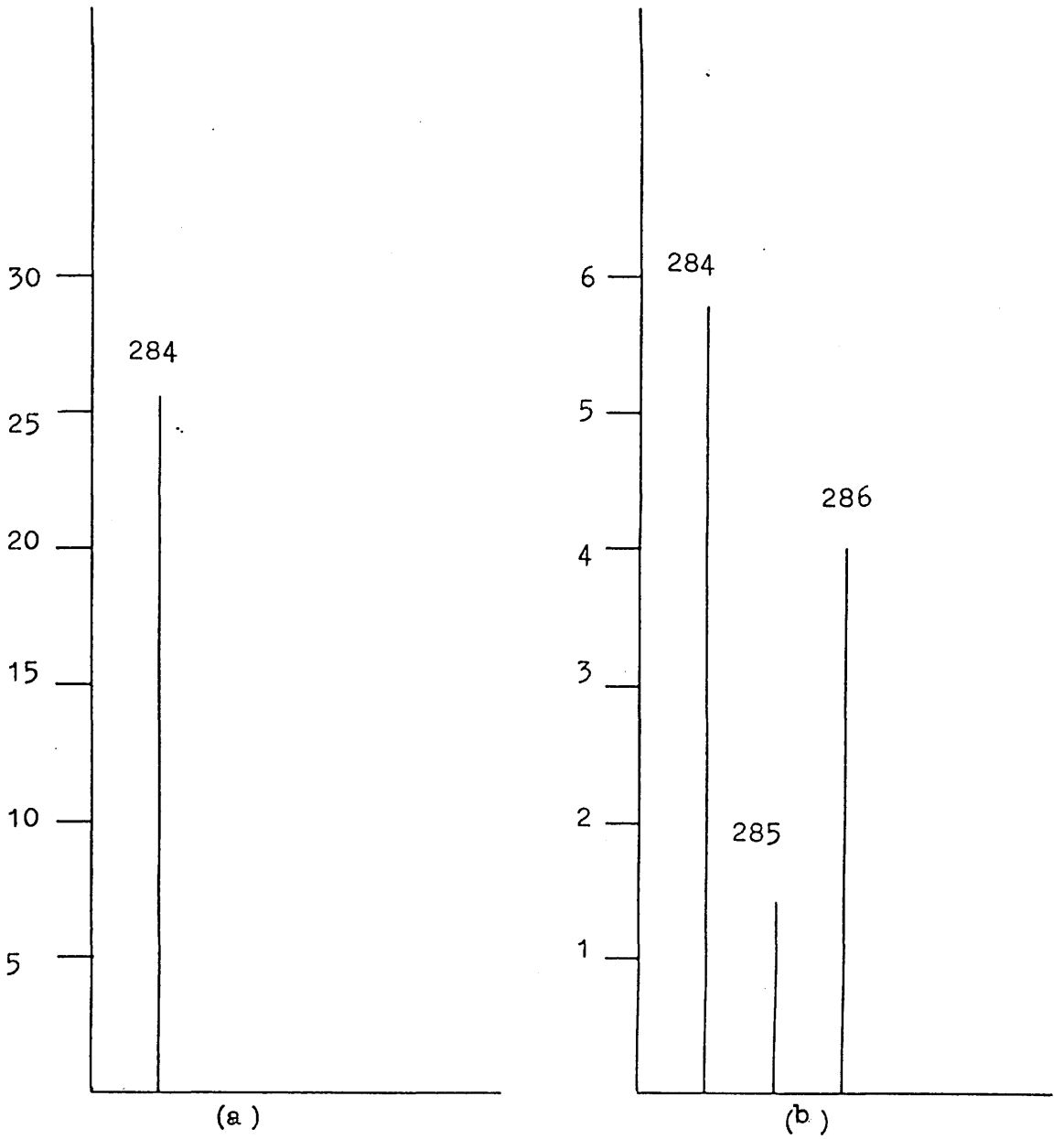

Fig.(4.7). Mass spectra of retinal extracted from meta 11 (b) and (a) reference retinal (Sigma). Both samples were run under the same conditions and in the same solvent.

Reaction: meta 1 (dried) $\xrightarrow{H_2O^{18}}$ H_2O removed without pH drop.

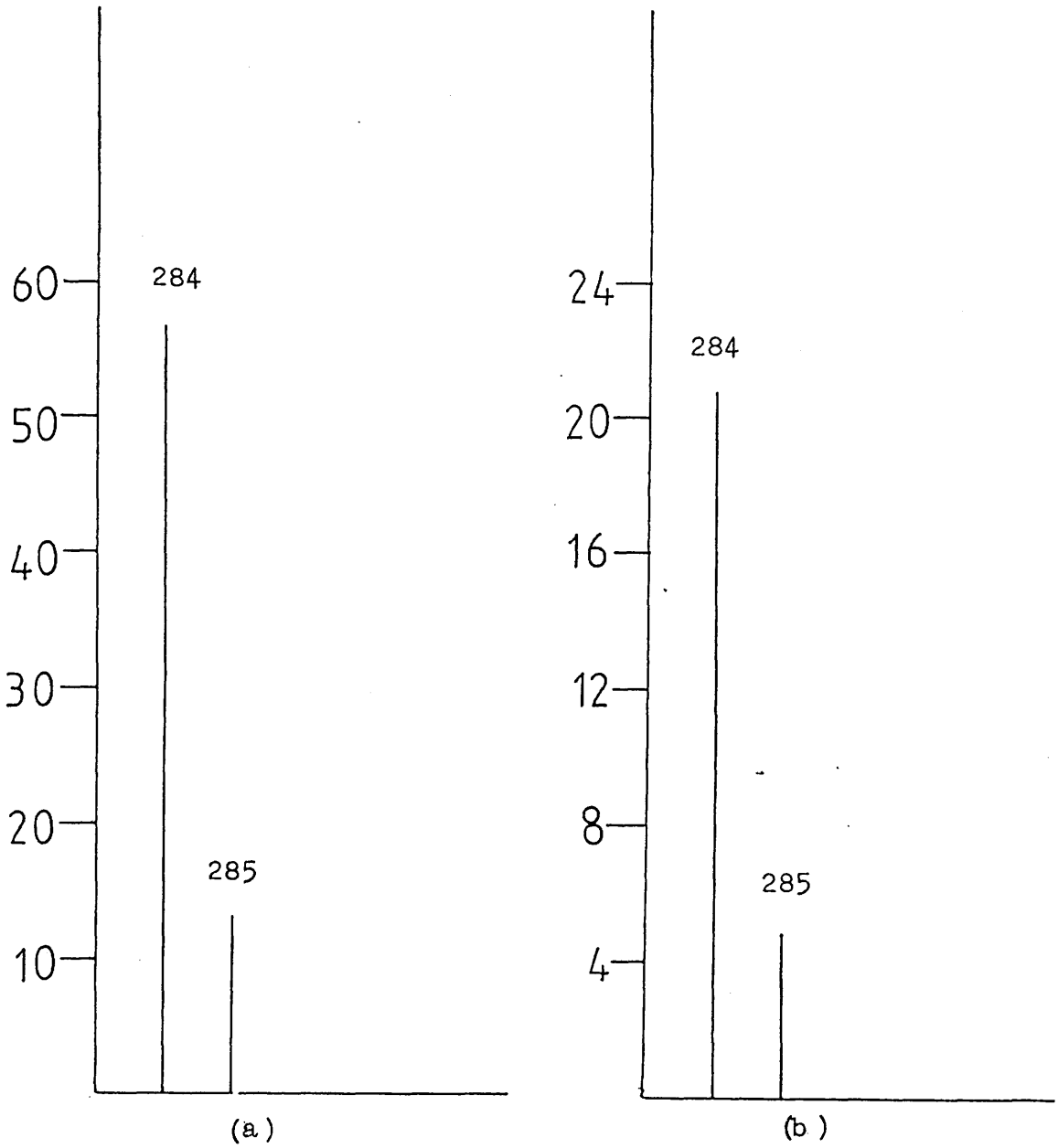

Fig.(4.8). Mass spectra of retinal extracted from meta 1 (b) and (a) reference retinal (Sigma). Both samples were run in the same solvent under the same conditions.

Reaction: Rhodopsin $\xrightarrow{H_2O^{18}}$ Meta 1

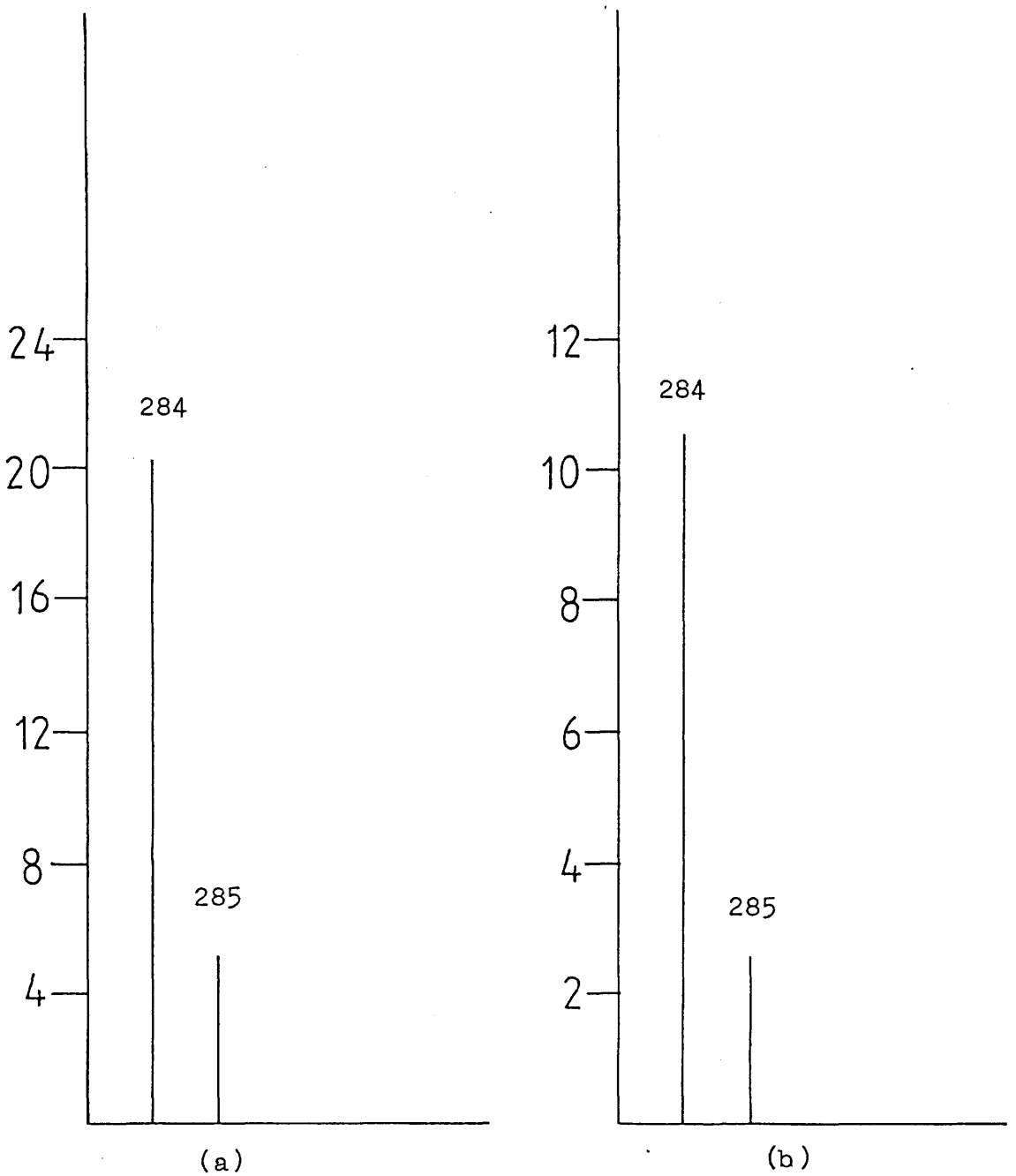

Fig.(4.9). Mass spectra of retinal extracted from rhodopsin bleached to meta 1 in the presence of H_2O^{18} (b) and (a) reference retinal (Sigma). Both samples were run in the same solvent under the same conditions.

4.6 Detection of label by infrared spectroscopy.

In many cases it is possible to detect incorporation of a labelled atom by the shift in its infrared spectrum.

Most of the O^{18}- labelled molecules investigated so far contain at least one double or triple XO bond, where X= C,N,P,S,V,Mn,As or U. In such cases, the potential energy of those vibrational modes which involve an appreciable XO stretching is localised to a large extent in these bonds. (Pinchas and Laulicht 1971). It is therefore possible to get an estimation of the O^{18}- induced shift of these modes by assuming it to be not much lower than for the corresponding diatomic X-O oscillator having the same stretching frequency.

The ν^i/ν ratio of isotopic frequencies of diatomic molecules being very nearly equal to $(\mu/\mu^i)^{\frac{1}{2}}$, one can write the following equation for this ratio in the case of the $X\text{-}O^{18}$ and $X\text{-}O^{16}$ oscillators :-

$$\nu^i/\nu = (\mu/\mu^i)^{\frac{1}{2}} = \left(\frac{16\times M_X \times (18+M_X)}{(16+M_X)\times 18\times M_X}\right)^{\frac{1}{2}} = \frac{2}{3}\left(\frac{2(18+M_X)}{16+M_X}\right)^{\frac{1}{2}} \text{----(4.1)}$$

where ν^i/ν = the ratio of the isotopic stretching frequencies.

$(\mu/\mu^i)^{\frac{1}{2}}$ = the ratio of the reduced masses of the isotopic molecules.

M_X = mass of the X atom.

Thus after M_x is substituted in to equation (4.1) by its value and the characteristic stretching frequency of the corresponding X-O^{16} group is multiplied by the resulting ν/ν ratio, the stretching frequency of the diatomic X-O^{18} vibrator and hence the respective expected O^{18} induced shift can be obtained from this equation.

Using this theory when X = carbon, the normal group frequency is $\simeq 1667$ cm^{-1}, the calculated isotopic group is $\simeq 1627$ cm^{-1}, thus the observed shift should be seen in the infrared signal for the carbonyl group on replacement of O^{16} by O^{18}.

An infrared spectrum of the retinal was run which showed incorporation of label Fig.(4.10). Compared to an infrared of extracted unlabelled retinal Fig.(4.11), it can be seen that a peak is present at 1638 cm^{-1} corresponding to where one would expect a C = O^{18} stretch to occur. The shift in peak = 29 cm^{-1} which is less than that predicted theoretically but is in the range observed experimentally by other workers labelling a ketone with O^{18} :-

eg. $(C_6H_5)_2CO$ normal frequency = 1667 cm^{-1}
labelled frequency = 1697 cm^{-1}
shift = 30 cm^{-1}

(Pinchas and Laulicht 1971).

To characterise the two C=O peaks, commercial retinal was labelled via a Schiff base as before. This too gave two

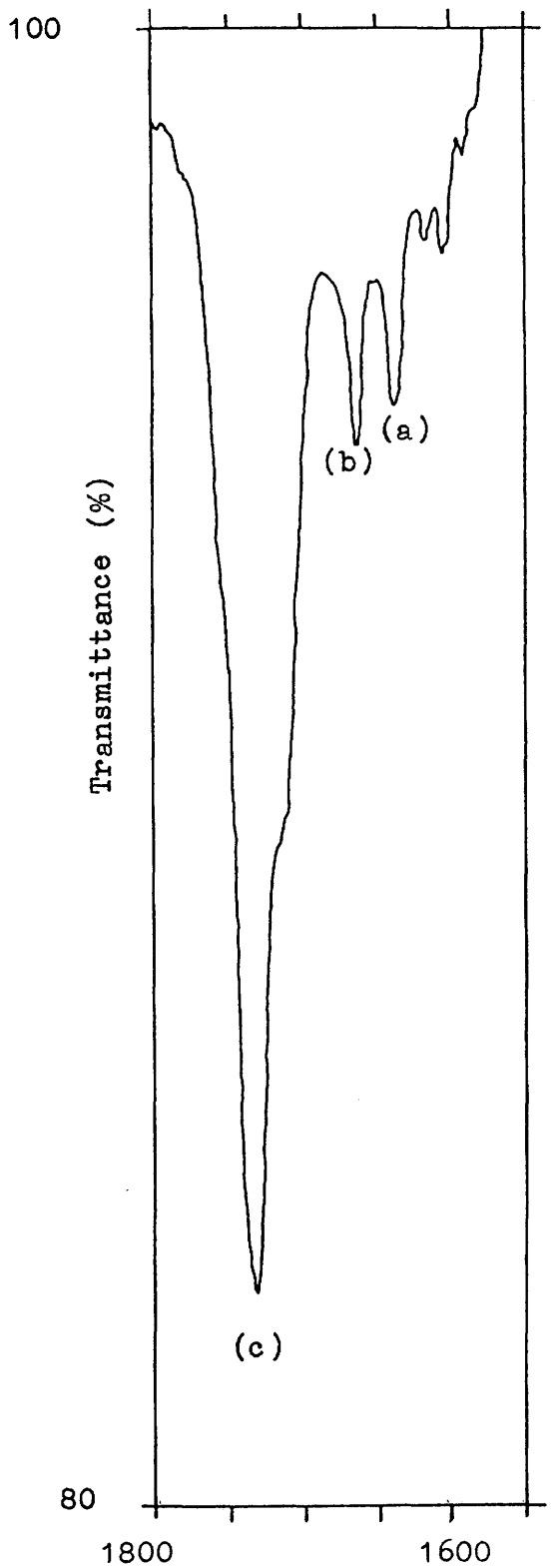

Fig.(4.10). Infrared spectrum of retinal extracted from rhodopsin showing incorporation of label.

(a) $C=O^{18}$ stretch.

(b) $C=O^{16}$ stretch.

(c) Peak due to impurities.

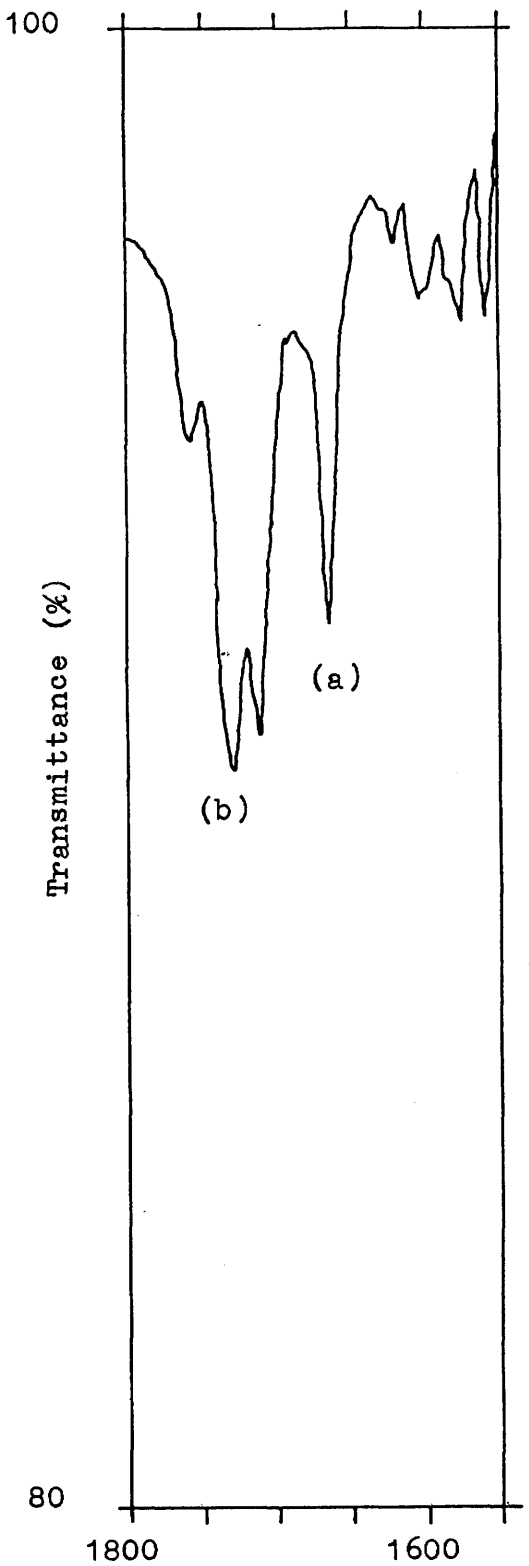

Fig.(4.11). Infrared spectrum of retinal extracted from rhodopsin.

(a) C=O stretch.

(b) Peak due to impurities.

carbonyl peaks, one at 1667 cm^{-1}, one at 1638 cm^{-1} Fig.(4.12). The extent of O^{18} incorporation was not high (either in infrared or mass spectroscopy), presumably due to dilution of label with water present in solvent. The mass spectrum is shown in Fig.(4.13).

Further work could be done in the area of labelling to reduce the uncertainties present. There are impurities present in the infrared spectra possibly due to plasticisers in the solvent which lack of time prevented a proper investigation of. It would be better and more convincing to obtain a labelled sample with a high incorporation of label and no impurities. This could perhaps be obtained if carefully distilled and dried solvent were used and if 90% enriched water could be used.

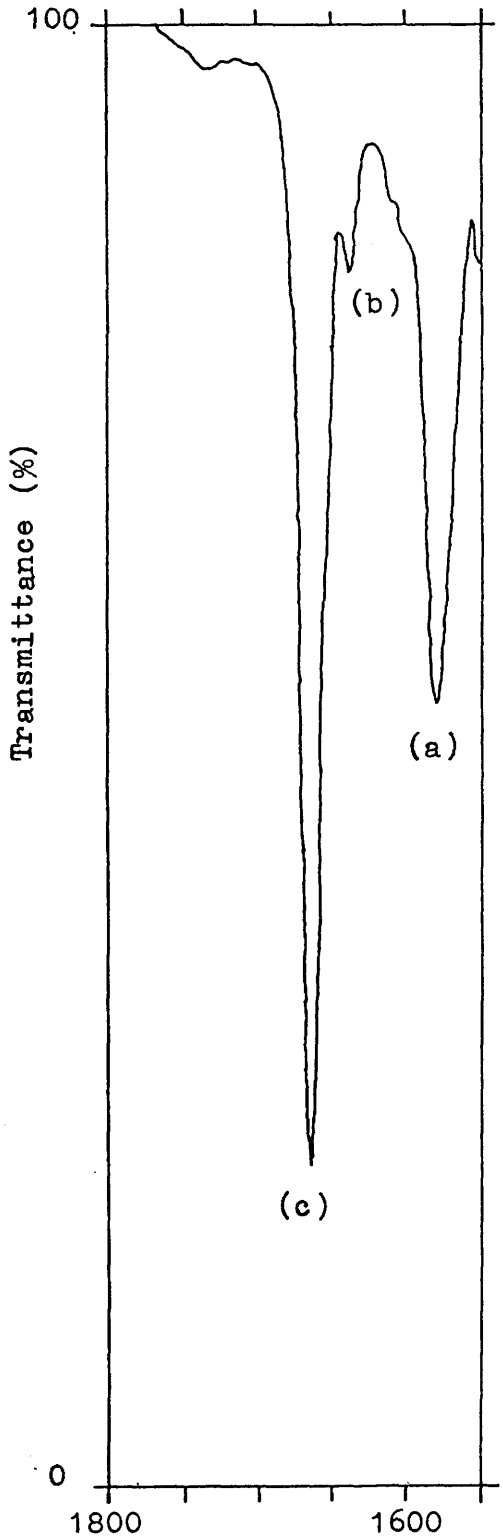

Fig.(4.12). Infrared spectrum of retinal from Schiff base hydrolysis showing incorporation of label.

(a) Peak due to impurities.

(b) $C=O^{18}$

(c) $C=O^{16}$

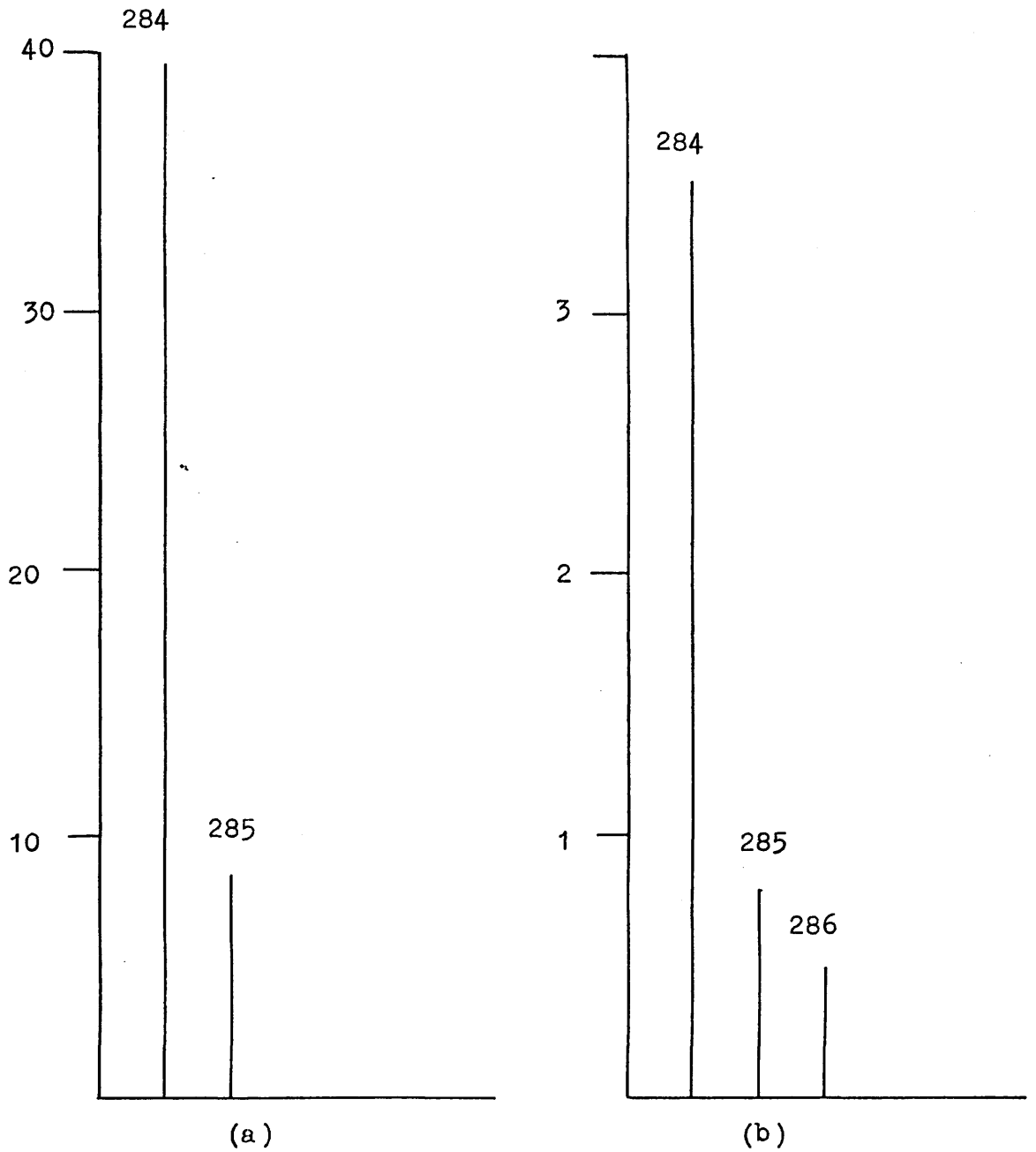

Fig.(4.13). Mass spectra of (b) retinal extracted from Schiff base hydrolysis and (a) reference retinal (Sigma). Both samples were run under the same conditions, in the same solvent.

4.7 Discussion.

The labelling experiments as monitored by mass spectroscopy and infrared spectra support the hypothesis of Schiff base hydrolysis during the meta I to meta II transition in cattle rhodopsin. The main fact which casts doubt on this hypothesis is the fact that sodium borohydride reduction of meta II suggests that at this point, the chromophore and protein are still attached. As discussed in the introduction however, studies on the binding site using reducing agents tend to give dubious results. Various investigators have found conflicting results for the binding site:- either a lysine residue or phosphatidylethanolamine or both. It seems likely that the chromophore can undergo transimmination to the phospholipid depending on the extraction conditions. Thus borohydride reduction conditions may have encouraged transimmination from protein to phospholipid instead of meta I to meta II.

In support of the hydrolysis theory, Matthews et al (1963) found that:-

1. Increasing the temperature of the solution favoured meta II.
2. Addition of glycerol favoured meta II.
3. Increasing the ionic strength of the medium favoured meta II.

Each of these factors may be interpreted to support Schiff base hydrolysis:-

1. Increasing the temperature will increase the rate of a reaction.

2. It has been found that decreasing the polarity of the medium will favour Schiff base hydrolysis in model Schiff bases (Pollack and Brault 1975). Addition of glycerol will reduce the polarity of the medium increasing Schiff base hydrolysis.

3. The effect of ionic strength of the medium can be interpreted in terms of the kinetic salt effect. According to this theory, the observed rate of a reaction k, is a function of the absolute rate plus terms involving the ionic strength of the reaction medium:-

$$\log k = \log k_o + 2Q Z_a Z_b \sqrt{U}$$

where Z_a = valency of ion a.

Z_b = valency of ion b.

Q = 0.51 for aqueous solutions at 25°C.

$U = \frac{1}{2} \sum Z_i^2 C_i$, the summation being taken over all the ions in solution. (Laidler 1979).

Thus varying the ionic strength of a solution will affect the observed rate of a reaction and if meta I to meta II is Schiff base hydrolysis, the ionic strength of the medium will affect this reaction.

In addition, the situation for cattle metarhodopsin may be contrasted sharply to the invertebrate acid to

alkaline metarhodopsin transition. In the invertebrate case, the equilibrium is thought to involve protonation and deprotonation of the Schiff base, and it is interesting to note that the position of its equilibrium is unaffected by glycerol or ionic strength of the medium.

The non-ideal protonation results obtained for the meta I to meta II transition are possibly due to subtle electrostatic effects. If the Schiff base hypothesis is true, subsequent titration of the amino group will be affected by its environment eg. solvent, ionic strength, presence of detergent, perhaps giving rise to unreproducible results.

The significance of hydrolysis or otherwise at the metarhodopsin stage is unclear. Since invertebrates like octopus also undergo a similar photoreaction without cleavage of chromophore, it seems questionable whether the breaking of the chromophore bond is active in transduction. As discussed in chapter 2, it may rather reflect differing regeneration mechanisms.

CHAPTER 5

Conclusions.

Conclusions

The work done in this thesis suggests that vertebrate and invertebrate visual pigments have a great deal in common despite their somewhat diverse development. Both exhibit high energy uptake as the first step in visual excitation. As discussed in chapter 2, this may suggest that photon energy storage is of prime importance in vision, its main function being to make visual excitation an energetically expensive step and hence reduce the extent of spurious signals resulting from thermal noise. Later steps involve dissipation of the stored energy, the crucial difference between the two pigments occuring at the metarhodopsin stage where in the case of vertebrates it has been postulated that the chromophore-protein bond is hydrolysed to give all-trans retinal plus opsin. In the invertebrate case, the photoreaction halts at the metarhodopsin stage with the chromophore -protein bond intact. It is suggested that this fundamental difference is due to different regeneration mechanisms which in turn may be due to the different lifestyles of the vertebrates and invertebrates. It is known that in vertebrates, the rhodopsin is free to move in the disc membrane and hence it will readily capture fresh chromophore. In invertebrates, the rhodopsin is in a fixed array, deliberately so to enable them to detect polarised light which they use for navigation and feeding, and so the chances of opsin regaining a fresh chromophore is much reduced. Photoregeneration

in situ is a much more efficient method of regeneration.

Studies on the acid ⇌ alkaline metarhodopsin equilibrium agree with the proposed mechanism of Schiff base deprotonation for the acid to alkaline metarhodopsin transition. Deviations from ideal titration behavior were attributed to ionic strength effects.

The quantum yield for the forward reaction in the octopus photocycle was calculated to be 0.689 $\pm$ 0.016. This is very similar to vertebrate visual pigments. The regeneration reaction had a quantum yield of 0.430 $\pm$ 0.017 which is relatively high presumably since photoregeneration is so significant for invertebrates.

As a final comparison of the two pigments, it has to be noted that invertebrates like octopus seem to have a less well developed visual system than vertebrates on two counts:- 1. They cannot see in colour. Although a second pigment retinochrome is present in octopus and squid its function is believed to be that of screening pigment and regeneration aid rather than that of colour pigment. 2. Some have a much lower photosensitivity ($\varepsilon\gamma$) than vertebrates.

These differences however may not be due to significant inferiority of the invertebrate visual system, but may rather reflect environmental influence on development. Octopuses do not require colour vision if they do indeed use polarised light to detect prey. Also in a medium such as water, visual accuity may not be quite so critical for self preservation as on land. Both systems may have

developed differently due to environmental pressures.

Finally, the study of the meta I to meta II transition using H_2O^{18} seems to support the theory of Schiff base hydrolysis during this transition. The incorporation of label was monitored using I.R. and mass spectroscopy and label uptake was clearly observed. The significance or otherwise of hydrolysis at this stage is still unclear. It may be due solely to the regeneration requirement of protein-chromophore cleavage or may be crucial in producing an "active" molecule for activating G-protein if the enzyme cascade theory is correct.

An interesting note which remains at the end of this work is whether the similarities observed between vertebrates and invertebrates represent true convergent evolution at the molecular level or simple conservation of a vital mechanism which had evolved before branching in the evolutionary tree occurred.

Appendix 1

S.D.S. Gel Electrophoresis of Octopus Microvilli Membrane Proteins.(In collaboration with Dr. S.A.H. Al-Mahdawi.)

Conventional S.D.S. slab gel electrophoresis was performed under the following conditions:-

Stock Solutions

1. Buffers.

	Lower Tris buffer	Upper Tris buffer	Reservoir buffer
Trizma base	36.34g	6.06g	12g
S.D.S.	0.8g	0.4g	glycine 57.65g
H_2O to	180 ml	90 ml	900 ml
adjusted to pH (6N HCl)	8.8	6.8	8.3
H_2O to final volume	200 ml	100 ml	1000 ml

2. 30% Acrylamide Stock Solution.

30g of acrylamide : 0.8g bis acrylamide made up to 100 ml with water.

3. 15% S.D.S. Denaturing Solution.

1.5g sodium dodecyl sulphate
0.211g Na_2EDTA
3 ml 42% sucrose
5.5 ml H_2O
1.5 ml β - mercaptoethanol.
10 ml

This is added to the sample before loading on to the gel.

The gel is composed of two layers, a lower gel composed of 10% acrylamide and an upper stacking gel of 3% acrylamide. These were prepared as follows:-

10% casting gel

10 ml of the 30% stock solution
7.5 ml of the lower Tris buffer
0.015g of ammonium persulphate
15 μl TEMED
12.5 ml H_2O
30 ml

3% stacking solution

3 ml of 30% stock solution

7.5 ml of upper Tris buffer

0.05g of ammonium persulphate

10 µl of TEMED

19.5 ml of H_2O

30 ml

The casting gel was poured first with the stacking gel on top. Small troughs were created on the stacking gel as it set.

Sample Preparation

The samples run on the gel were:-
Freshly thawed octopus microvilli (sample A). An octopus rhodopsin sample which had been bleached and regenerated several times (sample B).

Samples were mixed with 15% denaturing solution to give a final concentration of 2.5% S.D.S. . The total volume should be in the range 10-20µl with a sample content of ~5µg of material. The following solutions were prepared:- Samples A and B were taken up in 0.01 M Tris buffer pH 8 to give a final concentration of 1µg/µl. Then:-

1. 5μl of sample A + 1.25μl of 15% SDS.
2. 10μl of sample A + 2.5μl of 15% SDS.
3. 15μl of sample A + 3.75μl of 15% SDS.
4. }
5. } standard protein marker.
6. Pharmacia standard protein marker.
7. 5μl of sample B + 1.25μl 15% SDS.
8. 10μl of sample B + 2.5μl 15% SDS.

These were incubated for 15 minutes at 37°C, then loaded on to the gel. The gel was run at 150 V for 4½ hours.

Fixing and Staining

The gel was fixed overnight in trichloroacetic acid It was then stained with 50% trichloroacetic acid + 0.1% Coomassie brilliant blue for 1 hour, then destained for ~ 5 hours with 7% acetic acid at 37°C. A photograph was obtained Fig.(A1.1).

Interpretation of results

A calibration graph of log(molecular weight) versus distance travelled was drawn using the proteins in the marker gel:-

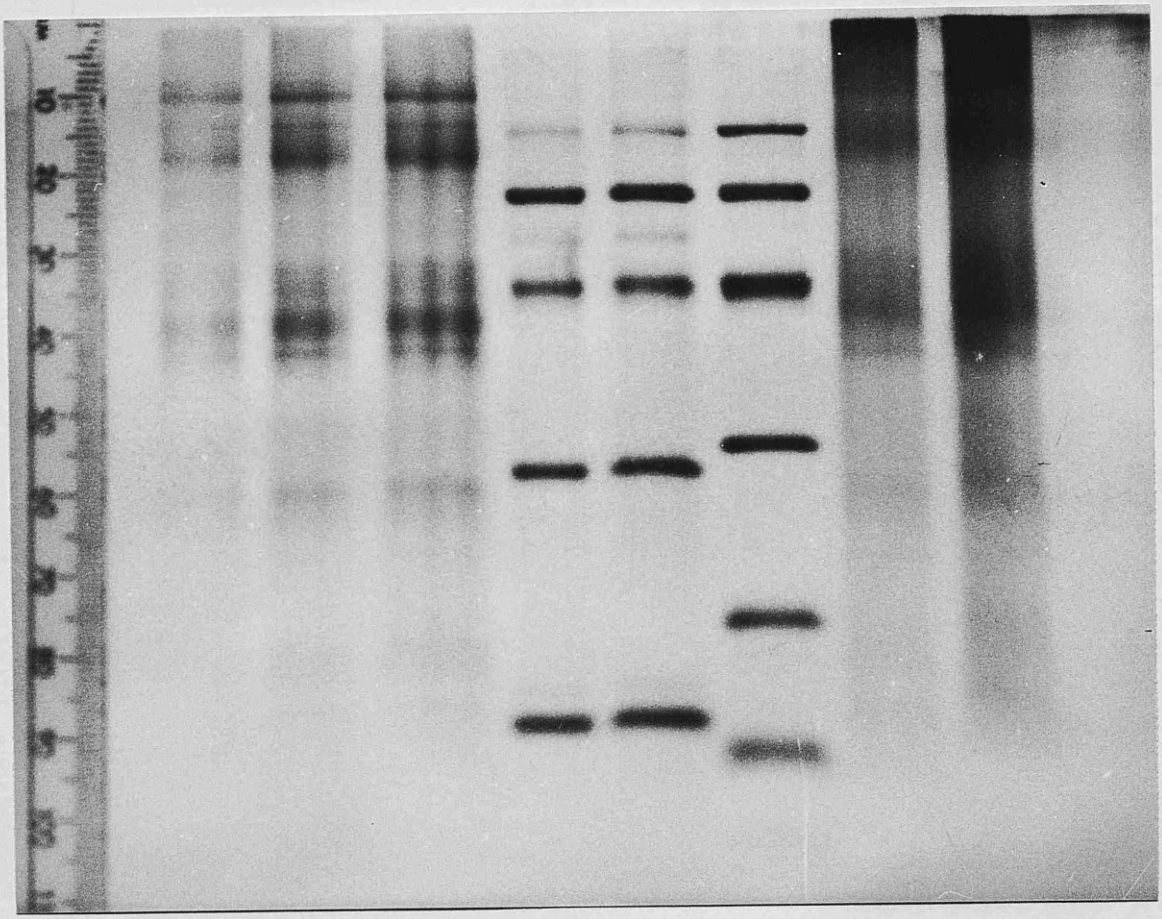

Fig.(A1.1). SDS gel electrophoresis on octopus microvilli. Columns 1,2 and 3 contain increasing concentrations of freshly thawed octopus microvilli. Columns 4 and 5 contain a standard protein marker. Column 6 contains a Pharmacia standard marker. Columns 7 and 8 contain octopus microvilli which had been bleached and regenerated several times.

marker	distance travelled (mm)	Mol. Wt.
α-lactalbumin	89	14,400
trypsin inhibitor	73	20,100
carbonic anhydrase	52	30,000
ovalbumin	32	43,000
albumin	21	67,000
phosphorylase b	13.5	94,000

This gave a calibration curve shown in Fig.(A1.2). From this it was possible to estimate the molecular weights of the proteins present in the microvilli sample. There were several bands corresponding to the range of molecular weights 27,000 to 88,000 AMU, showing the presence of other proteins in addition to the rhodopsin.

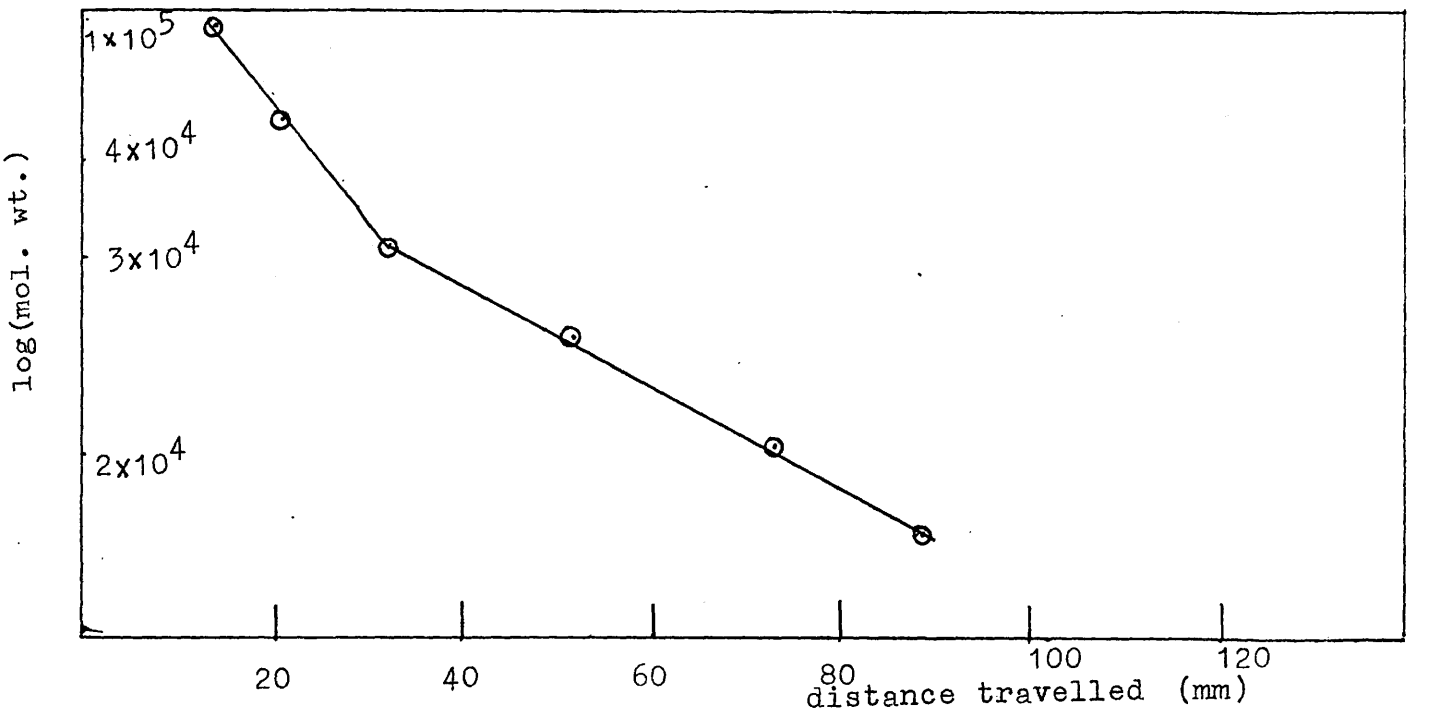

Fig.(A1.2). Calibration graph of log(Mol. Wt.) versus distance travelled.

From the gel the molecular weight of octopus rhodopsin is probably 39,000 Dalton since this is the major protein band in the correct region for an invertebrate rhodopsin. The strong band around 80,000 Dalton is probably due to presence of dimers of rhodopsin. Lower molecular weight proteins could be due to both the presence of impurities and rhodopsin degradation.

Appendix 2

Ouchterlony Gels:- An attempt to demonstrate the immunological cross-reactivity of octopus and bovine rhodopsins using antiserum to bovine rod outer segments.

Preparation of solutions.

1. Phosphate buffer:- 0.01M phosphate buffer pH 7.4 was prepared with 0.14M NaCl and 0.05% sodium azide.
2. Destaining solvent:- 400ml of absolute methanol was added to 400ml of H_2O and 80ml of glacial acetic acid.
3. Staining solution:- 1.25g of napthol blue black was added to 880ml of the destaining solvent.

Preparation of gel.

0.3g of agarose (electrophoresis grade from ICN Pharmaceuticals Inc.) was dissolved in 25ml of the phosphate buffer with stirring on a hot plate. Two immunodiffusion plates were placed on a level surface and 9ml of hot agarose was pipetted in to each using a pre-warmed pipette. The gels were allowed to set, then two hexagonal arrays of holes were cut on one plate using a 5mm hole cutter. The holes were filled as follows:-

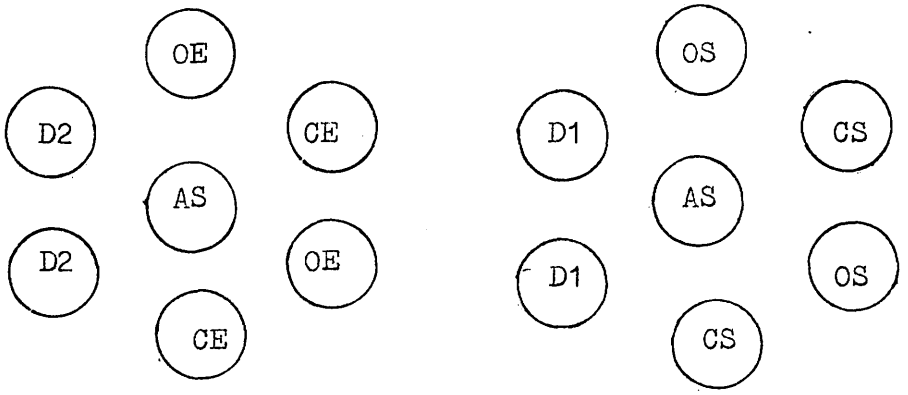

CE :- 180µl of bovine rod outer segments + 20µl of 1.5% emulphogene.

OE :- 180µl of octopus microvilli + 20µl of 1.5% emulphogene.

D1 :- 180µl of phosphate buffer + 20µl of 1.5% emulphogene.

CS :- 180µl of bovine rod outer segments + 20µl of 1% SDS.

OS :- 180µl of octopus microvilli + 20µl of 1% SDS.

D2 :- 180µl of phosphate buffer + 20µl of 1% SDS.

AS :- Rabbit-antibovine rhodopsin antiserum . (Courtesy of Dr. C.A. Converse.)

After four days, definite arcs were seen on the CS sample.

Staining of gel.

The gel was washed in 0.075M NaCl solution. This was achieved by floating the immunodiffusion plate upside down in 250ml of the saline solution. The saline solution was stirred continuously with a magnetic stirrer and changed at regular intervals. The gel was washed for two days then transferred to a $2\frac{1}{2} \times 3\frac{1}{2}$ glass slide with a piece of filter paper put on top. It was left to dry

overnight at room temperature.

The gel was stained with staining solution for 5 to 10 minutes, then destained with several washings of the destaining solution. A photograph of the resulting gel was obtained Fig.(A2.1).

Conclusions:- Although immunoprecipitation could be demonstrated for bovine rhodopsin samples, no such effects were seen with octopus microvilli. Thus no immunological cross-reactivity is apparent between bovine and octopus rhodopsins at the admittedly crude level of this experiment.

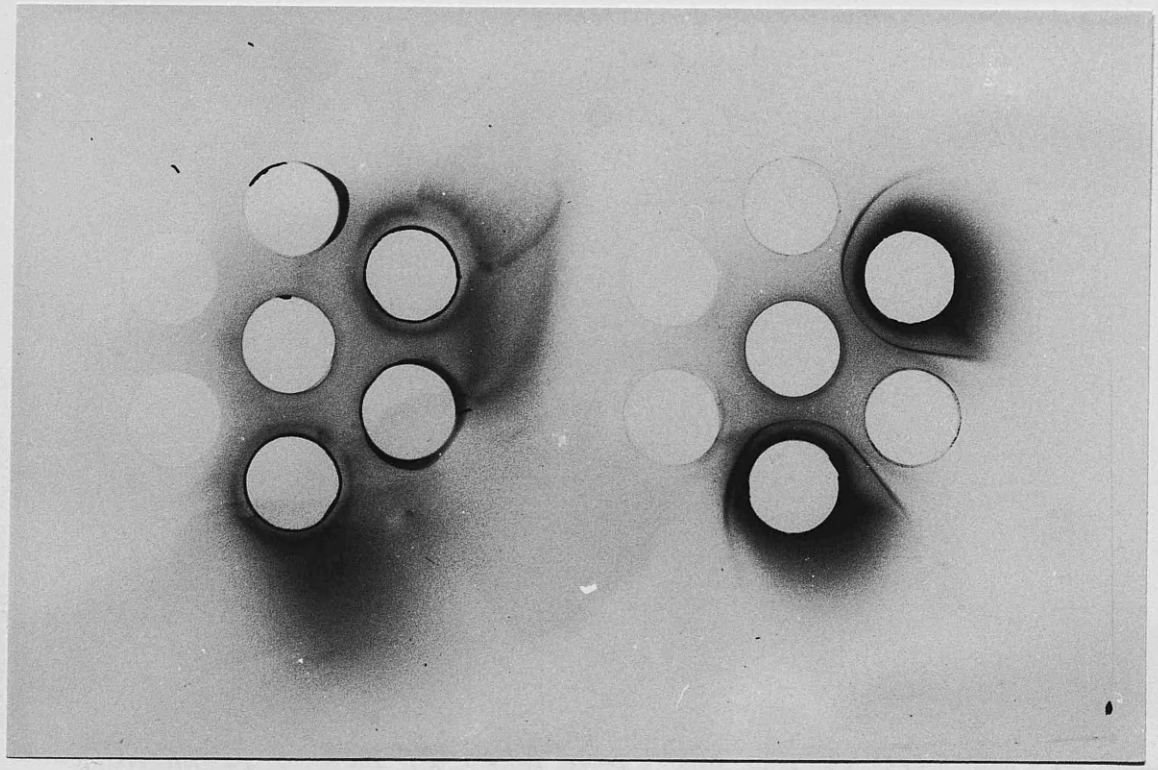

Fig.(A2.1). Ouchterlony gel testing for immunoprecipitation between octopus microvilli and vertebrate antiserum.

Appendix 3

Preparation of cattle rhodopsin.

The technique used for the preparation of cattle rhodopsin was based on that used by Papermaster and Dreyer (1974). All procedures were carried out under darkness or dim red light.

Stock Solutions.

1. 42% sucrose stock solution..

420g of sucrose was made up to 1 Kg with distilled water. The density was checked by weighing 10 ml in a volumetric flask. The density should be 1.1861 at 22°C.

2. 30% Homogenising Solution.

This consisted of 322g of 42% sucrose, 26 ml of 1.0M NaCl, 0.8 ml of 0.1M $MgCl_2$ and 2ml of 1.0M pH 7.4 Tris acetate buffer made up to 450g with distilled water. The Tris acetate contained 10mM EDTA and 15mM $CaCl_2$ to reduce oxidation effects.

3. Sucrose solutions for density gradients.

ρ = 1.15 :- 93.0g of 42% sucrose
100µl of 1.0M Tris acetate pH 7.4
100µl of 0.1M $MgCl_2$
distilled water added to give a final weight of 115g.

ρ = 1.13 :- 81.4g of 42% sucrose
100μl of 1.0M Tris acetate pH 7.4
100μl of 0.1M $MgCl_2$
distilled water to give a final weight of 113g.

ρ = 1.11 :- 68.4g of 42% sucrose
100μl of 1.0M Tris acetate pH 7.4
100μl of 0.1 M $MgCl_2$
distilled water added to give a final weight of 111g.

ρ = 1.10 :- 62.4g of 42% sucrose
100μl of 1.0M Tris acetate pH 7.4
100μl of 0.1 M $MgCl_2$
distilled water added to give a final weight of 110g.

Procedure:- 50 or 100 cattle eyes (collected fresh and dark adapted over ice) were dissected each time. The retinas were removed and added to a centrifuge tube containing 10ml of homogenising solution. 25 retinas were added to each tube.

The retinas were broken up with six passes of a teflon homogeniser which was then washed with a further 5ml of homogenising solution. The mixture was spun down at 4000rpm for 10 minutes on an MSE 18 centrifuge and the supernatant was carefully removed and placed in a

conical flask cooled in ice. The process was repeated and the two supernatants containing crude rod outer segments were pooled and diluted 1½-2 times with 10mM Tris acetate buffer pH 7.4. The resulting solution was spun down at 18,000 rpm for at least 30 minutes on an MSE 18 centrifuge. This gave pellets of crude rhodopsin-containing membranes which were taken up in ρ = 1.10 sucrose solution and homogenised using a glass homogeniser.

Centrifuge tubes with sucrose density gradients were prepared by carefully layering sucrose solutions of density ρ = 1.15, 1.13 and 1.11 on top of one another. The rhodopsin in ρ =1.10 sucrose solution was layered on the top. The centrifuge buckets were weighed and balanced where necessary with ρ = 1.10 sucrose solution. The gradients were spun at 13,500 rpm for 2 hours at 0°C on an MSE 25 centrifuge. The rod outer segments were found predominantly at the 1.11/1.13 g/ml interface and this was carefully removed using a syringe. It was diluted 1½-2 times with 10mM Tris acetate pH 7.4 buffer and spun down at 18,000 rpm for 30 minutes as before. The pellets were taken up in 10 mM Tris acetate for storage.

Appendix 4

Tables of Mass Spectra.

Table

4.1 Mass spectrum of retinal extracted from Schiff base hydrolysis. Data displayed in Fig.(4.2b).

4.2 Mass spectrum of reference retinal (Sigma). This was run in the same solvent immediately after the mass spectrum shown in table 4.1. Data displayed in Fig.(4.2a).

4.3 Mass spectrum of retinal extracted from meta II after the reaction :

$$\text{Meta I (dried)} \xrightarrow[\text{pH drop}]{H_2O^{18}} \text{Meta II}$$

Data displayed in Fig.(4.6b).

4.4 Mass spectrum of reference retinal (Sigma). This was run in the same solvent immediately after the mass spectrum shown in table 4.3. Data displayed in Fig.(4.6a).

4.5 Mass spectrum of retinal extracted from meta II after the reaction:

$$\text{Meta I (dried)} \xrightarrow[\text{pH drop}]{H_2O^{18}} \text{Meta II}$$

Data displayed in Fig.(4.7b).

4.6 Mass spectrum of reference retinal (Sigma). This was run in the same solvent immediately after the mass spectrum shown in table 4.5. Data displayed in Fig.(4.7a).

4.7 Mass spectrum of retinal extracted from meta I after the reaction :

$$\text{Meta I (dried)} \xrightarrow{H_2O^{18}} H_2O \text{ removed without pH jump.}$$

4.8 Mass spectrum of reference retinal (Sigma). This was run in the same solvent immediately after the mass spectrum shown in table 4.7. Data displayed in Fig.(4.8a)

4.9 Mass spectrum of retinal extracted from meta 1 after the reaction : $\text{Rhodopsin} \xrightarrow{H_2O^{18}} \text{Meta 1}$

Data displayed in Fig.(4.9b).

4.10 Mass spectrum of reference retinal (Sigma). This was run in the same solvent immediately after the mass spectrum shown in table 4.9. Data displayed in Fig.(4.9a).

4.11 Mass spectrum of retinal extracted from Schiff base hydrolysis. Data displayed in Fig.(4.13b).

4.12 Mass spectrum of reference retinal (Sigma). This was run in the same solvent immediately after the mass spectrum shown in table 4.11. Data displayed in Fig.(4.13a).

Table 4.1

Mass	%AR. Base	Mass	%AR. Base	Mass	%AR. Base	Mass	%AR. Base
25	0.2	90	0.3	148	1.6	205	0.8
26	1.6	91	13.5	149	12.2	206	0.3
27	6.3	92	3.4	150	1.3	207	0.5
28	100.0	93	6.1	151	1.3	208	0.1
29	8.9	94	3.3	152	3.3	210	0.4
30	0.6	95	9.9	153	1.4	211	0.5
31	1.6	96	2.6	154	0.9	213	0.8
32	20.5	97	5.2	155	1.8	214	0.2
37	0.5	98	1.2	156	1.4	215	0.3
38	0.8	99	1.4	157	3.0	217	0.4
39	8.2	100	8.2	158	1.2	218	0.4
40	3.2	101	0.4	159	3.6	219	0.4
41	24.6	102	0.6	160	1.4	220	0.1
42	3.5	103	1.9	161	2.8	221	0.3
43	18.1	104	2.2	162	0.9	222	0.2
44	2.6	105	9.4	163	1.2	223	1.1
45	2.7	106	2.0	164	0.4	225	0.4
49	0.2	107	5.5	165	1.8	227	0.2
50	1.9	108	1.8	166	0.8	231	0.1
51	2.5	109	5.6	167	1.8	232	0.1
52	1.1	110	1.8	168	0.7	233	0.1
53	4.9	111	3.3	169	1.4	235	0.1
54	1.7	112	0.7	170	0.7	239	0.1
55	19.0	113	1.6	171	2.1	241	0.7
56	5.2	115	4.7	172	0.7	249	0.1
57	16.0	116	1.6	173	4.2	251	1.2
58	1.5	117	3.9	174	1.1	252	0.1
59	0.6	118	1.4	175	1.6	253	0.2
60	1.6	119	7.6	176	0.7	255	0.7
61	0.4	120	2.7	177	3.0	256	0.1
62	0.4	121	4.1	178	1.1	259	0.2
63	1.5	122	1.8	179	1.1	266	1.3
64	0.5	123	3.6	180	0.6	267	0.6
65	4.6	124	1.2	182	0.6	268	0.1
66	1.6	125	1.9	183	1.2	269	1.1
67	8.8	126	0.6	186	0.6	282	0.2
70	4.1	129	5.3	187	1.4	284	4.2
71	7.5	130	1.7	188	0.8	285	1.1
72	0.7	131	4.2	189	1.1	286	0.2
73	0.9	132	1.9	190	0.2		
74	0.6	133	4.4	191	0.8		
75	0.9	134	1.4	192	0.6		
76	2.1	135	3.0	193	0.7		
77	7.6	136	1.4	194	0.4		
78	2.3	137	2.0	195	1.5		
79	8.2	138	0.7	196	0.7		
80	2.3	139	1.1	197	1.1		
81	10.4	140	0.2	198	0.2		
82	2.8	141	2.6	199	1.4		
83	7.1	142	2.1	200	0.5		
84	1.9	143	3.3	201	0.7		
85	3.9	144	1.7	202	0.5		
86	0.7	145	4.1	203	0.5		
87	0.6	146	1.7	204	0.1		
89	0.9	147	3.6				

Table 4.2

Mass	%AR. Base	Mass	%AR. Base	Mass	%AR Base
26	0.8	111	0.5	181	0.6
27	1.7	115	1.4	183	0.4
28	100.0	116	0.6	185	1.0
29	3.5	117	1.4	186	0.3
31	0.3	118	0.6	187	0.9
32	21.1	119	3.8	188	0.7
39	2.1	120	1.3	189	0.5
40	2.1	121	1.7	195	0.5
41	6.3	122	0.7	197	0.4
42	0.6	123	0.8	199	0.8
43	2.5	124	0.3	200	0.3
44	2.0	127	0.6	201	0.3
45	0.8	128	1.3	202	0.3
50	0.5	129	1.7	213	0.4
51	0.7	130	0.6	214	0.2
52	0.2	131	1.7	241	0.3
53	1.5	132	1.0	251	0.3
54	0.3	133	2.2	255	0.3
55	4.1	134	0.6	256	0.2
56	0.8	135	1.1	269	0.8
57	1.9	136	0.4	284	8.2
63	0.3	137	0.4	285	1.8
65	1.3	141	0.8		
66	0.5	142	0.8		
67	1.9	143	1.4		
68	0.4	144	1.4		
69	3.0	145	2.0		
70	0.6	146	1.0		
71	0.8	147	1.7		
77	2.8	148	1.1		
78	0.7	149	0.6		
79	2.7	152	0.2		
80	0.6	153	0.3		
81	2.4	155	0.6		
82	0.6	156	0.6		
83	1.1	157	1.3		
84	0.3	158	0.5		
85	0.4	159	1.8		
89	0.3	160	0.6		
91	4.7	161	1.8		
92	1.2	162	0.5		
93	2.1	163	0.2		
94	0.6	165	0.4		
95	3.0	166	0.2		
96	0.9	167	0.3		
97	0.8	169	0.4		
103	0.7	170	0.3		
104	0.3	171	1.0		
105	4.0	172	0.3		
106	1.1	173	2.8		
107	2.3	174	0.7		
108	0.7	175	0.9		
109	1.4	176	0.5		
110	0.3	177	0.8		

Table 4.3

Mass	%AR Base	Mass	%AR Base	Mass	%AR. Base	Mass	%AR Base
41	100.0	99	4.4	155	2.4	227	0.2
42	15.7	101	1.7	156	1.7	228	1.0
43	76.8	102	1.2	157	3.6	231	0.5
44	3.6	103	2.7	158	1.5	236	0.2
45	4.4	104	5.8	159	3.4	239	0.2
49	1.0	105	11.6	160	1.5	241	0.2
50	5.3	106	3.4	161	3.1	242	0.5
51	5.3	107	7.7	162	1.2	251	0.2
52	2.7	108	3.1	163	1.7	255	0.7
53	13.3	109	7.5	164	0.5	256	2.2
54	6.8	110	2.9	165	1.9	269	0.7
55	55.0	111	6.1	166	1.0	279	0.5
56	17.2	112	2.7	167	2.4	284	3.6
57	47.2	113	3.1	168	0.7	285	1.0
58	2.9	114	0.2	169	1.7	286	1.5
59	1.9	115	6.5	170	0.2	287	0.0
60	12.6	116	2.4	171	2.7		
61	2.4	117	5.3	172	1.0		
62	1.0	118	1.9	173	3.9		
63	2.2	119	8.2	174	1.2		
64	0.7	120	3.4	175	2.2		
65	8.7	121	6.1	176	0.7		
66	3.4	122	2.7	177	1.7		
67	20.6	123	5.6	178	0.7		
68	10.2	124	1.9	179	1.5		
69	58.4	125	3.4	180	0.2		
70	11.1	126	1.5	181	1.0		
71	19.6	127	2.2	182	0.2		
72	1.7	128	4.8	183	1.2		
73	9.4	129	7.0	185	2.9		
74	2.4	130	2.2	186	0.7		
75	1.7	131	4.6	187	1.5		
76	6.3	132	2.2	188	0.7		
77	12.1	133	5.3	189	1.2		
78	3.9	134	2.2	190	0.2		
79	14.0	135	3.9	191	1.0		
80	5.1	136	2.9	192	0.7		
81	24.0	137	4.4	193	1.0		
82	6.8	138	1.7	194	0.2		
83	15.0	139	1.9	195	0.5		
84	4.6	140	1.0	197	1.0		
85	11.1	141	3.4	199	1.7		
86	1.0	142	2.4	200	0.2		
87	2.4	143	4.1	201	0.7		
88	0.2	144	1.9	202	0.2		
89	1.2	145	4.4	203	1.0		
90	0.2	146	2.2	205	1.7		
91	16.9	147	3.6	207	0.5		
92	3.9	148	1.9	209	0.2		
93	10.7	149	29.5	211	0.2		
94	3.9	150	3.4	213	1.7		
95	14.5	151	1.9	215	0.5		
96	5.1	152	1.5	217	0.5		
97	10.2	153	1.9	218	0.2		
98	3.4	154	0.7	223	2.2		

Table 4.4

Mass	%AR. Base	Mass	%AR. Base
41	100.0	127	8.6
42	9.9	128	21.0
43	42.0	129	21.0
44	11.1	130	7.4
50	8.6	131	19.8
51	16.0	132	9.9
52	7.4	133	19.8
53	28.4	134	7.4
54	7.4	135	9.9
55	50.6	136	2.5
56	12.3	141	13.6
57	21.0	142	11.1
63	7.4	143	14.8
65	22.2	144	7.4
66	11.1	145	19.8
67	25.9	146	8.6
68	4.9	147	14.8
69	29.6	148	8.6
70	4.9	149	16.0
71	9.9	152	2.5
76	6.2	153	6.2
77	40.7	154	2.5
78	14.8	155	8.6
79	38.3	156	7.4
80	13.6	157	12.3
81	24.7	158	3.7
82	6.2	159	16.0
83	11.1	160	6.2
85	3.7	161	13.6
89	4.9	162	2.5
91	64.2	165	6.2
92	14.8	167	3.7
93	23.5	169	3.7
94	8.6	170	2.5
95	28.4	171	8.6
96	8.6	172	1.2
97	7.4	173	21.0
103	9.9	174	6.2
104	8.6	175	7.4
105	43.2	177	2.5
106	9.9	181	3.7
107	24.7	183	2.5
108	9.9	185	7.4
109	13.6	187	7.4
111	1.2	188	3.7
115	24.7	189	1.2
116	9.9	195	3.7
117	19.8	199	8.6
118	7.4	213	3.7
119	32.1	241	1.2
120	12.3	255	1.2
121	14.8	269	4.9
122	6.2	284	27.2
123	7.4	285	7.4

Table 4.5

Mass	%AR. Base	Mass	%AR. Base	Mass	%AR. Base
41	100.0	98	4.3	155	2.5
42	15.2	99	4.7	156	1.8
43	76.9	101	1.4	157	4.3
44	3.6	102	1.4	158	1.8
45	5.4	103	3.6	159	5.1
47	1.8	104	5.8	160	1.8
49	1.4	105	22.7	161	4.3
50	7.2	106	4.7	162	1.4
51	9.7	107	9.7	163	2.9
52	3.2	108	3.6	164	0.7
53	14.8	109	8.3	165	2.9
54	7.9	110	3.6	166	1.1
55	60.6	111	7.6	167	3.6
56	18.4	112	3.6	168	1.1
57	52.3	113	4.0	169	2.2
58	4.3	114	0.7	170	0,7
59	2.5	115	8.3	171	4.0
60	14.1	116	3.6	172	1.1
61	4.0	117	6.1	173	7.6
62	1.1	118	2.5	174	2.2
63	2.9	119	11.9	175	2.9
64	0.7	120	4.3	176	1.1
65	10.5	121	7.2	177	2.2
66	4.3	122	5.8	178	0.7
67	24.2	123	6.5	179	1.1
68	10.8	124	2.5	181	1.1
69	62.5	125	3.6	183	1.4
70	12.6	126	1.8	185	3.6
71	24.2	127	2.9	186	0.7
72	2.2	128	6.1	187	2.2
73	11.6	129	9.0	188	1.4
74	3.6	130	2.9	189	2.2
75	2.5	131	6.5	191	1.1
76	6.1	132	3.2	195	1.4
77	22.0	133	7.2	196	0.7
78	6.1	134	2.9	197	1.4
79	18.1	135	4.7	199	2.5
80	5.8	136	2.9	200	0.7
81	26.7	137	4.3	201	1.4
82	8.7	138	1.8	203	1.1
83	17.7	139	1.8	205	2.5
84	6.1	141	4.3	213	1.8
85	11.9	142	3.2	215	0.7
86	1.1	143	5.4	223	2.9
87	3.2	144	2.5	241	1.1
88	1.1	145	6.5	251	0.7
89	1.4	146	2.9	255	1.1
90	0.7	147	4.7	256	2.9
91	23.8	148	2.5	269	1.4
92	5.4	149	40.4	271	0.7
93	12.6	150	4.7	279	0.7
94	4.3	151	1.8	284	5.8
95	15.9	152	1.4	285	1.4
96	6.1	153	2.5	286	4.0
97	11.6	154	1.8		

Table 4.6

Mass	%AR. Base	Mass	%AR. Base
41	100.0	111	9.8
42	15.7	113	7.8
43	62.7	115	15.7
44	29.4	116	2.0
45	17.6	117	13.7
46	9.8	119	25.5
47	7.8	120	11.8
50	13.7	121	13.7
51	23.5	122	7.8
52	7.8	123	9.8
53	21.6	125	7.8
54	11.8	127	3.9
55	56.9	128	17.6
56	15.7	129	11.8
57	47.1	130	3.9
60	11.8	131	15.7
61	9.8	132	9.8
63	3.9	133	17.6
65	17.6	134	13.7
66	7.8	135	9.8
67	45.1	141	9.8
68	7.8	142	3.9
69	35.3	143	11.8
70	13.7	144	3.9
71	17.6	145	15.7
74	3.9	146	3.9
76	7.8	147	15.7
77	49.0	148	7.8
78	11.8	149	3.9
79	31.4	153	2.0
80	9.8	155	7.8
81	33.3	157	9.8
82	23.5	159	13.7
83	21.6	161	11.8
84	7.8	171	9.8
85	25.5	173	19.6
88	13.7	174	3.9
91	43.1	175	7.8
92	9.8	185	7.8
93	21.6	187	7.8
94	7.8	188	2.0
95	29.4	199	3.9
96	9.8	269	2.0
97	15.7	284	25.5
98	2.0		
99	2.0		
103	11.8		
104	2.0		
105	49.0		
106	11.8		
107	17.6		
108	9.8		
109	17.6		
110	2.0		

Table 4.7

Mass	%AR. Base	Mass	%AR. Base	Mass	%AR. Base
41	100.0	109	18.6	169	5.5
42	19.3	110	6.9	170	2.8
43	75.2	111	15.2	171	7.6
44	45.5	112	6.9	172	1.4
45	20.7	113	9.7	173	14.5
46	6.9	115	15.9	174	4.8
50	10.3	116	5.5	175	6.2
51	12.4	117	11.7	176	2.1
52	5.5	118	5.5	177	31.0
53	17.9	119	34.5	178	6.2
54	7.6	120	10.3	179	4.8
55	71.7	121	17.2	181	11.0
56	28.3	122	8.3	182	3.4
57	80.0	123	13.8	183	4.8
58	4.1	124	4.8	184	2.1
60	10.3	125	8.3	185	6.2
61	3.4	126	2.8	187	4.8
63	6.9	127	6.9	188	2.1
65	20.7	128	11.7	189	3.4
66	5.5	129	13.1	191	1.4
67	29.0	130	5.5	192	4.1
68	11.0	131	13.8	193	2.8
69	57.9	132	7.6	194	1.4
70	20.7	133	16.6	195	9.0
71	40.7	134	6.9	196	4.1
72	1.4	135	13.8	197	4.8
73	4.8	136	5.3	198	4.8
74	3.4	137	6.9	201	1.4
75	1.4	139	4.8	205	3.4
76	9.0	141	8.3	209	4.1
77	28.3	142	6.2	210	1.4
78	9.0	143	13.1	211	2.1
79	26.9	144	6.2	213	2.8
80	7.6	145	15.9	223	6.9
81	36.6	146	5.5	251	11.7
82	13.8	147	12.4	252	2.8
83	31.0	148	7.6	255	1.4
84	10.3	149	77.2	266	15.9
85	24.1	150	7.6	267	4.1
89	2.8	151	3.4	269	4.1
90	1.4	152	3.4	279	3.4
91	66.2	153	4.1	282	2.8
92	24.1	154	2.1	284	20.7
93	24.1	155	6.2	285	4.8
94	9.7	156	3.4		
95	33.1	157	10.3		
96	11.7	158	3.4		
97	24.1	159	15.2		
98	6.2	160	4.8		
99	9.7	161	12.4		
103	6.9	162	3.4		
104	8.3	163	2.8		
105	35.9	165	6.2		
106	8.3	166	2.1		
107	20.7	167	11.0		
108	8.3	168	2.1		

Table 4.8

Mass	%AR. Base	Mass	%AR. Base	Mass	%AR. Base
37	1.2	107	41.2	169	10.0
38	2.9	108	11.1	170	5.9
39	35.9	109	18.8	171	18.8
40	13.5	110	4.1	172	6.5
41	91.8	111	2.4	173	48.2
42	7.6	112	2.9	174	10.6
43	31.2	113	2.9	175	13.5
44	7.6	115	38.8	176	5.9
45	4.1	116	14.1	177	11.2
50	5.9	117	32.4	178	4.1
51	12.9	118	10.0	179	4.7
52	5.9	119	64.1	180	2.9
53	30.6	120	21.2	181	8.8
54	5.3	121	25.9	182	4.1
55	53.5	122	11.8	183	8.2
56	8.2	123	9.4	184	3.5
57	17.6	127	11.8	185	15.9
60	2.4	128	33.5	186	5.3
62	1.2	129	37.6	187	13.5
63	7.1	130	13.5	188	8.8
64	2.9	131	37.1	189	6.5
65	27.1	132	18.2	192	1.8
66	8.2	133	38.8	193	2.4
67	31.8	134	11.2	195	8.2
68	4.1	135	17.1	196	3.5
69	37.1	136	6.5	197	6.5
70	8.2	137	4.1	198	2.4
71	7.6	139	2.4	199	14.1
74	1.2	141	21.8	200	4.7
75	1.8	142	18.8	201	5.3
76	4.7	143	29.4	202	4.7
77	56.5	144	12.9	209	4.1
78	17.1	145	37.6	210	1.2
79	51.2	146	15.9	211	2.9
80	14.1	147	30.0	213	8.8
81	34.7	148	15.9	214	2.9
82	6.5	149	12.4	215	1.8
83	10.6	150	2.4	223	1.8
84	2.4	151	1.8	225	2.4
85	1.8	152	7.6	227	1.8
89	6.5	153	10.6	228	1.2
90	1.8	154	5.9	241	6.5
91	100.0	155	14.1	251	7.1
92	20.0	156	11.2	255	6.5
93	37.6	157	24.1	256	2.4
94	9.4	158	8.8	266	4.1
95	46.5	159	32.9	267	1.2
96	11.8	160	11.2	269	12.9
97	5.3	161	28.8	270	1.8
101	1.8	162	7.1	284	56.5
102	4.7	163	2.9	285	12.9
103	13.5	165	10.0		
104	8.2	166	5.3		
105	74.1	167	9.4		
106	16.5	168	4.7		

Table 4.9

Mass	%AR. Base	Mass	%AR. Base	Mass	%AR. Base	Mass	%AR. Base
37	2.1	99	5.3	155	5.3	223	3.2
38	3.7	100	1.1	156	3.7	231	0.5
39	28.9	101	2.6	157	7.4	241	2.6
40	11.1	102	1.6	158	3.2	251	1.6
41	100.0	103	5.3	159	10.0	255	1.1
42	16.3	104	10.0	160	4.2	259	0.5
43	79.5	105	25.3	161	8.4	269	2.6
44	7.9	106	6.8	162	3.2	279	5.3
45	17.9	107	17.4	163	4.7	284	10.5
50	7.4	108	6.8	164	1.6	285	2.6
51	8.4	109	21.1	165	4.2		
52	3.2	110	6.8	166	2.1		
53	16.3	111	13.7	167	12.6		
54	6.8	112	8.9	168	2.1		
55	77.9	113	8.4	169	3.7		
56	23.7	115	11.6	170	1.6		
57	75.3	116	4.2	171	5.8		
58	6.3	117	10.0	172	1.6		
59	4.7	118	4.2	173	11.1		
60	11.1	119	19.5	174	3.2		
61	3.2	120	7.4	175	4.7		
62	2.1	121	13.7	176	2.1		
63	4.2	122	5.8	177	5.8		
65	13.2	123	14.2	178	2.6		
66	4.7	124	5.3	179	3.7		
67	34.2	125	7.9	180	0.5		
68	11.6	126	2.1	181	3.2		
69	72.1	127	4.2	182	1.1		
70	23.2	128	9.5	183	2.6		
71	34.2	129	17.9	185	4.2		
72	3.7	130	4.7	187	4.2		
73	5.3	131	10.5	188	2.1		
74	3.2	132	5.8	189	3.2		
75	3.7	133	13.2	190	0.5		
76	8.9	134	4.7	191	3.7		
77	21.1	135	10.0	192	1.6		
78	6.3	136	4.7	193	2.1		
79	25.3	137	9.5	194	0.5		
80	7.4	138	3.2	195	3.2		
81	45.3	139	4.2	196	1.1		
82	12.6	140	0.5	197	2.1		
83	30.5	141	6.3	199	4.2		
84	8.9	142	5.8	200	0.5		
85	14.7	143	8.9	201	2.1		
86	2.6	144	4.2	202	0.5		
87	3.2	145	12.1	203	2.1		
89	2.1	146	4.2	205	3.2		
91	32.1	147	10.5	207	1.1		
92	7.4	148	4.2	209	0.5		
93	21.6	149	58.4	211	1.1		
94	13.2	150	6.8	213	2.6		
95	36.3	151	5.3	217	1.6		
96	9.5	152	3.2	218	1.1		
97	21.6	153	3.7	219	0.5		
98	4.7	154	1.1	221	1.1		

Table 4.10

Mass	%AR. Base	Mass	%AR. Base	Mass	%AR. Base	Mass	%AR. Base
41	98.2	108	12.1	167	7.3	267	1.8
42	7.3	109	19.4	168	3.6	269	11.5
43	33.3	110	5.5	169	10.3	270	3.0
44	20.0	111	4.2	170	4.8	282	0.6
45	4.2	113	1.8	171	18.2	284	20.9
49	3.0	115	35.2	172	6.1	285	5.1
50	7.3	116	12.7	173	43.6		
51	14.5	117	28.5	174	9.7		
52	6.1	118	10.3	175	12.7		
53	30.9	119	59.4	176	5.5		
54	5.5	120	21.2	177	14.5		
55	54.5	121	28.5	178	5.5		
56	8.5	122	10.9	179	5.5		
57	15.2	123	9.7	180	3.6		
60	0.6	124	0.6	181	10.3		
62	2.4	125	0.6	182	4.2		
63	9.7	126	0.6	183	7.9		
64	3.6	127	10.3	184	4.2		
65	30.3	128	31.5	185	13.9		
66	7.7	129	30.3	186	5.5		
67	29.7	130	11.5	187	10.9		
68	4.8	131	35.2	188	9.7		
69	39.4	132	15.8	189	6.1		
70	4.8	133	35.2	190	0.6		
71	7.3	134	11.5	191	1.8		
74	1.2	135	16.4	192	2.4		
75	2.4	136	7.3	193	3.0		
76	4.2	137	4.8	194	1.2		
77	53.9	139	2.4	195	8.5		
78	17.0	141	19.4	196	3.6		
79	49.7	142	16.4	197	6.1		
80	13.9	143	24.8	198	3.0		
81	34.5	144	12.1	199	13.3		
82	6.7	145	35.2	200	4.2		
83	11.5	146	15.8	201	5.5		
84	1.8	147	25.5	202	4.2		
85	4.2	148	14.5	203	2.4		
89	6.7	149	9.7	207	0.6		
90	1.8	150	3.0	209	4.8		
91	100.0	151	2.4	210	0.6		
92	22.4	152	7.3	211	3.6		
93	37.0	153	9.1	213	7.3		
94	9.1	154	6.1	214	3.6		
95	43.0	155	14.5	215	1.8		
96	10.9	156	10.3	223	1.8		
97	6.1	157	23.6	225	1.2		
98	0.6	158	7.9	226	0.6		
99	1.2	159	27.9	227	1.8		
101	1.2	160	10.3	228	1.2		
102	4.2	161	27.9	241	5.5		
103	13.3	162	7.3	242	0.6		
104	7.9	163	2.4	251	7.9		
105	70.9	164	0.6	255	6.7		
106	16.4	165	10.3	256	1.2		
107	37.0	166	5.5	266	6.7		

Table 4.11

Mass	%AR. Base	Mass	%AR. Base	Mass	%AR. Base	Mass	%AR. Base
41	7.2	97	0.9	154	0.6	213	0.6
42	0.9	98	0.3	155	0.8	214	0.2
43	3.1	99	0.3	156	0.7	215	0.2
44	1.6	101	0.2	157	1.4	223	0.1
45	0.5	102	0.5	158	0.6	225	0.2
47	3.2	103	0.9	159	1.9	226	0.0
48	1.5	104	0.7	160	0.7	227	0.2
49	14.4	105	100.0	161	1.8	228	0.1
50	9.0	106	8.3	162	0.5	241	0.4
51	27.7	107	2.8	163	0.3	242	0.1
52	2.1	108	0.7	164	0.2	251	0.4
53	0.2	109	1.5	165	0.9	252	0.1
54	0.5	110	0.5	166	0.4	255	0.5
55	4.3	111	0.6	167	0.6	256	0.2
56	1.0	112	0.2	168	0.3	267	0.0
57	2.4	113	0.3	169	0.6	269	0.8
58	0.2	114	0.0	170	0.4	270	0.2
59	0.1	115	2.1	171	1.1	284	3.5
60	0.3	116	0.8	172	0.5	285	0.8
61	0.4	117	1.8	173	3.0	286	0.5
62	0.7	118	0.7	174	0.7	287	0.0
63	1.2	119	4.1	175	0.9		
64	0.3	120	1.5	176	0.4		
65	1.9	121	1.7	177	0.5		
66	0.6	122	0.8	178	0.8		
67	2.4	123	0.8	179	0.5		
68	0.5	124	0.2	180	0.4		
69	3.3	125	0.3	181	0.7		
70	0.7	126	0.4	182	1.0		
71	1.2	127	0.8	183	0.5		
72	0.1	128	1.9	184	0.2		
73	0.5	129	1.8	185	1.0		
74	2.7	130	0.7	186	0.3		
75	2.0	131	2.3	187	0.9		
76	3.2	132	1.2	188	0.7		
77	62.9	133	2.5	189	0.5		
78	6.3	134	0.8	190	0.1		
79	3.4	135	1.2	191	0.1		
80	0.8	136	0.5	193	0.2		
81	2.7	137	0.5	194	0.2		
82	0.8	138	0.1	195	0.5		
83	1.6	139	0.3	196	0.2		
84	9.6	141	1.2	197	0.4		
85	0.9	142	1.0	198	0.2		
86	6.0	143	1.6	199	0.9		
87	0.3	144	0.7	200	0.3		
88	1.2	145	2.3	201	0.4		
89	0.7	146	1.0	202	0.3		
90	0.3	147	1.9	203	0.2		
91	5.6	148	1.0	204	0.0		
92	1.1	149	1.3	205	0.1		
93	2.4	150	0.4	209	0.2		
94	0.7	151	0.5	210	3.5		
95	3.1	152	1.2	211	0.7		
96	0.9	153	0.9	212	0.1		

Table 4.12

Mass	%AR. Base	Mass	%AR. Base	Mass	%AR. Base
41	72.7	118	9.4	182	6.5
42	8.6	119	53.2	183	9.4
43	48.2	120	15.1	184	5.0
44	33.1	121	22.3	185	10.1
45	17.3	122	10.1	186	2.2
46	7.9	123	10.1	187	8.6
50	7.2	127	7.2	188	6.5
51	15.1	128	21.6	189	5.0
52	4.3	129	19.4	192	4.3
53	23.0	130	7.9	193	3.6
54	2.2	131	23.0	195	14.4
55	42.4	132	12.2	196	6.5
56	8.6	133	27.3	197	6.5
57	15.1	134	8.6	199	9.4
62	1.4	135	17.3	200	2.2
63	8.6	136	6.5	201	2.2
64	1.4	137	2.2	202	2.2
65	23.7	141	12.9	209	6.5
66	6.5	142	11.5	210	2.9
67	22.3	143	20.1	211	2.2
68	1.4	144	10.8	213	5.0
69	32.4	145	25.2	214	1.4
70	6.5	146	11.5	223	5.8
71	7.2	147	20.1	241	2.9
76	2.2	148	11.5	251	15.8
77	38.8	149	8.6	252	3.6
78	11.5	152	5.0	255	4.3
79	37.4	153	7.2	266	24.5
80	8.6	154	2.9	267	5.8
81	26.6	155	10.1	269	9.4
82	3.6	156	7.9	282	2.9
83	10.8	157	18.0	284	39.6
85	3.6	158	5.8	285	8.6
89	6.5	159	25.9		
90	1.4	160	8.6		
91	100.0	161	19.4		
92	38.8	162	5.0		
93	28.8	163	1.4		
94	5.8	165	9.4		
95	29.5	166	5.0		
96	8.6	167	7.2		
97	7.9	168	2.2		
102	2.2	169	8.6		
103	10.1	170	3.6		
104	5.0	171	12.9		
105	56.1	172	3.6		
106	12.9	173	28.8		
107	31.7	174	7.2		
108	8.6	175	8.6		
109	14.4	176	4.3		
110	2.9	177	46.0		
111	3.6	178	8.6		
115	25.9	179	5.8		
116	10.1	180	2.9		
117	20.9	181	20.1		